Calcification patterns of the coccolithophore *Coccolithus braarudii* (Haptophyta), from the late Quaternary to present in the Southern Ocean

by

Joana Carolina Cubillos

BSc. Hons., University of Tasmania

Submitted in fulfilment of the
requirements for the degree of

Doctor

of

Philosophy

University of Tasmania

June, 2013

Declaration of Originality

I declare that the material presented in this thesis is original, except where due acknowledgement is given, and has not been accepted for award of any other degree or diploma

_____

Joana Carolina Cubillos

June, 2013

Authority of Access

This thesis may be available for loan and limited copying in accordance with the *Copyright Act* 1968

_____

Joana Carolina Cubillos

June, 2013

Statement regarding published work contained in the thesis

The publishers of the paper comprising Chapter 2 hold the copyright for that content, and access to the material should be sought from the respective journals. The remaining non-published content of the thesis may be made available for loan and limited copying and communication in accordance with the *Copyright Act* 1968.

Statement of authorship (Chapter 2)

The following people contributed to the publication of the work undertaken as part of this thesis:

Joana C. Cubillos (candidate) (50%), Jorijntje Henderiks (author 2) (35%), Luc Beaufort (author 3) (2.5%), Will R. Howard (author 4) (2.5%), Gustaaf Hallegraeff (author 5) (10%)

Details of authors roles:

Joana C. Cubillos (the candidate) and Jorijntje Henderiks contributed to the idea, method development and method refinement, presentation and formalization.

Luc Beaufort contributed to the original idea and training on the original methodology.

Gustaaf Hallegraeff contributed with his expertise, feedback, laboratory facilities, presentation and formalization.

Will Howard facilitated the samples and additional data.

We the undersigned agree with the above stated “proportion of work undertaken” for each of the above published peer-reviewed manuscript contributing to this thesis:

Signed: _____ _____

Professor Gustaaf Hallegraeff	Professor Millard Coffin
Supervisor	Executive director
Institute for Marine and	Institute of Marine and
Antarctic Studies	Antarctic Studies
University of Tasmania	University of Tasmania

Date: _____

Dedication

To my beautiful man Philip (Felipe), for his love, patience and kindness…

To our gorgeous son Gabriel and the strength he has already given me…

To my dear family: my dad, Mariano, my mum, Pola, my sisters Paula and Pamela, and my beautiful nephews Benjamin and Emilio…

Acknowledgments

I would like to acknowledge and thank the following people for their contribution to this thesis:

To my primary supervisor Professor Gustaaf Hallegraeff for his commitment to this project, his feedback and his ability to face the challenges that this project presented for all of us.

I had the pleasure to meet and work with Dr. Jorijntje Henderiks, based in Sweden, who also joined the supervision team. Jorijntje has been central to this research and without her constant feedback and tireless work I wouldn't have been able to finish this candidature. I wish to thank her for all her efforts, knowledge and precious time.

To the rest of my supervision team, Dr. Will Howard and Dr. Simon Wright for their input.

To Helen Bond for all her help and support at the lab and her infallible friendship.

To Associate Professor Ron Berry (ARC Centre of Excellence in Ore Deposits (Codes)), for providing the Leica DM6000 cross-polarised microscope used for all image gathering and method development, and thank him also for sharing his expertise and knowledge in the field of mineralogy and microscopy.

To Dr. Tom Trull and Dr. Stephen Bray (Antarctic Climate and Ecosystem Cooperative Research Centre (ACE, CRC)) for providing the sediment trap samples (SAZ Project), used for method development, and also for their advice and valuable time. Special thanks to Stephen for last minute calculations and his precious time in such last notice.

To Dr. Andrew Moy (Australian Antarctic Division (AAD), Antarctic Climate and Ecosystem Cooperative Research Centre (ACE, CRC)) for his availability, valuable feedback and time.

Professor David Ratkowsky and Dr. Greg Jordan were crucial in the statistical

analysis of the data and their judgment and feedback were central to the results of this thesis. Thanks you both for your sharing your expertise and mostly your valuable time.

To Dr. Karsten Goemann, in charge of the SEM unit (Central Science Laboratory), who provided support in all aspects of image gathering and quality, for which we are very grateful.

To Luc Beaufort for welcoming me into his lab at CEREGE (Aix-en Provence, France), and giving me his time and expertise in the training of the original methodology used as the base for this research.

To Rick van den Enden for his help with the SEM Unit at the Australian Antarctic Division.

To Professor Patrick Quilty at the School of Earth Sciences for his advice, expertise and generous time.

To Miguel de Salas for the isolation of the *Coccolithus* cultures used on this research.

To Suellen Cook, Kate Perkins and Juan Jose Dorantes and Marius Muller, Giselle Astorga and Fabiola Aburto for their friendship and support throughout this process, and all my friends and family.

To all whom I shared music this past five years, which allowed me to keep my sanity in hard times.

Content

Abstract

Ocean acidification, caused by a decrease in pH due to elevated anthropogenic CO_2 input from the atmosphere into the ocean, is the focus of intense current research with regard to biological impacts. Allegedly, the most affected species will be those that produce hard calcite and aragonite shells. In the present study, we assessed calcification and morphometry of the large-sized, heavily calcified coccolithophore genus *Coccolithus*, in the Southern Ocean, south of Tasmania.

Firstly, we characterised the species, past and present, in the Southern Ocean using the following source materials: fossil core-top material from Core GC07 (South Tasman Rise); recent sediment trap samples collected during Sept 2003 - Feb 2004 from the Subantarctic Zone (SAZ) south of the subtropical front (STF); and two newly isolated culture strains from coastal Tasmania. Results showed that only a single taxon , designated *Coccolithus braarudii* [(Gaarder, 1962) Baumann et al., 2003] sensu Geisen et al. (2002) and Young et al., (2003), was consistently present in the Southern Ocean, with coccolith length ranging from 10-16 μm and consistent presence of a central bar across the central area. Core-top sediments showed its presence for at least the past ~1000 years, and recent sediment trap samples demonstrated a well-established population from Sept 2003 to Feb 2004 (coccolith and coccosphere fluxes of ~ 6.87×10^3 and ~ 2.11×10^2 counts/m^2/day, respectively in September to over ~ 6.41×10^6 and 1.23×10^4 counts/m^2/day in January 2004, respectively). Tasmanian culture material proved that this species was equally present both north and south of the STF (~ 46°S).

To evaluate calcification patterns, a method to estimate coccolith weight was newly adapted in order to suit this large, heavily calcified species. This method is based on the intensity of birefringence of individual coccoliths under cross-polarised light, measured in grey levels, which is converted into relative weight (picograms per pixels) through a calibrated transfer function. In its original approach, the birefringence technique is unsuitable for partially non-birefringent coccoliths in standard orientation, such as those of the family Coccolithaceae. However, we

here consider only the birefringent parts of the coccoliths, the proximal shield (PS) and central area (CA) to determine intra-specific coccolith weight variation. Since only part of the coccolith is measured, this constitutes a relative weight measurement, here called weight index (WI). In contrast to other methods that exclusively rely on coccolith length to estimate calcification, the advantage of this approach is that it decouples coccolith weight from length, to provide separate estimates of how each morphological feature of coccoliths responds to environmental changes. Furthermore, we advocate for a combined approach of WI and morphometry, to depict allometric relationships within coccoliths, i.e. how coccolith shape varies with size.

Sediment trap samples from the Subantarctic Zone (SAZ) were analysed for seasonal variations in the morphology of *C. braarudii*. Distal shield length (DSL), WI, and various other parameters of individual coccoliths were measured (N = ~ 3000), as well as coccolith and coccosphere concentrations estimated. Results showed an increase in WI, DSL and cell concentration from spring to summer, correlated with the seasonal increase in phytoplankton chlorophyll *a*. No correlation was found between WI and environmental parameters (Atmospheric CO_2, $[CO_3^{2-}]$, DIC, sea surface temperature (SST) and nutrients), which appears to confirm earlier observations that this species is insensitive to chemical variations. However there was a positive correlation between DSL and SST. We also recorded the occurrence of a lighter, slightly smaller phenotype during early spring - which could be the remnant of a winter population - and a larger, heavier phenotype in mid-summer. Although this might indicate a constant allometric relationship between size and weight at a seasonal scale, the appearance of healthier populations in summer may suggest certain seasonal plasticity of *C. braarudii* coccoliths.

In order to analyse changes in WI and morphological parameters at a geological time scale, fossil material from sediment Core MD972106 was investigated from the Last Glacial Maximum (LGM, ~ 20 ka) through to the late Holocene (~ 4.2 ka), and compared with recent sediment trap samples. Additionally, we incorporated a novel estimator for intra-specific variations in the degree of calcification, combining WI and DSL, resulting in a calcification index (CI). Coccolith weight (WI) in *C. braarudii* in the Southern Ocean has significantly increased (not decreased) from the

late Quaternary to the present, further confirming that this genus could be insensitive to changes in ocean chemistry composition.

Lighter, larger coccoliths during the LGM could imply degrees of calcification would be lower as a trade-off for larger coccolith under glacial conditions. Holocene material contained a smaller, heavier phenotype, while a larger, heavier phenotype was present in contemporary oceans. While variations in DSL were correlated with environmental parameters such as SST, atmospheric CO_2 (ppmv) and CO_3^{2-} concentrations ($[CO_3^{2-}]$), WI was not related to any of these variables. Our results showed that the scaling between size and weight (allometry) of coccoliths was not constant over geological time, indicating subtle but significant changes in the mean shape of *C. braarudii*, and that the allometric relationships at a seasonal scale may represent short term adaptation processes. CI exhibited a clear response to environmental parameters, especially SST, implying that variable allometry between size and weight underpins phenotypic plasticity in this species, which is assumed to be an adaptive response to changing environmental conditions.

List of Figures

Figure 5.10. CI (from Equation 5.1) response to SST (^{o}C), atmospheric CO_2 (ppmv), CO_3^{2-} concentrations ([CO_3^{2-}] in µM Kg^{-1}) and age (ka) through LGM, deglaciation and late Holocene (three samples per time interval, N= ~ 300 per sample). CI, SST, CO_2 and [CO_3^{2-}] have been transformed by natural logarithm. Environmental variables are available for each data point only, therefore no error bars are available. Error bars for CI are ± 1 s.e. (pp 99).

List of Tables

Chapter 1 General Introduction

1.1 Coccolithophores

1.1.1 Background

Coccolithophores are unicellular marine algae from the Division Haptophyta, characterized by their ability to form calcite ($CaCO_3$) scales intracellularly (coccoliths), which are extruded and cover the entire cell (coccosphere) (Figure 1.1). The vast majority of known haptophytes is included in the scale-bearing Prymnesiophyceae and within this class, around half of the described species have the ability to biomineralize organic scales (De Vargas and Probert, 2004). Hence, De Vargas et al. (2007) proposed the erection of a new subclass Calcihaptophycidae, for calcifying Haptophytes. This group is responsible for 20 to 60% of the pelagic marine carbonate production (Baumann, 2004). Their robust coccoliths, together with their global, stratigraphically-continuous distribution in marine sediments, combine to make these organisms ideal candidates to recreate analysis of Mesozoic to Holocene diversity records (Bown, 2005).

Two types of coccoliths can be produced, holococcoliths and heterococcoliths, formed by a very different type of biomineralization, now understood to comprise the haploid and the diploid form of the life cycle, respectively (Young et al., 2003) (Figure 1.2). Holococcoliths consist of a large number of small, equant calcite crystals, around 0.1µm, held together by organic material and only rarely preserved in the fossil record, while heterococcoliths consist of radial arrays of complex crystal units (Henriksen et al., 2004c; Young et al., 1999). The most common type of heterococcolith are placoliths, whereby the expansion from a central tube, the proto-coccolith ring, forms two disks composed of calcite crystals arranged radially, normally forming a rhomboid shape (Henriksen et al., 2003; 2004a).

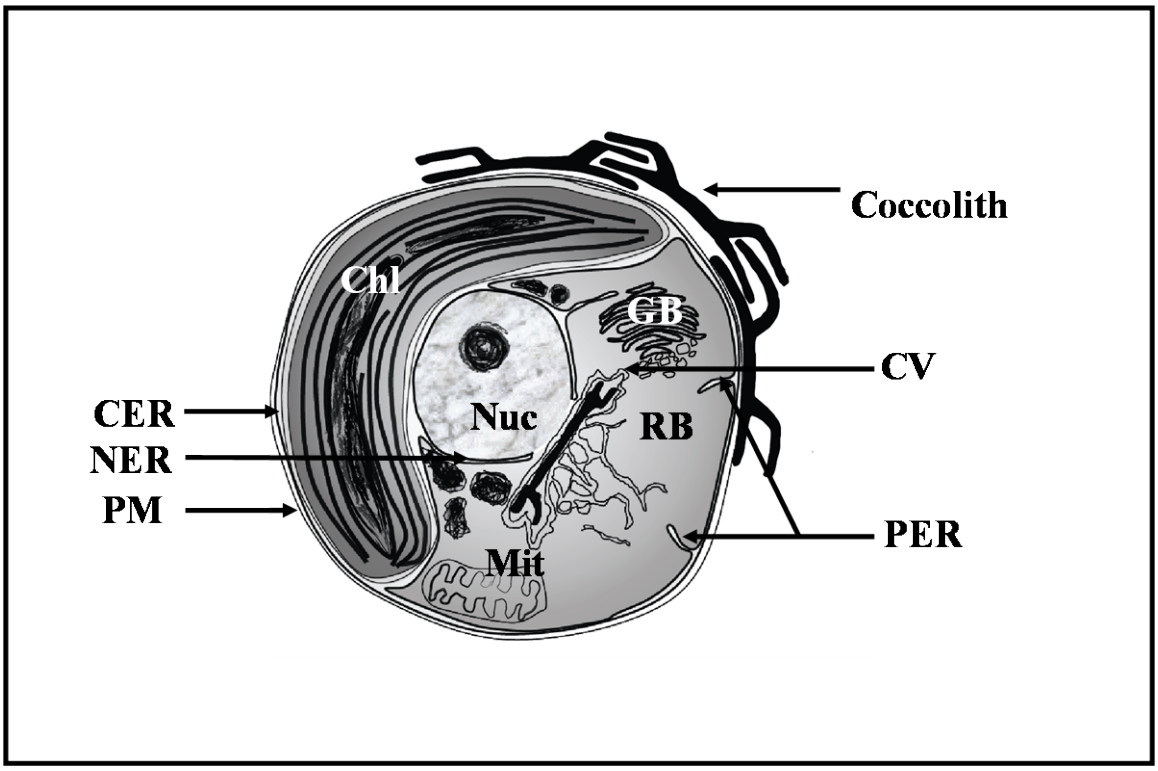

Figure 1.1. Schematic representation of the internal structure of a coccolithophore cell. Nuc, nucleus; Chl, chloroplast; PM, plasma membrane; Mit, mitochondria; GB, Golgi Body; RB, reticular body; CV, coccolith vesicle; CER, chloroplast endoplasmic reticulum; PER, peripheral endoplasmic reticulum; NER, nuclear endoplasmic reticulum. Modified from Brownlee and Taylor (2004).

Comprising a great genetic and morphological diversity - around 280 morphologically defined coccospheres described by Young et al. (2003) - coccolithophores are widely distributed around all oceans, also displaying various life strategies. The cosmopolitan *Emiliania huxleyi* is a fast growing species of reduced size (coccolith distal shield length ~ 3 to 6 μm), capable of forming extensive blooms, and hence described as an r-strategist. It is the only member of the Isochrysidales known to lack a life cycle stage producing holococcoliths (De Vargas and Probert, 2004).

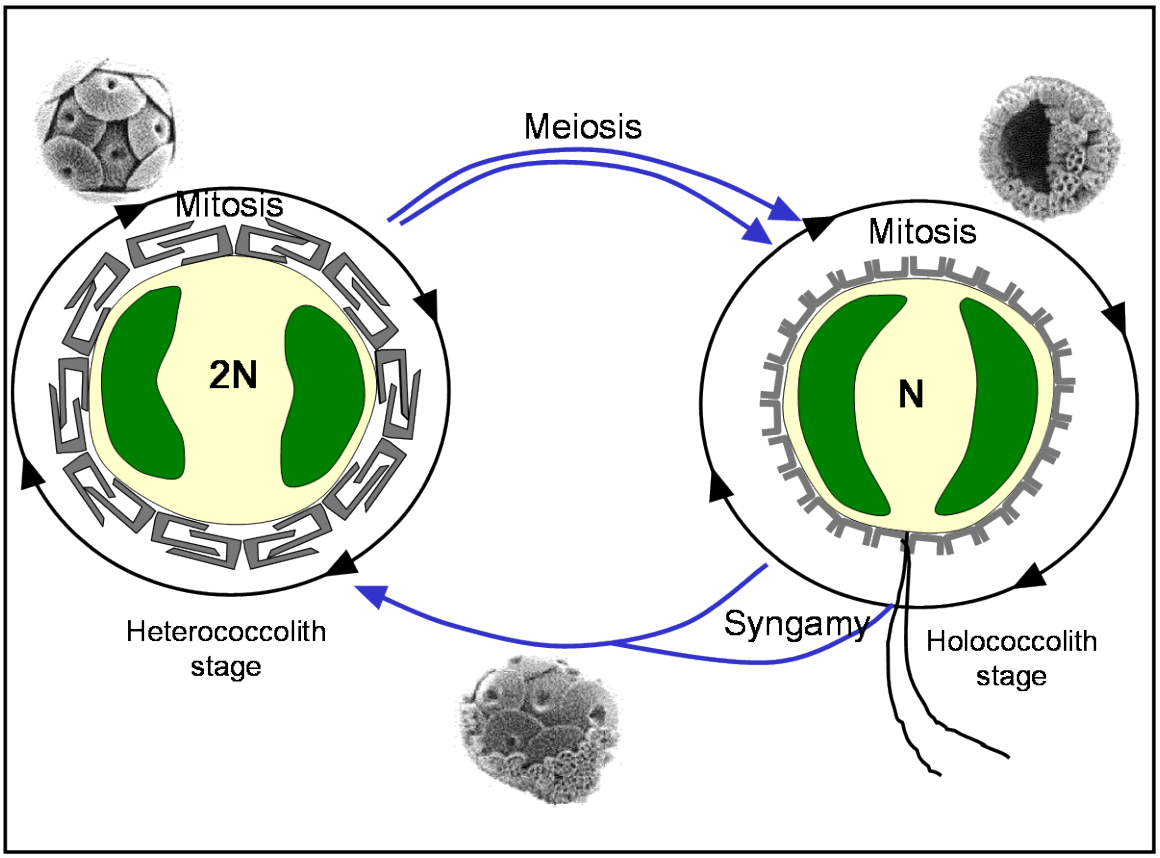

Figure 1.2. Schematic representation of a coccolithophore life-cycle. The diploid stage produces heterococcoliths intracellularly, while the motile haploid stage produces holococcoliths extracellularly (outside the cell membrane). The combination coccosphere, bearing both holococcoliths and heterococcoliths, would be the result of syngamy between two haploid gametes. Modified from Geisen et al. (2002).

Even though not typical of most coccolithophores, its ability to grow well in culture has meant that until recently, research was almost exclusively done on this species, and results extrapolated to others. Today, we know that coccolithophores exhibit very diverse life strategies, growth rates and calcification strategies, with species-specific (Langer et al., 2006) and even strain-specific (Langer et al., 2009) responses to ocean chemistry. Larger, slow growing species such as *Calcidiscus leptoporus*, and the subspecies *Coccolithus pelagicus* ssp. *pelagicus* and *Coccolithus pelagicus* ssp. *braarudii*, are examples of species with life cycle approaches tending to a k-selected strategy (Margalef, 1978).

1.1.2 Biomineralization and crystallography

Biomineralization refers to the process by which organisms form minerals (Lowenstam and Weiner, 1989; Weiner and Dove, 2003). Until the early 1980s, the

field was known as “calcification”, reflecting the predominance of biologically formed calcium-containing minerals. Calcium carbonate minerals are the most abundant biogenic minerals, both in terms of the quantities produced and their widespread distribution among many different taxa (Lowenstam and Weiner, 1989). As more and more biogenic minerals were discovered that contained other cations, the field became known as biomineralization (Weiner and Dove, 2003). Today, biologists, and especially palaeontologists, depend upon the products of the biomineralization process for identification and classification of coccolithophores (Young et al., 2004).

Coccolithogenesis, the process of coccolith formation, is a distinctive mode of biomineralization -unusual among eukaryotes as it occurs intracellularly (Figure 1.2) (De Vargas et al., 2007). The systematic presence of heterococcoliths from the Triassic Norian, ~ 205 million years ago (Ma) to the present, points to a stable pattern of biomineralization over ~ 225 million years, and therefore most likely a single evolutionary origin (Young et al., 1992b). However, the presence of non-calcifying taxa among coccolithophores suggests that some biochemical pathways involved in coccolithogenesis might have shut down and reactivated several times in the course of their evolution (De Vargas and Probert, 2004). De Vargas et al. (2007) hypothesised a reinvention of coccolithogenesis in the form of holococcoliths in the Jurassic Pliensbachian, ~ 185 Ma, from the already present heterococcoliths, some 23 million years before, during early Triassic, pointing to multiple origins of coccolithogenesis.

Heterococcolith formation consists of nucleation and crystal growth (Young et al., 1992a). A proto-coccolith ring of calcite is formed by nucleation intracellularly in vesicles derived from the Golgi body (Young et al., 1992a; Young and Henriksen, 2003). Crystal growth then takes place, with the formation of initially simple crystals closely regulated, deriving into complex genus-characteristic ultrastructures (Young et al., 1992a). After the completion of the coccolith, the vesicle dilates, and a dense organic coating becomes visible around and between coccolith crystals (Young and Henriksen, 2003). Coccolith calcite crystallography consists of two unit types, one with approximately vertically oriented C-axes (V units), the other with approximately radially oriented C-axes (R units) (Young and Bown, 1991), termed

the V/R model, which provides a powerful tool for phylogenetic characterization (Figure 1.3) (Young et al., 1992a).

Coccoliths represent an example of highly regulated biomineralization at a very small scale and, as in all biomineralization systems, the interplay between organic and inorganic components is the key to advanced crystal regulation (Henriksen et al., 2004a; Young et al., 2004). From an ecological point of view, their high calcite yield means that coccolithophore biomineralization plays a major role in controlling the alkalinity and carbonate chemistry of the photic zone (De Vargas et al., 2007). Coccolithophore biomineralization was originally selected in a high CO_2, low pH environment, where aragonite would most likely be precipitated, most likely due to the high open ocean, and which conditions may resemble those by the years 2100, on a business as usual scenario (De Vargas et al., 2007; Ridgwell and Zeebe, 2005).

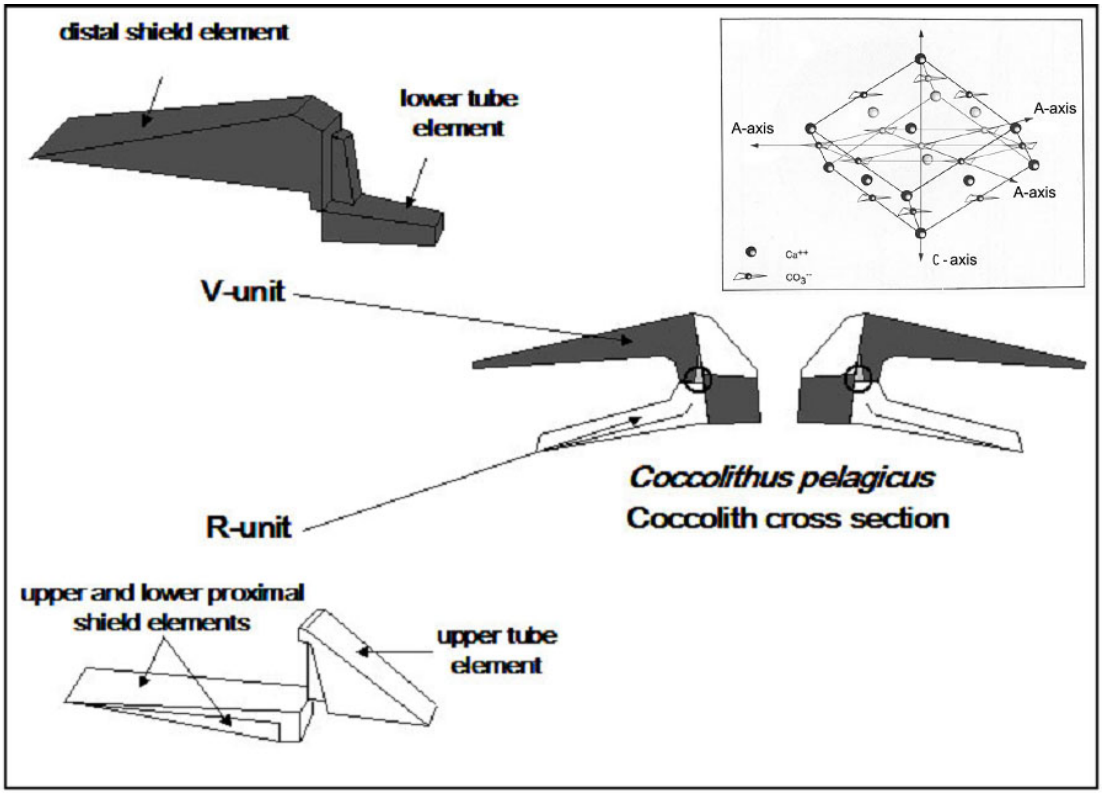

Figure 1.3. V/R model interpretation of *Coccolithus pelagicus* structure and coccolith cross-section with V (white) and R-unit (grey). Note location of protococcolith ring (circle). Inlet: Schematic representation of the atomic structure of a calcite crystal and its crystallographic axes. Modified from Young (1992).

1.1.3 Stratigraphy and evolution

Calcareous coccolithophores play a vital role at a biological level, as much as at a geological level. After death, coccoliths accumulate to form the largest single component of carbonate ooze sediment (Young et al., 1999). The term “calcareous nannofossil” is usually defined as including all calcareous fossils smaller than 30 µm (Bown and Young, 1998).The consistent and widespread presence of calcareous nannofossils in the stratigraphic record not only has assisted in the detailed research of their evolution, biodiversity and geographic distribution, but they have also served as proxies for past climate and carbonate budget reconstructions. Biases can occur, however, caused by dissolution in the upper part of the water column, leading to the loss of up to 70% of diversity from the recent fossil record (De Vargas et al., 2007). Sedimentation rates and consequent stratigraphical resolution can also influence biodiversity reconstructions outcomes. Therefore, special considerations need to be taken when studying coccolithophorid in the fossil record (Young et al., 2005).

Coccolithophores (most specifically coccoliths) first appeared in the fossil record in Upper Triassic sediments (~ 225 Ma) (Bown et al., 2004). This appearance does not necessarily confirms the biological origins of the coccolithophore lineage, because this lineage also contains non-calcifying haptophytes (De Vargas and Probert, 2004). The group diversified extensively during the Mesozoic, despite episodes of extinction at the Triassic/Jurassic boundary, declining dramatically at the Cretaceous/Tertiary (K/T) boundary, and again experiencing a rapid rise during the Cenozoic, with a peak in the early Palaeogene and a minimum during Oligocene (Aubry, 2007; Baumann and Freitag, 2004; Bown, 2005; Bown et al., 2004). The Neogene witnessed a diversity increase during the Miocene and decline during the Pliocene and Pleistocene, most likely due to climate shifts (Bown, 2005).

The evolution of nannoplankton resulted in a major shift in the locus of global calcification from the continental shelves toward deep oceans, with accompanying effects on deep-ocean CO_2 budgets, calcite compensation depths (CCD) and geological carbonate turnover rates (Bown and Young, 1998).

1.2 Ocean system

1.2.1 Carbonate system and calcium carbonate sedimentation

Current geochemical models estimate that the atmosphere exchanges about one third to one fifth of its total CO_2 every year with terrestrial and oceanic reservoirs. During glacial periods, the ocean served as a storage for atmospheric CO_2, while during glacial-interglacial transitions, it acted as a source of CO_2 to the atmosphere (e.g. Archer et al., 2000; Brovkin et al., 2012; Raven and Falkowski, 1999; Sigman and Boyle, 2000).

It has now been revealed that phytoplankton do not utilise major elements, including carbon, at a fixed ratio, as previously thought (see Redfield et al., 1963) and that construction of carbon budgets and biogeochemical cycles cannot be modelled on such simplification (Boyd and Trull, 2007). Together with planktonic foraminifera (Schiebel, 2002), which became prominent in the Middle Cretaceous (~ 100 Ma), and pteropods (e.g. Sarmiento et al., 2002), coccolithophores are mainly responsible for creating and maintaining the ocean's vertical gradient in seawater alkalinity (Rost and Riebesell, 2004). CO_2 is absorbed in the upper mixed layer, reacting with water to form carbonic acid (H_2CO_3), which in turn breaks up to form bicarbonate (HCO_3^-) and carbonate ions (CO_3^{2-}), used by primary producers such as coccolithophores. This process results in organic material, some of which will resurface through upwelling, in a process called remineralisation, and some will sink to the ocean floor and contribute to sedimentation. This CO_2 net drawdown is known as the Organic Carbon Pump and operates in a time scale of over 100.000 years. In contrast, the biogenic production and export of calcium carbonate has the opposite effect on air/sea CO_2 exchange, causing a net release of CO_2 to the atmosphere, referred as the Carbonate Counter Pump (Rost and Riebesell, 2004). Current production of $CaCO_3$ in the world ocean is calculated to be ~ 5 billion tonnes per year (bt y^{-1}), of which 3 bt y^{-1} (60 %) accumulates in the sediment, while the rest is dissolved (Milliman, 1993). The consequent $CaCO_3$ sedimentation in the ocean represents the largest carbon sink in the combined atmosphere, biosphere, and ocean system, and thus strongly influences the global carbon cycle (Griffith et al., 2008).

1.2.2 Anthropogenic changes: Ocean acidification

One of the most far-reaching perturbations of the environment since the beginning of the industrial period has been the increased emission of anthropogenic CO_2 into the atmosphere as a result of fossil-fuel burning and the consequent absorption of CO_2 into the ocean, making the second largest sink for anthropogenic carbon dioxide after the atmosphere itself (Riebesell et al., 2007; Pelejero et al., 2010; Honisch et al., 2012).While the past 400,000 years have experienced a rather stable concentration of atmospheric CO_2 -between 200 and 280 part per million (ppm) - current CO_2 levels are now reaching 380 ppm (Feely et al., 2004). Moreover, present-day CO_2 levels are unprecedented for at least the past 800,000 years (Siegenthaler et al., 2005), with the Southern Ocean as some of the most important areas of uptake, with apparent glacial/interglacial oscillations (reduced uptake during ice ages) (Sigman et al., 2010). In 2008, the total human CO_2 emissions were estimated at ~ 10 bt y^{-1} of carbon (Gruber et al., 2009). In a business as usual scenario, atmospheric CO_2 levels are predicted to increase, potentially reaching levels exceeding 1000 ppm by 2100, higher that anything experienced on Earth for several millions of years (The Royal Society, 2005).

In a normal scenario, as discussed, atmosphericCO_2 is absorbed by the ocean surface (CO_2 (aq)), and reacts with water to produce H_2CO_3, which in turn forms HCO_3^- and consumes carbonate ions CO_3^{2-}, with both reactions releasing hydrogen ions (H^+) (Figure 1.4). All the dissolved inorganic species of carbon - CO_2 (aq), HCO_3^-, CO_3^{2-} - combine to form dissolve inorganic carbon, or DIC. Seawater pH controls the relative proportion of carbonate species while the concentration of DIC remains constant (Iglesias-Rodriguez et al., 2008). In the current scenario, increased CO_2 absorption by the ocean is driving a chemical change in the carbonate species composition of seawater and DIC concentration, where a decrease of carbonate ions causes a shift in the ocean pH. Oceanic absorption of CO_2 from fossil fuels usage

thus may result in larger pH changes over the next several centuries than any inferred from the geological record of the past 300 million years (Caldeira and Wickett, 2003).

Critically, present Ca^{2+} concentrations ([Ca^{2+}]) in the ocean are at their lowest level in more than half-billion years. This, combined with a reduction of CO_3^{2-}, will produce an exceptionally low saturation state for seawater with respect $CaCO_3$ (Stanley, 2008), consequently reducing the availability of the prominent forms of $CaCO_3$, such as calcite and aragonite. This large-scale decrease in the calcite and aragonite saturation over the global ocean could have a profound effect on calcification rates of $CaCO_3$ shell-forming species (Feely et al., 2004).

The magnesium/calcium ratio (Mg/Ca) is another player in the mechanism of biomineralization. Coccolithophores usually precipitate calcium carbonate under low Mg/Ca ratio, producing low Mg-calcite. Coccolithophores' production of vast chalk deposits in the Late Cretaceous has therefore been attributed to the low Mg/Ca ratio and high [Ca^{2+}] in ambient seawater (~ 5.2) (see also Ries, 2005). Stanley (2006) claimed that the high Mg/Ca ratio and low [Ca^{2+}] of modern ocean can limit population growth for the large majority of coccolithophores today, while Stanley et al. (2005) found that Cretaceous Mg/Ca ratios (~ 1) did lead to higher growth rates.

However, Muller et al. (2011) found a decrease in the growth rates of *E. huxleyi* and *C. braarudii* at Mg/Ca ratio of ~ 2, the latter species showing less sensitivity. This can further point to an inter-specific physiological plasticity and response among coccolithophores to variations in element composition of seawater. This is particularly relevant when studying species of diverse ancestral background (Muller et al., 2011).

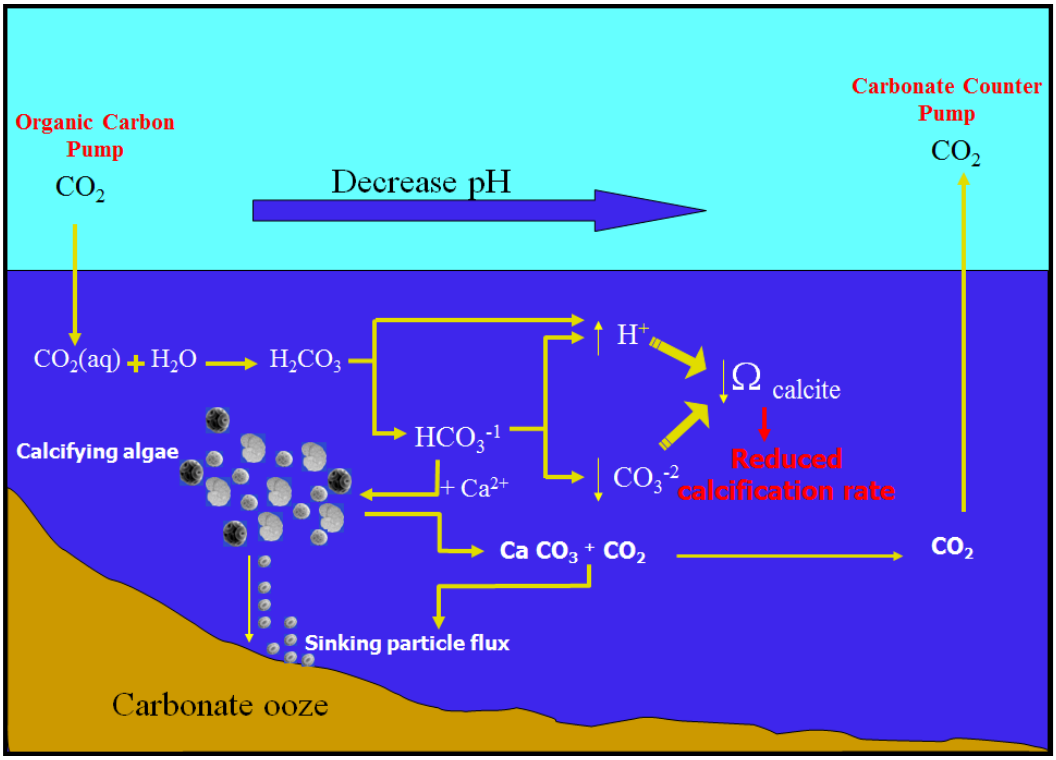

Figure 1.4. Diagram illustrating the ocean carbonate system, the role played by coccolithophores and the effect of ocean acidification. Equations are schematic and not at equilibrium. Atmospheric CO_2 (CO_2) is absorbed in the ocean, producing a net drawdown of CO_2 (Organic Carbon Pump). Part will be used for biogenic $CaCO_3$ causing a release of CO_2 to the atmosphere (Carbonate Counter Pump). Increased CO_2 intake into the ocean ultimately will cause a decrease in the saturation state with respect to Calcite (Ω_{cal}). See text for more details.

1.3 Background to this study

Ocean acidification and hence the shift in the saturation state of the oceans with respect to calcium carbonate ($CaCO_3$) (Feely et al., 2004), means a decrease in its availability to calcifying organisms, particularly in the form of calcite and aragonite. Research has already shown decreased calcification in some corals (Langdon and Atkinson, 2005; Tribollet et al., 2009), coccolithophores (Riebesell et al., 2000; Delille et al., 2005) and foraminifera (Moy et al., 2009; Dissard et al., 2010). Work by Moy et al. (2009) on planktonic foraminifera from a sediment core in the Southern Ocean indicated a tight relationship between changes in shell weight and glacial-interglacial episodes, as well as reduction in shell weight from the Holocene to present. More recently, Lohbeck et al. (2012) found adaptive responses to high CO_2 in *E. huxleyi*, in long term laboratory experiments (500 generations). These findings raise questions about the past, current and future calcification state of

other organisms, particularly coccolithophores, since this group represents a wide genetic variability and species diversity.

Further investigation in long-term coccolithophore calcification strategies is needed to understand past and present responses to shifts in ocean chemistry and implications for the carbon cycle.

1.4 Study Area

Two sediment cores from the South West Pacific sector of the Southern Ocean (Moy et al., 2006) were used for the paleontological survey. Piston Core MD972106 (45^{o} 09'S, 146^{o} 16'E, 3310 m water depth), was located North of the Subtropical Front (STF), in the South Tasman Rise (STR). Core-top of gravity Core GC07 (45^{o} 09'S, 146^{o} 17'E, 2334 m water depth) was also used in this study, as the location of the core in the northeast slope of the rise may provide protection from the east flowing currents, allowing for the preservation of younger sediments in the region (Findlay and Flores, 2000). Both cores were located North of the STF, as recognized by Belkin and Gordon (1996) (Figure 1.6). The average sedimentation rate of the cores was ~ 9.3 cm kyr^{-1} (Moy et al., 2006). These cores were selected for their position above the calcite saturation horizon, which is located at 4030 m depth. This ensured that despite intensification of the Antarctic Circumpolar Current (ACC) in this area, a potential cause for corrosion, the species of interest are less likely to be affected by dissolution than if they had been deposited at or below the calcite saturation horizon.

Additionally, eleven sediment trap samples were included in this study (46^{o} 49'S, 141^{o} 38'E, 2000 m depth), collected from the South East Indian Basin, south of the STF, from September 2003 to February 2004, as part of the SAZ (Subantarctic Zone) project. Strains from the coast of Tasmania were isolated and included in this study.

1.5 Regional oceanography

The Southern Ocean is now understood to play a critical role in the overturning circulation and large scale budgets of heat, carbon and freshwater (Rintoul, 2008). Its diversity in regional hydrographic conditions, coupled with extreme seasonality, results in spatial and temporal variability in the abundance of biological productivity (Mohan et al., 2011). During the past two decades, comprehensive data have been gathered to establish front locations and water masses associated with the Antarctic Circumpolar Current (ACC) (Figure 1.5). New technologies allowed circumpolar coverage of sea surface height (SSH) and sea surface temperature (SST) which has made it clear that the frontal structure of the ACC is more complex than once thought (Sokolov and Rintoul, 2009a). The result is a series of conspicuous fronts determining a stepwise transition from warm, salty, low nutrient water, to cooler, fresher, nutrient-rich polar water (Rintoul and Trull, 2001). Each front is circumpolar in extent and extends from the sea surface to the seafloor (Rintoul and Bullister, 1999), rarely crossing regions shallower than 2000 m (Sokolov and Rintoul, 2009b).

From North to South, the fronts are known as the Subtropical Front (STF), which is located in a bathymetric “saddle” of the STR, the Subantarctic Front (SAF), the Polar Front (PF), and the Southern Boundary (SB) of the ACC. The zone between the Southern part of the Australian continent and the STF is the Subtropical Zone (STZ), between the STF and the SAF lays the Subantarctic Zone (SAZ), and between the SAF and the PF lays the Polar Frontal Zone (PFZ). The zone between the PF and the SB of the ACC is known as the Antarctic zone (Figure 1.5).

Many of the major ACC fronts consist of multiple branches or filaments, which merge and diverge along the circumpolar path (Sokolov and Rintoul, 2007a). This is particularly important when interpreting data from sediment traps, collected along a relatively long time span (one year, in fortnightly intervals) at several different depths.

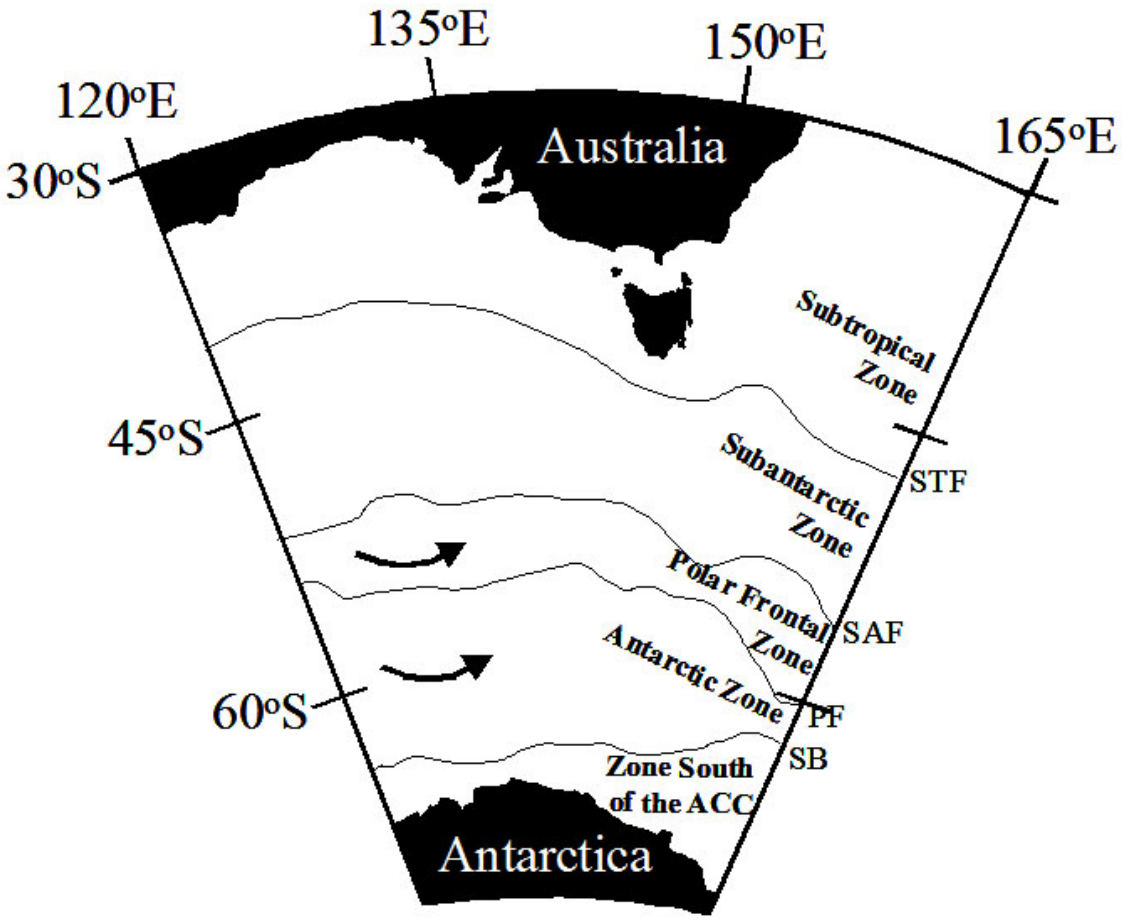

Figure 1.5. Location of Southern Ocean fronts and water masses. ACC = Antarctic Circumpolar Current, STF = Subtropical Front, SAF = Subantarctic Front, PF = Polar Front and SB = Southern Boundary of the ACC. Arrows indicate ACC easterly flow. Modified from Moy et al. (2006); front locations from Orsi et al. (1995).

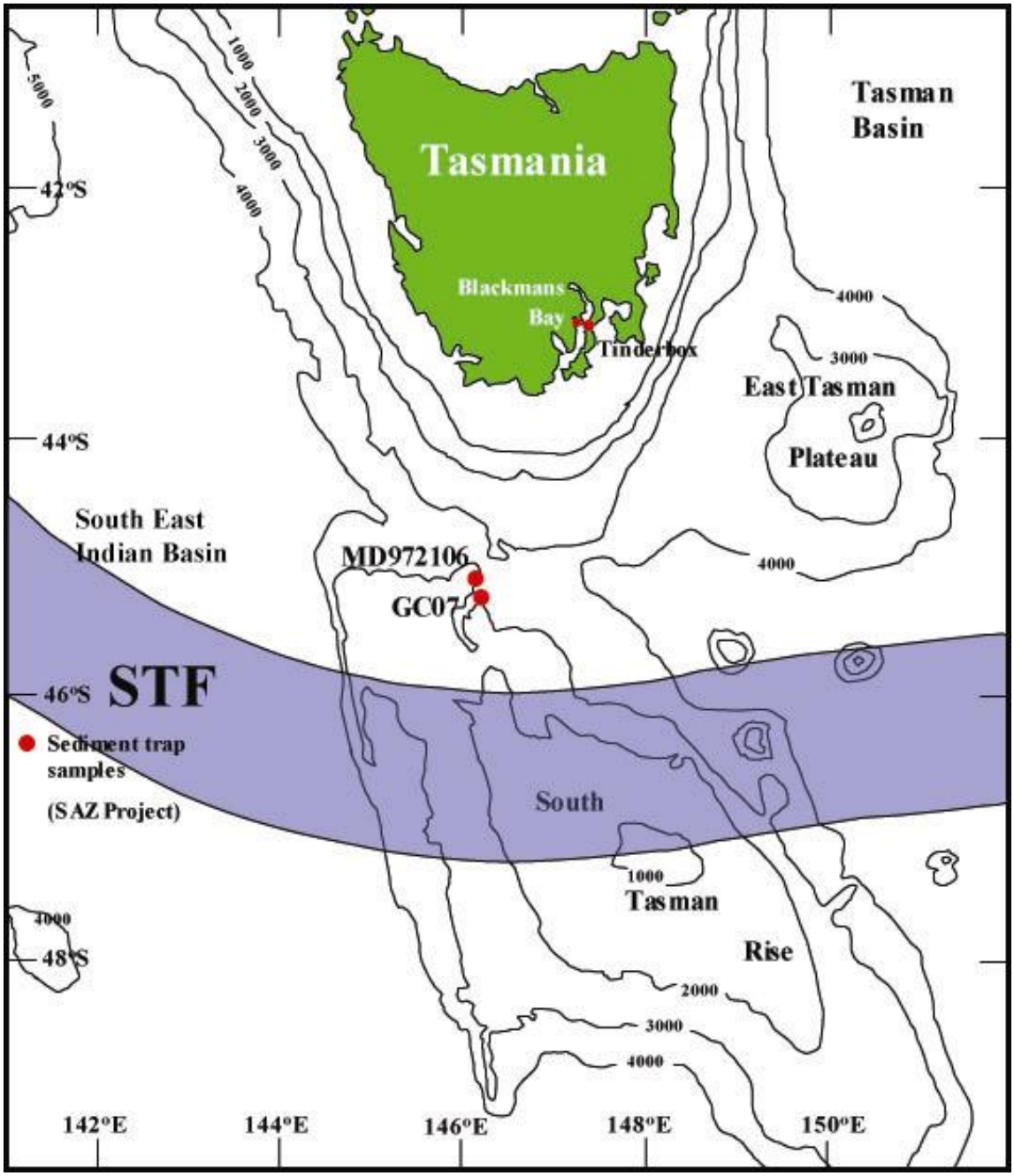

Figure 1.6. Biometry of the study area and location of all samples used in this study. Core MD972106 (3310 m), core GC07 (2334 m), sediment trap samples (2000 m), and culture material collected from Tasmanian coastal water at Blackmans Bay and Tinderbox. Modified from Findlay and Giraudeau (2002); front locations from Belkin and Gordon (1996).

Table 1.1. Description of all sampling material used in this study.

Sample material	Location	Latitude /longitude	Water depth at collection site (m)
Sediment traps	South Tasman Rise	46° 49'S, 141°38'E	2000 m
Core MD972106	South Tasman Rise	45° 09'S, 146° 16'E	3310 m
Core GC07	South Tasman Rise	46°09'S, 146°17'E	3307 m
Culture CPBMB02	Blackmans Bay	43° 00'S, 147° 20'E	Surface
Culture CPTX01	Tinderbox	43° 02'S, 147° 20'E	Surface

1.6 Coccolithophores in the Southern Ocean

1.6.1 Physiological considerations

Distributions of primary production, macronutrients and iron are not uniform in the Southern Ocean (Sokolov and Rintoul, 2007b). Within these frontal systems, relatively uniform water mass properties occur (Rintoul and Trull, 2001), with distinctive biological communities within these zones, with similar seasonal succession. South of the STF, the SAZ is characterized by a deep winter mixed layer, low silicic acid concentration and a phytoplankton community dominated by coccolithophores (Sokolov and Rintoul, 2007b). Silicate, nitrate and phosphate concentrations increase with latitude and with depth from the STZ to the PFZ (Cassar et al., 2011). This all year round pattern, associated with less seasonal variability in mixed layer depth south of the PF, allows for a diatom dominated phytoplankton (Sokolov and Rintoul, 2007b).

More recently, Moderate Resolution Imaging Spectroradiometer (MODIS) identified elevated PIC concentrations near the SAF and the PF (Balch et al., 2011). These authors identified this circumpolar feature as the "Great Calcite Belt", running from ~ 30°S to ~ 60°S, and were able, at least partially, to associate it with high concentrations of loose coccoliths in this area.

Nishida (1986), one of the first authors to document the diversity of extant coccolithophores in this area of the Southern Ocean, found the dominant species to be *Emiliania huxleyi* across the ACC frontal zones, followed by *Gephyrocapsa*

ericsoni, although the latter was most abundant north of the STF, identified at 47°S. Other common species were *Calcidiscus leptoporus*, *Syracosphera hystrica* and *Caneosphera molischii*. Findlay and Giraudeau (2000) found that diversity of coccolithophores decreased with increased latitude, and again was dominated by *E. huxleyi*. They identified three morphotypes of this species, a highly calcified (type A), a less calcified (type C) and another morphotype (type D), which they believed was the result of dissolution. Among other species they recognized *G. oceanica* as subdominant species and *C. leptoporus* and *Umbellosphaera tenuis* as subordinate species. Mohan et al. (2008) confirmed this poleward decrease in diversity in the area south of Madagascar, where *E. huxleyi* was also dominant, which he discriminated into types A and B/C. Findlay and Giraudeau (2000) and Nishida (1986) declared this *E. huxleyi*, more specifically type (B/C), to be sparse or absent south of 60°S. However, Cubillos et al. (2007) consistently found this morphotype at a concentration of ~ 100 cells ml^{-1} between 60 and 65°S. These authors also found that *E. huxleyi* type A rarely occurred past the northern boundary of the PF, with some exceptions (early summer 2002-03, spring 2004). More recently, Cook et al. (2011), scrutinising chloroplast pigments and photosynthetic performance of Southern Ocean strains of type A and type B/C, found enough morphological and genetic differentiation to describe type B/C as *E. huxleyi* var. *aurorae* S.S. Cook et Hallegr. A correlation between *E. huxleyi* type A and sea surface temperatures (SST) was demonstrated by Hiramatsu and De Deckker (1996) in the same area. The tight relationship between coccolithophores and their environment points to a potentially rapid change in the environmental conditions of the Southern Ocean, associated with temperature and salinity, which may imply a change in the carbonate system.

E. huxleyi (Family Noëlaerhabdaceae) is the most abundant and ubiquitous coccolithophores species, and although its ability to grow in culture has allowed extensive research on this taxon, we now know that extrapolating results to most other families of this group is inadequate and misleading (Langer et al., 2006; 2009). *E. huxleyi* is a species of small cell size, fast growth rate, and with the ability to form blooms, which, with a few exceptions (Tyrrell and Merico, 2004), is considered to be exclusive not only to this taxon, but also confined to the morphotype A.

In terms of calcite production, research has shown that species abundance is not

necessarily proportional to carbonate estimates. Baumann (2004) studied moored sediment trap samples off the North-West coast of Africa, and found a high discrepancy between numerical coccolith flux and coccolith carbonate mass flux, where small coccoliths of *E. huxleyi*, *F. profunda and G. ericsonii* accounted for 60% of the assemblage, while their mass flux only reached a maximum of 25%. In regards to larger species, these authors found that their mass flux was 5 to 10 times higher than numerical coccolith flux. Similar results were found by Sarmiento et al. (2002) who found that non-blooming coccolithophores, pteropods and foraminifera have a greater contribution to the calcite budget than previously thought. This calls for a better understanding of the response of larger species to changes in their environments.

1.6.2 Evolution of Coccolithophores

The long geological history of coccolithophore evolution accounts for its considerable morphological plasticity, with new species evolving throughout the Mesozoic and the Cenozoic, under various atmospheric and oceanic conditions. *E. huxleyi* is a relatively new species, having evolved only ~ 273 ka ago, during the Pleistocene when atmospheric CO_2 fluctuated between 294 and 330 ppmv (De Vargas et al., 2007). In contrast, *C. pelagicus* (Family Coccolithaceae) evolved during the Paleocene, ~ 63 Ma, when levels of atmospheric CO_2 were ~ 480-800 ppmv (De Vargas et al., 2007). One could then argue that the physiological adaptations that prompted the evolution of the Coccolithaceae would therefore be very different from those of the Noëlaerhabdaceae. *E. huxleyi* has been widely recognized for its vulnerability to changes the carbonate systems, mostly in culture studies (Riebesell et al., 2000; 2008), affecting its ability to calcify and form complete and well-formed coccoliths, while *C. pelagicus* has been observed to be insensitive to changes in carbonate chemistry (Langer et al., 2006). Additionally, these authors found that another heavily calcified species, *C. leptoporus*, was highly affected by these changes in carbonate chemistry, highlighting the importance of species-specific observations. From an evolutionary perspective, *C. leptoporus* evolved during the Miocene (~ 23 Ma), when atmospheric CO_2 levels fluctuated between ~ 260 and ~ 500 ppm, closer to contemporary levels. Henderiks and Rickaby (2007) proposed that extant species with an older genetic profile, having

evolved in a high CO_2 world, such as *C. pelagicus*, may have an "evolutionary memory", which enables them to cope with high variability of atmospheric CO_2 concentrations, making them insensitive to high CO_2, while at the same time able to calcify normally under low levels of CO_2. In contrast, species having evolved in a low CO_2 are adaptive to variability of CO_2 during glacial-interglacial times. Even though these authors advice caution at the notion of this evolutionary memory as a tools for constraining past atmospheric CO_2 estimates, the potentially different adaptive responses of various species (e.g. Langer et al., 2006; Lohbeck et al., 2012) call upon studies of calcification in selected coccolithophores at geological scales.

Geological observations are subject, however, to factors such as core resolution, dissolution and reworking. In order to understand intrinsic variability to short-term changes in ocean chemistry, resolution of seasonal observations might therefore be helpful.

1.6.3 Taxonomical notes

This thesis explores the taxonomy of genus *Coccolithus*, although treating *Coccolithus* spp. as a whole for the purpose of the method development. Therefore we initially refer to the species as *Coccolithus pelagicus* (*sensu lato*) in Chapter 2. We later refer to each subspecies in Chapter 3, unless not specified by the literature. Finally, we refer to the species found to be extant in the Southern Ocean in Chapter 4 and 5. These taxonomical notes are detailed throughout this thesis.

1.7 Significance, aims and thesis structure

The purpose of this thesis is to contribute to the understanding of calcification strategies of *C. pelagicus* ssp. *braarudii* in the Southern Ocean. This species is of interest due to its apparent insensitivity to high levels of CO_2 in laboratory experiments (Langer et al., 2006).

Several techniques have been used to assess calcification of individual coccoliths. The method used in this project is the estimation of coccolith weight by birefringence (Beaufort, 2005), based on the conversion of coccolith grey levels

under cross-polarised light, into picograms per pixel of calcite, through a previously calibrated transfer function. This method has been modified to suit the large partially non-birefringent coccolith of this Southern Ocean taxon.

We also scrutinised the genotypic and taxonomic description of *Coccolithus pelagicus* ssp. *braarudii*, which has previously been claimed to be absent south of the STF (~ 47^{o}S). Coccospheres found off the Tasmanian coast thus were dismissed as present via transport from upwelling regions southwest of South Australia and/or ballast water translocation (Findlay and Giraudeau, 2000).

Finally, both long-term and seasonal variations in calcification and morphology are examined, in order to understand environmental factors that influence biomineralization in the Southern Ocean.

1.7.1 Thesis aims

This thesis aims to:

1.- Present an adapted methodology of coccolith weight estimate by birefringence, suitable to larger, partially non-birefringent coccoliths-bearing species.

2.- Describe the *Coccolithus* morphotype currently present on the Australian area of the Southern Ocean, its taxonomical features, and current location.

3.- Study seasonal variations in coccolith weight and coccolith size (coccolith allometric characteristics) and in response to environmental parameters, in order to understand the factors causing these morphological variations.

4.- Compare between degrees of calcification of coccoliths (coccolith weight, volume and thickness) and calcification strategies (morphometry) from the late Quaternary with those from sediment trap samples, representing their current calcifying status.

1.7.2 Thesis structure

Chapter One, “General Introduction” provides a general background on

coccolithophores biology, life strategies, evolution, as well as some taxonomical facts, also stressing their importance as fossil material and proxies for environmental and stratigraphic studies. It describes their process of biomineralization and general crystallographic arrangement, and their role in to the carbon, calcium and magnesium cycle and as well as possible responses to ocean acidification.

Chapter Two, "Reconstructing calcification in ancient coccolithophores: Individual weight and morphology of *Coccolithus pelagicus* (*sensu lato*)" explains in detail the method used in the bulk of the thesis. This is an adaptation of the existing method of estimate weight by birefringence (Beaufort, 2005), developed to calculate the weight of individual coccolith. This chapter describes the application of this method to larger partially non-birefringent species such as *C. pelagicus* (*s.l*), previously considered unsuitable for this method. We acknowledge potential errors within the method, but also stress the benefits by providing a consistent tool across diverse sampling materials. Combined with morphometric analysis, it can be used as a proxy for depicting coccolith weight variation in response to changes in the ocean carbonate state.

Chapter Three, "Morphotaxonomy of *Coccolithus* spp. from the Southern Ocean, South of Tasmania" reviews the geographical presence of *C. pelagicus* ssp. *pelagicus* and *C. pelagicus* ssp. *braarudii* at a global level, from field samples to the stratigraphic record. This is followed by a detailed examination and description of the morphology of *Coccolithus* in the Southern Ocean, by exploring coccolith morphometry and estimating other parameters such as coccosphere size and cell concentration, in order to verify the existence of only one morphotype in the area of the South Tasman Rise.

Chapter Four, "Seasonal variability in calcification and abundance of the coccolithophore *Coccolithus braarudii* [(Gaarder, 1962) Baumann et al., 2003] in the Subantarctic Zone (SAZ) of the Southern Ocean, South of Tasmania" looks at seasonal variations in the morphology of *C. pelagicus* ssp. *braarudii*, from sediment trap samples from September 2003 to February 2004, and the short term relationship between morphological patterns of calcification and environmental parameters. Quantitative analysis was also conducted to assess flux variability during this period

of time.

Chapter Five, "*Coccolithus braarudii* [(Gaarder, 1962) Baumann et al., 2003] during the late Quaternary: Calcification patterns from the Last Glacial Maximum to the present" looks at changes in coccolith weight of *C. pelagicus* ssp. *braarudii*, in response to the environmental conditions of the Last Glacial Maximum (LGM), deglaciation, the Holocene and the present. It examines allometric relationships between weight and morphometrical dimensions, in response to environmental factors and ocean chemistry.

Chapter Six, "General conclusions" draws overall conclusions and outlines future research.

Chapter 2 Reconstructing calcification in ancient coccolithophores: Individual weight and morphology of *Coccolithus pelagicus* (*sensu lato*)

Joana C. Cubillos

Institute for Marine and Antarctic Studies (IMAS), Hobart, Tasmania 7001, Australia

Jorijntje Henderiks

Dept. of Earth Sciences, Palaeobiology, Uppsala University, Villavägen 16, SE-752 36 Uppsala, Sweden.

Centre for Ecological and Evolutionary Synthesis, Department of Biology, University of Oslo, PO Box 1066 Blindern, N-0316 Oslo, Norway.

Luc Beaufort

CEREGE, CNRS UMR 6635, BP80, 13545 Aix-en-Provence Cedex 04, France

William R. Howard

Office of the Chief Scientist, Department of Innovation, Industry, Science and Research, GPO Box 9839, Canberra, ACT, 2601, Australia

Gustaaf M. Hallegraeff

Institute for Marine and Antarctic Studies (IMAS), Hobart, Tasmania 7001, Australia

**Accepted for publication in Marine Micropaleontology on 23/4/2012*

This chapter has been removed for copyright or proprietary reasons.

Chapter 2

Reconstructing calcification in ancient coccolithophores: Individual weight and morphology of *Coccolithus pelagicus* (*sensu lato*)

Published in:

http://www.sciencedirect.com/science/article/pii/S0377839812000357

Reconstructing calcification in ancient coccolithophores: Individual weight and morphology of *Coccolithus pelagicus* (*sensu lato*). *Marine Micropaleontology.* Joana C. Cubillos, Jorijntne Henderiks, Luc Beaufort, William R. Howard, Gustaaf M. Hallegraeff. 2012. 92-93 p29-39.

Chapter 3 Morphotaxonomy of *Coccolithus* spp. from the Southern Ocean, South of Tasmania

Abstract

In order to confirm the distribution and taxonomical identity of the *Coccolithus* spp. in the Southern Ocean area south of the subtropical front (STF), near Tasmania, samples from three sources were collected. (1) Two strains were cultured from Southern Tasmanian onshore waters; (2) Holocene core-top material from Gravity core GC07 (~ 1.1 ka) was gathered from the South Tasman Rise (STR); and (3) sediment trap samples from the same area, available for spring-summer 2003-04, were examined. Morphometric analysis showed that the species present is *Coccolithus braarudii*, with no presence of *C. pelagicus* for at least the last 1160 years. Continuous sampling provided by the sediment trap samples also showed consistent presence of this species south of the STF from September 2003 to February 2004, with maximum coccolith and coccosphere fluxes of ~ 6.41 x 10^6 and 1.23 x 10^4 counts/m^2/day, respectively, in January 2004. Culture material indicated that this species is also present north of the STF, although some morphological features are not congruent with those of other sampling sources. We attribute this to malformation due to slow growth, which led to suboptimal culture conditions in later growth stages. This study helps clarify previous knowledge of this species, often claimed to be absent south of the STF, and provides evidence of a thriving, extant population during spring and summer in the Southern Ocean near Tasmania.

3.1 Introduction

3.1.1 Species varieties in the genus Coccolithus *Schwartz 1894*

Coccolithus Schwartz 1894 is a coccolithophore genus of the order Coccolithales (De Vargas et al., 2007), previously called order Coccosphaerales (Young et al., 2003), family Coccolithaceae Poche 1913 (Jordan and Kleijne, 1994) emend. Young and Bown 1997 (Jordan et al., 2004), which forms placolith-type coccoliths composed of two shields separated by a tube (Young et al., 2003). These large coccoliths (8-16 µm) are well preserved in the fossil material.

Although *Coccolithus pelagicus* (*sensu lato*) is recorded in fossil material since the Paleocene, this long fossil record is based on a very broad species concept (Geisen et al., 2004). Geisen et al. (2002) proposed that today this genus consists of two extant subspecies: *Coccolithus pelagicus* ssp. *pelagicus* (Wallich, 1877) Schiller, 1930 and *C. pelagicus* ssp. *braarudii* (Gaarder, 1962) Geisen et al., 2002. These exhibit overlapping geographical distributions (Saez et al., 2003), although *C. pelagicus* ssp. *pelagicus* is dominant in the Artic and sub-Artic regions and *C. pelagicus* ssp. *braarudii* dominates temperate and upwelling regions (e.g. Baumann et al., 2000; Geisen et al., 2002; Parente et al., 2004).

C. pelagicus ssp. *pelagicus* coccolith size ranges from 6 to 11 µm, whereas the larger *C. pelagicus* ssp. *braarudii* coccolith size ranges from 10 to16 µm. More recently, Parente et al. (2004) described a third morphotype, *C. pelagicus* ssp. *azorinus*, ranging in size from 14 to 16 µm, present around the Azores islands, relating its larger size to the intensification of the North Atlantic Oscillation, leading to a stronger Azores Current and Front. However, so far genetic evidence is only available for *C. pelagicus* ssp. *pelagicus* and C. *pelagicus* ssp. *braarudii* (De Vargas et al., 2007).

3.1.2 Taxonomical notes

In view of the genetic differences between the two main subspecies described above, and following the lead of other authors (e.g. Saez et al., 2003; De Vargas et al., 2007), for the remainder of this study, we will call them *C. pelagicus* and *C.*

braarudii when appropriate, and *Coccolithus* spp. to refer to the genus when the species has not been clarified.

3.1.3 Current global distribution

Extensive research has been done on the distribution and taxonomy of coccolithophores in the Northern Atlantic, Pacific and Indian Oceans. The Atlantic Ocean was studied in a broad seasonal survey by McIntyre and Bé (1967), who claimed that *C. pelagicus* was restricted to the Northern Hemisphere. Okada and McIntyre (1979) surveyed the Western North Atlantic Ocean, and found this species down to 100 m depth. Cachao and Moita (2000) found *C. braarudii* off the western coast of Iberia, an area known for seasonal coastal upwelling.

However, it is now well established that *C. pelagicus* is also present in the Southern Hemisphere (Figure 3.1). West of the Cape Peninsula (south-western South Africa) Mitchell-Innes and Winter (1987) reported a sparse population of this species. Hasle (1960) failed to find *C. pelagicus* in the Subantarctic and Equatorial Pacific. However, Mostajo (1985) observed it frequently in core-tops off the east coast of Argentina, suggesting a preference for cold water, and proposing the presence of an extant population in this area.

Presence of *C. pelagicus* has been found in the Pacific Ocean and western Pacific (Okada and Honjo, 1973, 1975). In the Tasman Sea, the presence of *C. pelagicus* has been documented off the Northern Island coast of New Zealand (Burns, 1975) and sparsely off western Tasmania (Hallegraeff, 1984) (Figure 3.2), as well as in South-East Tasmania, just north of the STF (Nishida, 1986). The latter author also found the motile form (haploid stage) throughout the water column in this area, with small numbers of loose heterococcoliths of the non-motile form (diploid stage) only in surface waters, mostly north of the STF. Note that the cited literature makes no specification on whether these forms are linked to *C. pelagicus* or *C. braarudii* and they failed to describe coccolith size and morphology. However, their description and illustrations match that of the larger *C. braarudii.*

Most areas where *C. braarudii* have been found are associated with upwelling. Giraudeau et al. (1993) reported *C. pelagicus* in the northern Benguela upwelling

system, and also found signs of malformation in this species offshore, which they attributed to possible bacterial effect as supposed to undersaturation of calcite. Giraudeau and Bailey (1995) associated high coccolithophore standing crops, including *C. pelagicus* -now identified as *C. braarudii*- to periods of active upwelling in the Southern Benguela region. Boeckel and Baumann (2004), looking at sediment samples from the south-eastern South Atlantic, found *C. pelagicus* associated with a highly fertile area of upwelling filamentous zone. More recently, Henderiks et al. (2012), observed *C. braarudii* during active coastal upwelling offshore Namibia, both in surface waters and at 50 m depth.

Verbeek (1989) found no trace of *C. pelagicus* south of Cape Town (~ 35 to 52^{o}S), and neither did Mohan et al. (2008) in the Indian Ocean, south of Madagascar. Findlay and Giraudeau (2000) found only one coccosphere of this species off Northwest Tasmania and proposed it was the result of upwelling from South Australia. They found no evidence to suggest an established presence south of the STF.

3.1.4 Depositional distribution in the Southern Ocean, south of Tasmania

Morphology of fossilisable organisms such as coccolithophores is a commonly used proxy for the study of evolutionary and potentially palaeoecological processes. Morphological change through time, however, can indicate either evolution, environmental change or, most likely, a combination of both (Bollmann, 1997).

Villa et al. (2005) found *C. pelagicus* as well as *C. braarudii* in late Quaternary sediment cores from the Weddell Sea, Bellingshausen Sea and the Maud Rise near the Antarctic Peninsula. Flores et al. (1999) observed *C. pelagicus* in a piston core below the Agulhas Current.

Hiramatsu and De Deckker (1997b) investigated Core GC-3, located near the Subtropical Convergence (now the STF) in the Southern Ocean, and observed the consistent presence of *C. pelagicus* along the 4.7 meter long core, with increased abundance during glacial periods. Burns (1975) consistently found this species off the Northern Island of New Zealand, while Wells and Okada (1997) found *C. pelagicus* east of New Zealand's South Island, under the path of the modern STF.

Findlay and Flores (2000) found this species present in a Holocene core-top just north of the STF, south of Tasmania, while Findlay and Giraudeau (2002) found *Coccolithus* spp. among Holocene sediment samples in the sub-Antarctic zone. However, the latter authors claimed it was absent from living assemblages north of the STF.

Figure 3.1. Map of the Southern Hemisphere representing documented presence and absence of *Coccolithus* spp., in core, water samples and sediment trap material.

3.1.5 Purpose of this study

We examined three different sampling sources of coccolithophore material in which the genus *Coccolithus* was present in order to clarify the distribution of *Coccolithus* species currently extant in the Southern Ocean, especially south of Tasmania (Table 1.1).

Sediment trap samples from the STR were recovered from September 2003 to February 2004 and extensive morphometric analysis was conducted on all samples. A random subset of these data was analysed for morphometry in this chapter, but will be discussed in more detail in Chapter 4. All samples will be accounted for when discussing factors such as the presence of a central bar and total coccolith and coccosphere fluxes.

Findlay and Flores (2000) analysed core-top sediments from Core GC07 (STR, 46^{o}09’S, 146^{o}17’E) and noted the presence of *C. pelagicus* as a subordinate species.

Here we revisit this core to focus on the morphometry of this species.

Additionally, two strains of this species were isolated from surface samples collected from the Tasmanian coastal areas of Blackmans Bay and Tinderbox, and grown in culture (Figure 3.2). Morphometric analysis of these two species will allow us to compare morphology with that observed in sediment trap samples and core sediment. Phenotypically, these strains are identical, although attempts of genetic analysis have so far been unsuccessful due to slow growth and subsequent bacterial contamination.

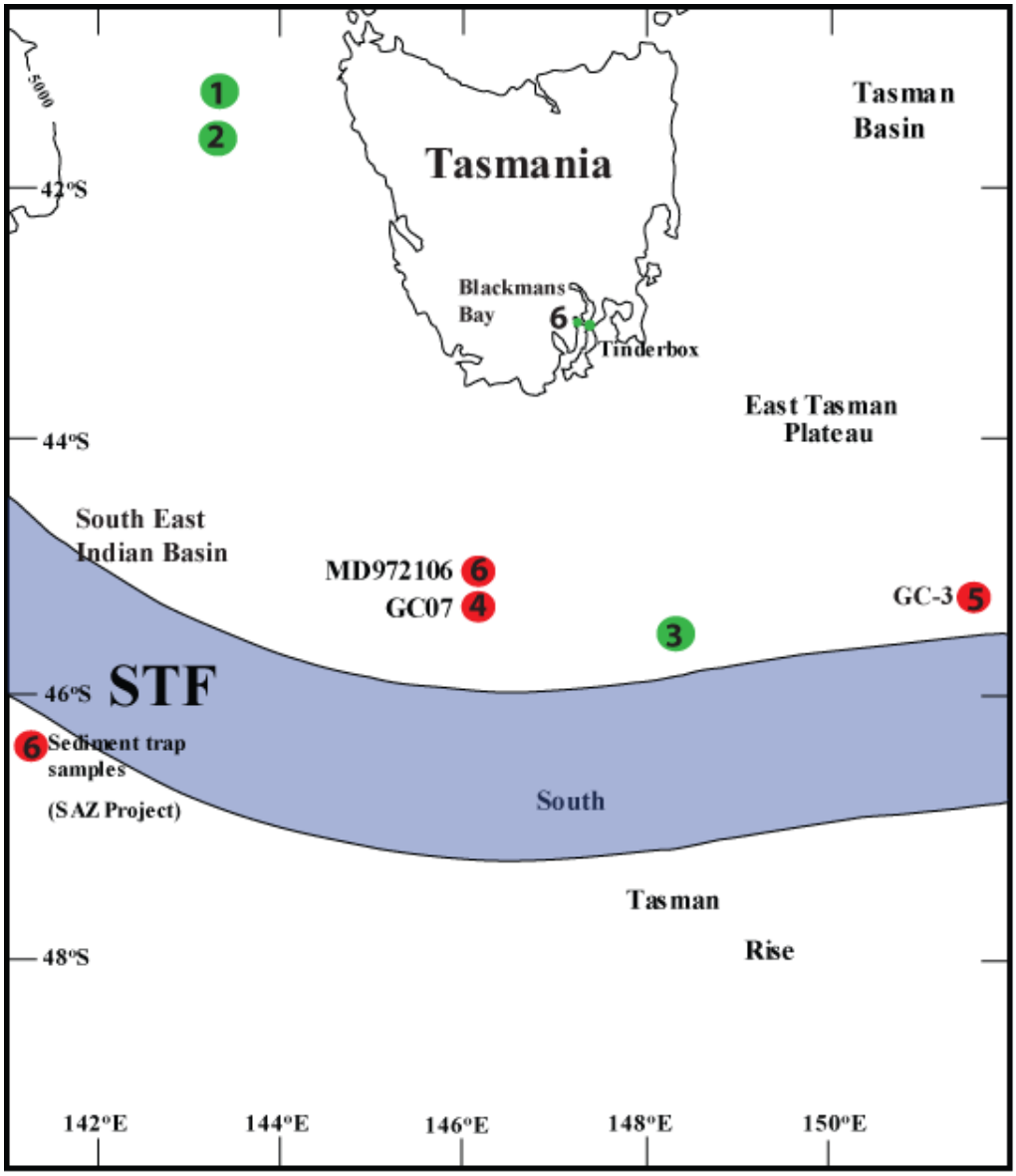

Figure 3.2. Specific location of reported *C. pelagicus* spp. south of Tasmania.

1. Hallegraeff (1984); 2. Findlay and Giraudeau (2000); 3. Nishida (1986); 4. Findlay and Flores (2000); 5. Hiramatsu and De Deckker (1997b); 6. This study.

3.2 Methods

3.2.1 Sediment Traps

The sediment trap samples used in this study are part of a long term program of moored sediment traps deployed in the Subantarctic Zone (SAZ) and Polar Frontal Zone (PFZ), called the SAZ Project, organized by the Antarctic Climate and Ecosystem Cooperative Research Centre (ACE CRC) with contributions from the Commonwealth Scientific and Industrial Research Organization (CSIRO) and Woods Hole Oceanographic Institution (Trull et al., 2001c).

Sediment traps were deployed on the 15th September 2003 from the research vessel Aurora Australis (Voyage Aurora 03/04 V01), at mooring site 47^{o}S (STR 46^{o} 49.47'S, 141^{o} 38.73'E), located at 2000 m depth, and a water depth of 4540 m. The trap had a total of 21 cups. Flux was collected through a large funnel with a baffle at the top (0.5 m^2 surface area) and a narrow opening at the bottom through which the particles fall into the individual cups (Trull et al., 2001c). Cup solution consisted of poisoned brine prepared with filtered seawater (Whatman GF/F, 0.7µm), collected at 65^{o}S, 141^{o}E. Surface water for brine preparation is generally collected south of 60^{o}S to ensure naturally elevated silicate concentration. To this, 5 g/L sodium chloride were added to increase density, 2.2 g/L strontium chloride, 3 g/L mercury chloride, acting as a biocide, and 1 g/L sodium tetraborate (buffer) (Bray, pers. comm.). The first cup opened on the 21st September 2003 and all studied cups had an opening time of 14 days. The mooring was collected on the 6th October 2004 (Voyage 04/05 V01).

Upon recovery, cups were preserved with 100µl of saturated mercury chloride and stored at 4^{o}C in the dark. Samples were allowed to settle and excess solution was drawn off. Samples were sieved through 1mm nylon mesh. The > 1 mm fraction was stored and the <1 mm fraction was split into ten fractions for chemical and biological analysis. This was done using a rotating splitter (McLane), using filtered seawater with sodium tetraborate as rinse solution. All fractions were stored in this solution, along with residual mercury chloride (Bray, pers comm.). Fraction 8 was used for analysis of *Coccolithus* spp. Only samples from 28th September 2003 to the

15th February 2004 were available for this study (cups 1-11). These samples were prepared for light microscopy (LM), with three replicates per sample.

For LM slide preparation, 1 ml of solution was transferred into micro-centrifuge tubes (1.5 ml) and centrifuged at 3000 rpm for five minutes. Supernatant was removed and samples were resuspended with buffered deionised water (DIW) stock solution to get rid of salt crystals. This process was repeated twice. The solution was homogenised carefully by resuspension and manual mixing, and 0.5 ml was pipetted onto a slide and left to air-dry, then fixed with Eukitt® (Fluka Analytical).

One hundred images per replicate of individual *C. braarudii* coccoliths were randomly collected with a Leica DM6000 cross-polarised microscope using a 100x oil immersion objective lens with a Leica DFC420C colour camera, under cross-polars (POL) and brightfield (BF). The same approach was used for image collection of culture material and gravity core samples. Images in POL were not used in this study. Images in BF were used to measure length and width of distal shield (DS), proximal shield (PS), central area (CA), central opening (CO) using the software Image J (Version 1.41o). From these measurements the area of each part of the coccoliths was calculated: DS area (DSA), PS area (PSA), CA area (CAA) and CO area (COA).

3.2.2 Coccolith and coccosphere concentrations

For coccolith and coccosphere counting, another set of slides (single replicate) were prepared following the same protocol, but only 100 µl of homogenised solution was pipetted into the slide, let to air-dry and fixed with Eukitt®. All coccoliths and coccospheres of *Coccolithus* spp. were counted for each slide. This resulted in relative concentrations of coccoliths and coccosphere ml^{-1} per centrifuge tube volume (CT, fraction 8). An additional step was to estimate coccolith and coccosphere flux per cup solution (fraction 1-10) and finally to counts/m^2/day, shown in Table 3.1.

3.2.3 Culture material

Two strains were collected from Southern Tasmania. Strain CPTX01 was collected at Tinderbox (43° 02'S, 147° 20'E) and strain CPBMB02 was collected at Blackmans Bay (43° 00'S, 147° 20'E). Strains were isolated by Miguel de Salas at the University of Tasmania (15/03/07) and grown in K medium at 14°C, 34‰ salinity, under a 16:8 light:dark cycle and a light intensity of 150 µmol m^{-2} s^{-1}. Growth has proven to be significantly slower than that reported for other *Coccolithus* culture strains from the Southern Hemisphere such as Strain RCC 1200 isolated from the coast off Namibia (Roscoff Culture Collection; e.g. Krug et al., 2011; Muller et al., 2009). The strains were prepared for LM and SEM observation. For both purposes, 1.5 ml of culture material was collected in micro-centrifuge tubes (1.5 ml), and centrifuged at 7000 rpm for five minutes. Supernatant was removed and 1 ml of distilled water was added. The material was resuspended and the process was repeated twice. For LM, a drop of material was added onto slides and let to air-dry. Samples were fixed with Eukitt®. For SEM observation, 1 ml of material was filtered onto 1.0 µm pore filter (Millipore) let to air dry and mounted onto SEM stubs. Samples were platinum coated, and analysed with a JEOL JSM-6701F Field Emission Electron Microscope.

3.2.4 Core-top sediment

In addition, core-top sediment from gravity Core GC07 (STR, 46°09'S, 146°17'E, 3307 m water depth) was examined. Dates based on C^{14} data were estimated at 1,167 years ago (1.1ka; 0-3 cm) (Findlay and Flores, 2000). Three replicate smear slides were prepared for LM. Fifty images per replicate were gathered in POL and BF, and measured for morphological parameters as described above.

3.2.5 Statistical Analysis

Primer 6 was used for PCA of morphometrical parameters. Time series and correlations were performed in Excel 2010. Morphological variations were analysed as a nested mixed model with the SAS System, which consisted of pair-wise comparisons between source materials for all parameters. The Tukey-Kramer test

was used for test of significance.

Table 3.1. Details of total mass flux calculation per cup (10/10 = fraction 1-10), coccolith and coccosphere counts per centrifuge tube volume (CT vol, 1/10 = fraction 8), counts per cup, and counts per area per day (counts/m^2/day).

Deployment year	Mooring location (lat/depth)	Cup (10/10)	Time cup open	mass/cup	Mass flux <1mm (10/10) mg/m2/day	Mass flux <1mm (10/10) mg/m2/yr	coccolith counts/100µL of CT vol	coccosphere counts/100µL of CT vol	Vol in CT (1/10) (ml)
2003	47_2000	1	14	161.47	23.07	8.43	13	4	37
2003	47_2000	2	14	426.47	60.92	22.25	2210	33	36
2003	47_2000	3	14	365.18	52.17	19.05	624	4	43
2003	47_2000	4	14	369.32	52.76	19.27	1002	6	34
2003	47_2000	5	14	874.93	124.99	45.65	4886	109	32
2003	47_2000	6	14	1065.22	152.17	55.58	6222	104	35
2003	47_2000	7	14	970.75	138.68	50.65	5313	105	32
2003	47_2000	8	14	521.32	74.47	27.20	5788	138	47
2003	47_2000	9	14	828.50	118.36	43.23	11825	227	38
2003	47_2000	10	14	1201.65	171.66	62.70	4539	117	48
2003	47_2000	11	14	1127.72	161.10	58.84	3007	66	42

Cont.

Cup (10/10)	coccoliths/CT	coccospheres/CT	coccolith counts/cup	coccosphere counts/cup	coccoliths (counts/m^2/day)	coccospheres (counts/m^2/day
1	4810	148	48100	1480	6871.43	211.43
2	795600	1188	7956000	11880	1136571.43	1697.14
3	268320	172	2683200	1720	383314.29	245.71
4	340680	204	3406800	2040	486685.71	291.43
5	1563520	3488	15635200	34880	2233600.00	4982.86
6	2177700	3640	21777000	36400	3111000.00	5200.00
7	1700160	3360	17001600	33600	2428800.00	4800.00
8	2720360	6486	27203600	64860	3886228.57	9265.71
9	4493500	8626	44935000	86260	6419285.71	12322.86
10	2178720	5616	21787200	56160	3112457.14	8022.86
11	1262940	2772	12629400	27720	1804200.00	3960.00

3.3 Results

3.3.1 Coccolithus braarudii *in the Australian sector of the Southern Ocean*

Sediment trap samples from the Southern Ocean South of Tasmania showed the consistent presence of *Coccolithus* spp. coccoliths from September 2003 to February 2004. Coccolith and coccosphere fluxes ranged from ~ 6.87 x 10^3 and ~ 2.11 x 10^2 counts/m^2/day in September, respectively, to over ~ 6.41 x 10^6 and ~ 1.23 x 10^4 counts/m^2/day in January 2004, respectively (Plate 3e, f; Plate 4c, d). There was a good relationship between loose coccolith and coccosphere fluxes (Figure 3.3), which may be an indicator of the reliability of the sediments traps in capturing water column coccospheres. Coccolith and coccosphere fluxes followed the same pattern in a time series trend and both suggested a seasonal variability, with an increase during spring and early summer and a decrease in late summer. More details of this variability will be discussed in Chapter 4. Of the total number of coccoliths

measured (N = 3397), 75.5% showed the presence of a central bar. This factor, together with size range, suggested that this species is *C. braarudii* (Plate 3a).

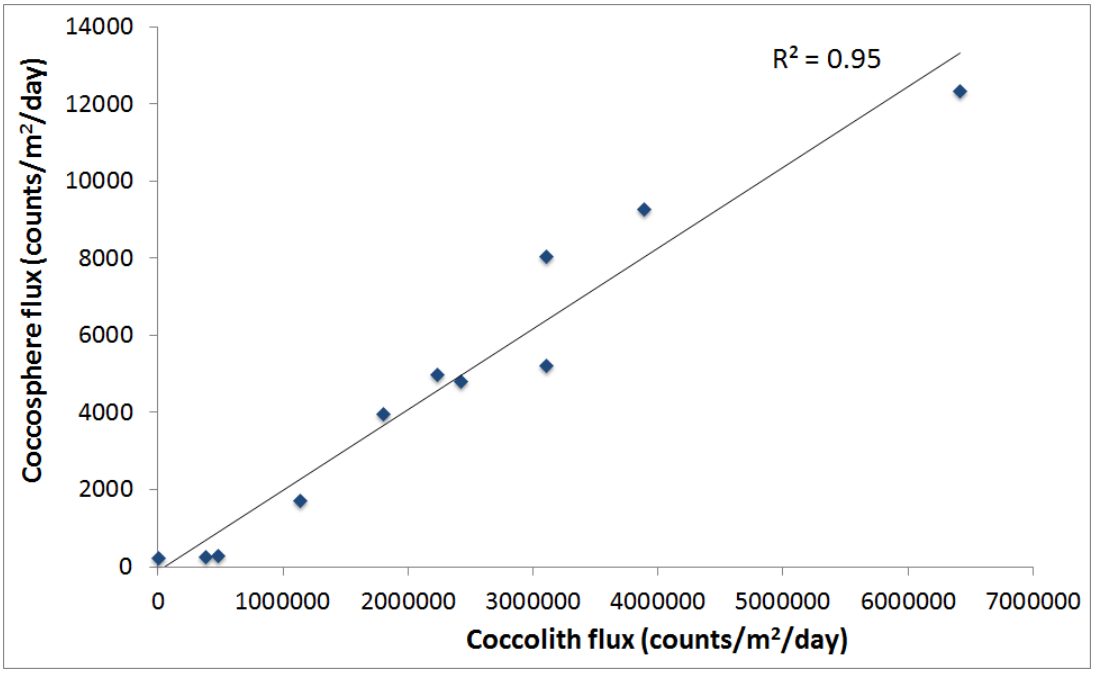

Figure 3.3. Correlation between coccolith and coccosphere fluxes (counts/m^2/day) of *C. braarudii* in sediments trap during spring-summer 2003-04 (fortnightly samples).

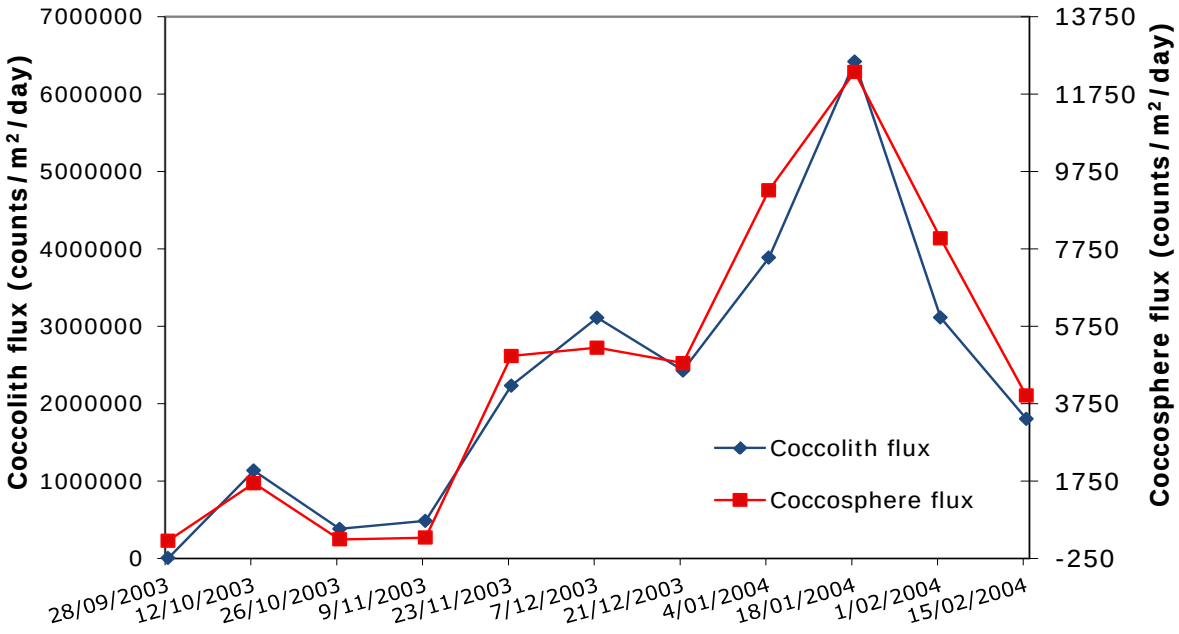

Figure 3.4. Time series of *C. braarudii* coccolith and coccosphere fluxes (counts/m^2/day) during spring-summer 2003-2004, from sediment trap samples (STR, 46^o 49.47'S, 141^o 38.73'E) at 2000 m depth.

3.3.2 Coccolith Morphometry

All measurements are summarised in Table 3.2. Maximum DS length (DSL) was observed in core-top samples (Plate 3b), ranging between 10.2 to 15.4 µm, whereas culture strain CPBPM02 showed the smallest DSL (Plate 3d), ranging from 9.8 to 13.7 µm. Nevertheless, pair-wise comparisons showed there was no significant variability between sources (p = 0.08) (Table 3.3). Sediment trap samples showed the largest DS width (DSW) (9.3 - 12.8 µm) and the smallest PS length (PSL) (7.3 - 12 µm).

Table 3.2 Range of morphometric measurements (in µm) for *Coccolithus braarudii* in culture, sediment trap samples and core-top sediment. Length (L) and width (W) of distal shield (DS), proximal shield (PS), central area (CA), central opening (CO), coccosphere diameter (CD) and number of DS elements. Standard deviations are included.

	Length DS (µm) N=50	Width DS (µm) N=50	Length PS (µm) N=50	Width PS (µm) N=50	Length CA (µm) N=50	Width CA (µm) N=50	Length CO (µm) N=50	Width CO (µm) N=50	Coccosphere Diameter (µm)	N° DS elements N=20
CPTX01	9.8 - 14.8 (stdev= 0.53)	8.1- 12.1 (stdev= 0.62)	8.1 - 12.1 (stdev= 2.71)	6.2- 10 (stdev= 3.07)	4.5-8.5 (stdev= 0.52)	3.1- 6.4 (stdev= 0.39)	1.6 - 6 (stdev= 0.55)	0.6- 2.8 (stdev= 0.40)	20 - 26 (stdev= 1.99)	48 - 63 (stdev= 3.68)
CPBMB02	9.8 - 13.7 (stdev= 0.75)	8.1 - 11.9 (stdev= 0.70)	8.1 - 11.7 (stdev= 1.41)	5.7 - 9.9 (stdev= 1.57)	5 - 8.4 (stdev= 0.63)	3.2 - 6.8 (stdev= 0.49)	2.3 - 5.8 (stdev= 0.60)	1.1 -3.4 (stdev= 0.41)	17 - 25.5 (stdev= 2.45)	44 - 70 (stdev= 6.71)
Sediment trap	10.5-15 (stdev= 0.95)	9.3 - 12.8 (stdev= 0.89)	7.3 - 12 9 (stdev= 1.92)	6.3 - 10 (stdev= 2.96)	4.1 - 8.1 (stdev= 0.56)	3 - 5.2 (stdev= 0.35)	0.9 - 4.3 (stdev= 0.53)	0.3 - 1.7 (stdev= 0.32)	25 -28 (stdev= 1.89)	48 - 54 (stdev= 1.16)
Core top Sediment	10.2- 15.4 (stdev= 1.07)	8.7 -14 (stdev= 1.03)	8.3- 13.2 (stdev= 2.02)	7-11.5 (stdev= 2.14)	4.3 - 7.9 (stdev= 0.70)	4.3 - 7.5 (stdev= 0.45)	0.9 - 4.6 (stdev= 0.69)	0.4 - 2.4 (stdev= 0.41)	N/A	48 - 60 (stdev= 3.48)

3.3.2.1 Morphological variation among cultures

For *C. braarudii* strains CPBMB02 and CPTX01, coccosphere diameter ranged from 17 to 25.5 µm and 20 to 26 µm respectively, and DS elements ranged from 44 to 70 µm and from 48 to 63 µm, respectively (Plate 4a, b). The CA was consistently open in 100% of observed coccoliths, showing the consistent presence of a central

bar (Plate 3c, d). Each area of the coccolith was compared as a separate parameter, but no significant difference between cultures was evident ($p = 0.45$).

Principal component analysis (PCA) showed a similar pattern, with all parameters contributing similarly to PC 1 and PC 2, except for COA, which contributed significantly (0.69) to the variation along PC 2 (Figure 3.5). Overall, PC 1 and PC 2 accounted for 90% of the variation in morphology of the cultures. Phenotypically, coccoliths present in the cultures were identical to each other and to those of the sediment trap and core-top sediment (Plate 3a, b; Plate 4a, b).

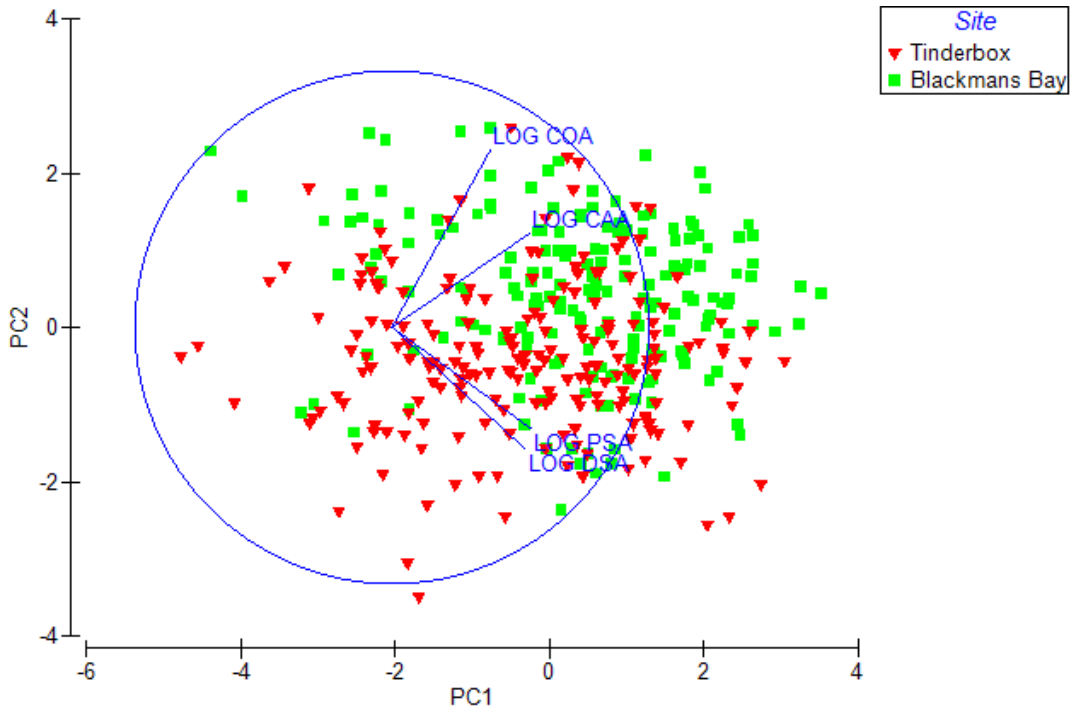

Figure 3.5. Principal component analysis of coccolith parameters (DSA, PSA, CAA and COA) of *Coccolithus braarudii* strains CPTX01 (Tinderbox, Tasmania) and CPBMB02 (Blackmans Bay, Tasmania). Data was transformed by natural logarithm. Blue circle indicates the direction of parameters vectors.

3.3.2.2 Variation among all sampling sources

An overall significant variation between all sampling sources was evident, driven by a significant difference between combined core-top and sediment traps, and culture material. There was no significant difference in parameters of core-top material and sediment trap samples. However, DSA of coccoliths in cultures were significantly

smaller than those of coccoliths from the core-top and sediment trap samples, while all other parameters were comparable between source materials (Table 3.3).

A PCA of coccolith parameters for all materials showed a significant variation of culture material along PC 2 (Figure 3.6), mostly driven by variation in COA (0.75) while all other parameters showed a non-significant variation. Overall PC 1 and PC 2 accounted for 90% of the variation among source materials.

Table 3.3. Summary of significant values for pairwise comparison between sampling material, sediment trap samples, core-top material and cultures. Values in bold indicate significance at p = 0.05 by the Tukey-Kramer test.

	DSA	PSA	CAA	COA	DSL
Overall p	**0.009**	0.21	0.23	0.13	0.08
Core-top-sedtrap	0.57	0.31	0.99	0.99	0.56
Core-top-culture	**0.009**	0.93	0.25	0.16	0.07
Sedtrap-culture	**0.01**	0.25	0.26	0.15	0.25

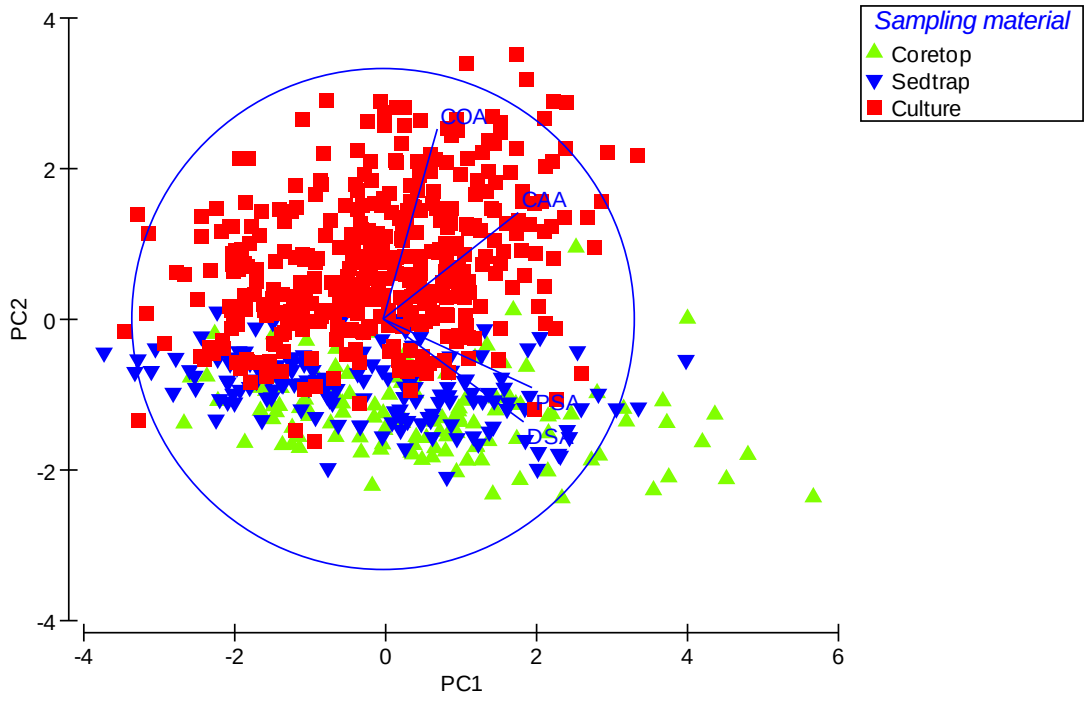

Figure 3.6. Principal component analysis of coccolith parameters (DSA, PSA, CAA and COA) of *Coccolithus braarudii* from core-top sediment, sediment trap samples and culture material. Blue circle indicates the direction of parameters vectors.

3.4 Discussion

3.4.1 Comparative morphometry

Coccolithophores and the coccoliths they produce vary in size as a result of both genotypic variability and varying growth response to different ecological conditions and an example of this size variation includes *Coccolithus* (Young and Ziveri, 2000). The present study, however, provided statistical evidence that there was no significant variability in the average morphology of this species between core-top sediment and sediment trap samples. The variability observed is in accordance with size ranges reported by other authors (Young and Ziveri, 2000; Parente et al., 2004). All materials studied showed the consistent presence of a central bar. While this is not consistent with findings in down core sediment (Chapter 2), where there was inconsistent presence of central bar, it indicates none the less the presence of *C. braarudii* in the Tasmanian sector of Southern Ocean for at least the last millennium. While observations by Young and Ziveri (2000) depicted the presence of two differently sized subtypes, our study shows a continuous size variation. This suggests the existence of only one extant species in the Southern Ocean, i.e. *Coccolithus braarudii* [(Gaarder, 1962) Baumann et al., 2003] sensu Geisen et al. (2002) and Young et al., (2003).

The Tasmanian culture material also exhibited the same morphological characteristics, although with a smaller DSL and an overall larger COA, which may be a pattern of malformation due to suboptimal culture conditions (Plate 3c, d) leading to older coccoliths. The small distance between collection sites, and their environmental and oceanographic similarities may explain that variability was not significant between strains.

3.4.2 **Coccolithus** ***presence south of the STF***

Sediment trapping is a valuable tool, both to estimate carbonate production and to link the dynamics of the pelagic plankton zone (Baumann, 2004) to deep sea deposits. In this study, this method allowed the gathering of reliable material to confirm the presence of the *C. braarudii* south of the STF, where substantial

amounts of coccosphere were found throughout all the studied months, evidence of a well-established population. Seasonal variations were also recorded, and more details on *C. braarudii* counts will be discussed in Chapter 4.

Most studies in the Southern Ocean agree that *C. pelagicus* spp. is a subdominant and overall rare species. The usual source material for these studies has been individual water sampling (e.g. Findlay and Giraudeau, 2000; Hallegraeff, 1984; Nishida, 1986), which failed to collect substantial cell numbers to demonstrate an established presence of this species. The culture strains were collected in the coastal waters of Southern Tasmania, which could suggest that the Upper Circumpolar Deep Water (UCDW) plays a role in the transport of this species into the area of the STF.

Claims by Findlay and Giraudeau (2000) that *C. pelagicus*, now redefined as *C. braarudii*, was the product of ballast water discharge and upwelling, need to be corrected. The fossil record indicated that this species has been present since at least the last glaciation (discussed in Chapter 5), and core-top sediment showed consistent presence until 1,167 years ago. Our sediment trap samples from September 2003 to February 2004 showed the presence of a species with the same morphometrical features, including consistent present of central bar and same size range as in core-top material, which again point to the identity of *C. braarudii*. The presence of this species in the SAZ, South of Tasmania, implies an established population in the region south of the STF, contrary to what Findlay and Giraudeau (2000) claimed.

The process of settling material into sediment traps can be subject to some alteration, and caution needs to be taken at its interpretation. A study by Deuser et al. (1988) showed that there can be high variability between particle fluxes in different years, although this could not be tested in this study. The sediment trap used in this study was positioned at 2000 m water depth. Besides obscuring the exact location of this coccolithophore population in the water column, high depths of positioned trap samples can delay flux settlement (Deuser et al., 1988). These authors described the connection from the sea surface to the trap as a funnel, which position and range in the sea surface is mostly unpredictable. However, the similar trend followed by coccoliths and coccospheres during the time series (Figure 3.4) could be an indicator of an *in situ* production, possibly existent in the lower part of the photic zone.

Additionally, Sokolov and Rintoul (2007) described several multiple branches or "filaments" building the ACC major fronts, which merge and diverge along its circumpolar path. However, the SAZ has been identified as having a deep mixed layer, low silicate concentration and the phytoplankton community dominated by coccolithophores (Sokolov and Rintoul, 2007b). Most fronts of the ACC encompass the whole water column and are rarely shallower than 2000 m (Sokolov and Rintoul, 2009a). In this regard, it would be expected that the collected specimens are local and endemic to the region. Further evidence is the presence of the local Antarctic diatom *Fragilariopsis kerguelensis* (Plate 4f) in the traps (Hallegraeff, pers.com.; Scott and Thomas, 2005). Even though this is the most abundant diatom in Antarctic waters, with a circumpolar distribution (Cefarelli et al., 2010; Mohan et al., 2011; Olguin and Alder, 2011) and spread from the STF to the Polar frontal Zone (PFZ) (Mohan et al., 2011), this indicates further presence of local populations of *C. braarudii* in the ACC, although the exact distribution of this species in the Tasmanian sector of the ACC remains to be described.

3.5 Conclusion

Coccolithus braarudii was found to be an established species in the Southern Ocean, located specifically southwest of the STF, where it was consistently observed in sediment traps deployed between September 2003 and February 2004, South of Tasmania. *C. braarudii* counts reached a maximum coccolith and coccosphere fluxes of ~ 6.41 x 10^6 and ~ 1.23 x 10^4 counts/m^2/day, respectively, in January 2004.

Coccolith morphometry was consistent between sediment traps located south of the STF and core-top sediments, north of the STF and consistent phenotypic evidence points to the presence of only on subspecies, *Coccolithus braarudii* (Gaarder, 1962) Baumann et al., 2003.

Laboratory observations were carried out in order to establish a healthy culture of the isolated strains. Isolated culture strains of coastal waters of Tasmania showed same phenotypic characteristics as sediment traps and core-top sediments, with consistent presence of a central bar. Growth was observed to be very slow, although

cells remained alive for several months to years. Coccoliths showed large variation in the morphology of the central area, central opening, and variations in DS length, which we can conclude to be evidence of malformation.

Chapter 4 Seasonal variability in calcification and abundance of the coccolithophore *Coccolithus braarudii* [(Gaarder, 1962) Baumann et al., 2003] in the Subantarctic Zone (SAZ) of the Southern Ocean, South of Tasmania

Abstract

Sediment trap samples were studied from September 2003 to February 2004 from the Subantarctic Zone (SAZ) in the Southern Ocean, south of Tasmania, in order to characterise seasonal variations in morphology of *Coccolithus braarudii*. Weight index (WI), distal shield length (DSL) and various morphological parameters of individual coccoliths were measured, as well as coccolith and coccosphere fluxes. Results showed a positive trend of WI, DSL and cell flux, in line with seasonal increases in levels of chlorophyll *a*. This study also resolved the presence of a lighter, smaller phenotype during early spring, in contrast to larger, heavier phenotypes in mid-summer. No correlation was found between seawater chemical composition (including nutrients) and morphological parameters. This confirms previous claims of insensitivity of this species to known environmental variations. Finally, the appearance of healthier, morphologically different populations of *C. braarudii* coccoliths in summer may suggest seasonal plasticity of this species.

4.1 Introduction

4.1.1 The Southern Ocean influence in global ocean circulation

The Southern Ocean exerts a great influence on global ocean circulation. The main branch of Southern Ocean water, the Antarctic Circumpolar Current (ACC) comprises a cluster of circumpolar fronts (Figure 1.5, see Chapter 1 for more details), which serve as boundaries as well as deep reaching jets flowing eastward (Orsi et al., 1995). The ACC carries North Atlantic Deep Water (NADW) from the Atlantic to the other ocean basins, forming an important interlinking circulation, which permits global overturning circulation to occur, which, in turn, dominates the global transport of heat, freshwater and other properties that drive global climate (Rintoul and Trull, 2001).

Cooling of the upper ocean water in the North Pacific induces sinking and a southward flow, reaching the Southern Ocean via the tip of Africa (Broecker, 1997), and resulting in the main water supply into the Pacific and Indian Oceans. Winter mixing at the equator side of the ACC forms the Subantarctic Mode Water (SAMW) which is vertically well mixed and high in oxygen (Rintoul and England, 2002; Rintoul and Trull, 2001) (Figure 4.1). This water mass is also influenced by buoyancy fluxes associated with fresh water input and heat gain, which decreases density of upwelling waters (Lumpkin and Speer, 2007).

Meanwhile, nutrient-rich Upper Circumpolar Deep Water upwells south of the SAF (UCDW) where part of it loses buoyancy near Antarctica and consequently forms the Antarctic Bottom Water (AABW) (Trull et al., 2001c). The remainder gains buoyancy due to warming and freshwater input, ultimately sinking to form the Antarctic Intermediate Water (AAIW) and the SAMW (Speer et al., 2000; Trull et al., 2001c). Additionally, as the NADW is exported into the Indian and Pacific Oceans by the ACC, and becomes entangled in the overturning circulation of the Southern Ocean, it is also associated with the AAIW and the AABW formation (Zhengyu and Philander, 2001), also supplying the more saline Lower Circumpolar Deep Water (LCDW).

The Southern Ocean serves as a window to the large volume of water contained in the entire deep ocean (Sarmiento and Orr, 1991). Hence, water masses formed in the Southern Ocean return excess macro-nutrients to the ocean interior, in contrast to the equatorial Pacific where excess nutrients are advected into the sub-tropical gyres and consumed there (Trull et al., 2001a).

In terms of changes in ocean chemistry and consequent ocean acidification (OA), this makes the Southern Ocean of particular importance, along with the need to understand its seasonal patterns and predict its changes in the next century. McNeil and Matear (2008) predicted aragonite undersaturation for the Southern Ocean as early as 2030, when atmospheric CO_2 levels, under a business as usual scenario, will reach 450 ppm, contrary to previous estimation of undersaturation in the year 2100 (e.g. Caldeira and Wickett, 2003; Kleypas et al., 1999).

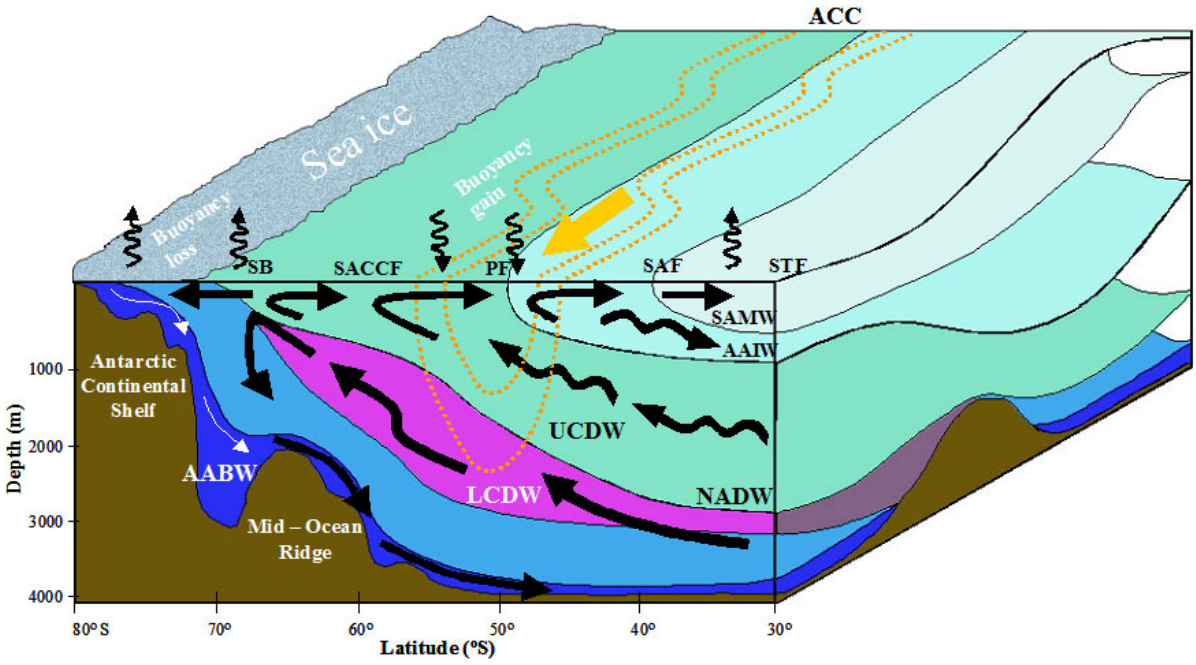

Figure 4.1. Schematic representation of the overturning circulation of Antarctic deep water masses. Water fronts are: STF = Subtropical Front; SAF = Subantarctic Front; PF = Polar Front; SACCF = Southern Antarctic Circumpolar Current Front; SB = Southern Boundary. Water masses are: SAMW = Subantarctic Mode Water; AAIW = Antarctic Intermediate Water; NADW = North Atlantic Deep Water; UCDW = Upper Circumpolar Deep Water; LCDW = Lower Circumpolar Deep Water; AABW = Antarctic Bottom Water. Curved arrows indicate loss and gain of buoyancy. Yellow arrow indicates direction of the ACC. See text for more details. Modified from http://dimes.ucsd.edu/; fronts locations from Trull et al. (2001c).

4.1.2 The Subantarctic Zone (SAZ)

Extensive studies using water samples and sediment trap samples, along with isotopic composition of biological samples, have derived accurate estimations of the seasonal fluctuations of the physical and environmental properties of the SAZ. Trull et al. (2001c) determined carbon export through particle flux, and concluded a high export to the deep sea, despite its high nutrients levels and low productivity (HNLP) characteristics. Lourey and Trull (2001) compared seasonal nitrate and phosphate depletion in the SAZ with that of the PFZ and found a greater nutrient depletion in the SAZ compared with the PFZ. More recently, McNeil and Tilbrook (2009) used carbon tracers and nutrients to calculate a seasonal carbon budget, and estimated a marked down-gradient of DIC from winter to summer. The SAZ is a sink for atmospheric CO_2, which results from seasonally low sea surface fugacities of CO_2 during the Austral summer, implying that the SAZ could be a major site of organic carbon export from the mixed layer (Borges et al., 2008; McNeil et al., 2007; McNeil and Tilbrook, 2009; Takahashi et al., 2002).

Salt deficiency is another characteristic of polar surface waters, due to the transportation of freshwater, in the form of vapour, from low to high latitudes, where it enters the ocean as precipitation and continental runoff (Broecker, 1997). The SAZ average salinity is 34.2 ‰ (Rintoul and Trull, 2001).

4.1.3 Coccolithophores seasonality patterns

The seasonal variability of coccolithophores in the Southern Hemisphere has thus far been poorly documented. For other calcifying groups, Howard et al. (2011) studied seasonal variations in pteropod flux from sediment trap samples from the SAZ, and identified marked peaks during late spring and mid-summer.

In the Northern Hemisphere, work by Broerse et al. (2000b) documented that *C. pelagicus* abundance peaked in late autumn and during spring in the subarctic region of the Sea of Okhotsk, north of Japan. Similarly, coccolith and coccospheres maximum abundance were recorded during spring in the subtropical north-east Atlantic (Broerse et al., 2000c), with *C. pelagicus* exhibiting a marked seasonal pattern with peaks in early summer, which might have been caused by local eddy

activity. Maximum coccolithophore fluxes have been related to periods of upwelling (Broerse et al., 2000a) and more recent studies have determined that weakened upwelling conditions during the summer-autumn deglaciation seem to also favour coccolithophore growth, in combination with increased SST, at the coast of Portugal (Silva et al., 2009). Similarly, Malinverno et al. (2009), looking at sediment trap samples in the Mediterranean Sea, found a high surface productivity during intervals of maximum water mixing, although this study recorded higher coccosphere flux in the spring-summer transition, and so did Haidar et al. (2000). Coccolith abundance peaks have also been recorded in late winter off Bermuda (Haidar and Thierstein, 2001; Haidar et al., 2000).

For the Southern Hemisphere, studies have been conducted on the physiological responses of phytoplankton communities in general (Cassar et al., 2011), and of coccolithophore distribution at particular points in time (e.g. Findlay and Giraudeau, 2000; Cubillos et al., 2007; Balch et al., 2011). All these studies were focussed on the more abundant species *Emiliania huxleyi* and *Gephyrocapsa oceanica*. However, to date no studies have reconstructed the seasonality of coccolithophore standing stock in the Southern Ocean.

4.1.4 Purpose of this study

Despite the recognized importance of biological carbon export in the Southern Ocean, there has been very little study of modern Southern Ocean sinking particle flux to the deep sea (Trull et al., 2001c). Intercepting this flux during sinking through sediment trap samples constitutes a crucial research tool; it not only allows the characterization of species at a particular time and place, but also allows the monitoring and calculation of a wealth of physical parameters. This, combined with other biological parameters such as chlorophyll *a*, a proxy for primary production, enables the reconstruction of population dynamics and a detailed study of their physiological and morphological variations at a seasonal level and at an inter-annual level (e.g. Roberts et al., 2011; Trull et al., 2001a; 2001c).

The aim of this study is to understand the morphological variation of the coccolithophore *Coccolithus braarudii* in the SAZ, South of Tasmania, in relation to

seasonal (bio) chemical changes (DIC, [CO_3^{2-}], atmospheric CO_2 and nutrients), intrinsic environmental factors such as *in situ* SST, as well as chlorophyll *a*.

This study also intends to improve our understanding of the rate of morphological adaptation of coccoliths of *C. braarudii* in response to environmental factors on a short time scale, to later compare with morphological variability at geological time scales (~ 20,000 years) in upcoming chapters. These morphological adaptations will be estimated in terms of levels of calcification based on weight index (WI) and coccolith size parameters. We also include a fortnightly quantification of coccoliths and coccospheres in order to understand population dynamics at a seasonal level.

4.2 Methods

4.2.1 Sediment traps

The sediment trap samples used in this study are part of a long-term program of moored sediment traps deployed in the SAZ and PFZ, called the SAZ project, organized by the Antarctic Cooperative Research Centre (ACE CRC) with contributions from the Commonwealth Scientific and Industrial Research Organization (CSIRO) and Woods Hole Oceanographic Institution (see Trull et al., 2001b; 2001c for details).

Sediment traps for this study were deployed on the 15th September 2003 from the research vessel Aurora Australis (Voyage Aurora 03/04 V01), at mooring site 47°S (South Tasman Rise (STR) 46° 49.47'S, 141° 38.73'E), at 2000 m depth. Seafloor depth in this area is 4540 m. The mooring had a total of 21 cups, of which cups 1-11 were used for this study. For cups preparation and preservation refer to Chapter 3. The first cup opened on the 21st September 2003 and all studied cups had an opening time of 14 days. The mooring was collected on the 6th October 2004 (Voyage 04/05 V01). Only samples from 28th September 2003 to 15th February 2004 were available for this study.

Upon recovery, cups were preserved with 100µl of saturated mercury chloride and stored at 4°C in the dark. Sediment was separated into ten fractions for chemical and

biological analysis (see Chapter 3 for details). Fraction 8 was used for analysis of *C. braarudii*. A subset of eleven samples, from September to January, was prepared for light microscopy, including three replicates per sample.

For slide preparation, 1 ml of solution was transferred into micro-centrifuge tubes (1.5 ml) and centrifuged at 3000 rpm for five minutes. Supernatant was removed and samples were resuspended with buffered deionised water (DIW) stock solution. This process was repeated twice. The solution was homogenised carefully by resuspension and manual mixing, and 0.5 ml was pipetted onto a slide and left to air-dry, then fixed with Eukitt® (Fluka Analytical).

One hundred images per replicate of individual *C. braarudii* coccoliths were randomly collected with a Leica DM6000 cross-polarised microscope (LM) using a 100x oil immersion objective lens with a Leica DFC420C colour camera, under cross-polars (POL) and brightfield (BF). POL Images were used for weight estimate by birefringence, resulting in weight index (WI), while images in BF were used for morphometric analysis (see Chapter 2). All coccolith parameters were measured, including lengths and widths of distal shield (DS), proximal shield (PS), central area (CA) and central opening (CO) (Figure 2.1). From these parameters each area of the coccolith was calculated.

For counting, another set of slides was prepared using the same method, but only 100µl of homogenised solution was pipetted onto a slide, left to air-dry and fixed with Eukitt®. All coccoliths and coccospheres of *C. pelagicus* were counted in each slide, resulting in relative concentration per millilitre. Table 3.1 shows full details on calculations of coccolith and coccospheres flux (counts/m^2/day).

4.2.2 Environmental data

Seasonal carbonate system variability was estimated for the 47^{o}S sediment trap site using empirical relationships between DIC and alkalinity, derived by McNeil et al. (2007) using seasonal records of SST, surface salinity, silicate, phosphate and nitrate, sourced from the World Ocean Atlas (http://iridl.ldeo.columbia.edu/SOURCES/.NOAA/.NODC/.WOA05/).

Other carbonate system variables such as dissolved inorganic carbon (DIC), carbonate ion concentrations ($[CO_3^{2-}]$ in µM Kg^{-1}) atmospheric CO_2 (ppmv) were calculated from estimated DIC (from G. bulloides δ13C and modern surface water DIC, modern deep water DIC, modern δ13C of surface water DIC, modern δ13C of deep water DIC, ΔDIC/Δδ13C (Moy, 2005)) and alkalinity using the carbonate system program "CO_2SYS" (Pierrot et al., 2006) including pH and calcite saturation state (Ω_{cal}). Carbonate dissociation constants were those derived by Mehrbach et al. (1973) and later refit by Dickson and Millero (1987).

Chlorophyll data was sourced from SeaWiFS from a selected averaging area at latitude [47°S, 46 °S], and longitude [141°E, 143°E].

4.2.3 Statistical analysis

Time series and correlations were performed in Excel 2010. Primer 6 was used for PCA of morphometrical parameters. In order to test for (in)dependencies within our multivariate biometric dataset, pair-wise linear regression models between morphological parameters and their correlations were produced in Excel 2010 and SPSS.

Morphological data was transformed using the natural logarithm so that any non-linear, power-law allometry (Equation 4.1) between the different size (length and area) and volume (WI) variables is accounted for by a linear regression model (Equation 4.2; e.g. Warton et al., 2006):

$$y = \gamma x^{\beta} \qquad \text{Equation 4.1}$$

$$\leftrightarrow \ln(y) = \ln(\gamma) + \beta \cdot \ln(x) \qquad \text{Equation 4.2a}$$

$$\leftrightarrow \ln(y) = \alpha + \beta \cdot \ln(x) \qquad \text{Equation 4.2b}$$

Where y and x are two variable, β is a constant and ln is natural log. Natural log transformations were also conducted for DIC, CO_2 and $[CO_3^{2-}]$.

4.3 Results

4.3.1 Environmental parameters

During the spring-summer season, SST increased from 9.5^{o}C in September to 12.4^{o}C in January. As expected, DIC and atmospheric CO_2 decreased with increased SST, ranging from 2080.5 to 2042 µM kg^{-1} and from 331.3 to 296.8 ppmv, respectively. DIC remained relatively stable from September to the end of November, while CO_2 reached its maximum level in November. Carbonate ion concentrations increased with increased SST, ranging from 152.4 to 177.6 µM kg^{-1} (Figure 4.2). All parameters underwent a marked change from late November to early December.

4.3.2 Seasonal population

4.3.2.1 Population averages

Coccosphere and coccolith fluxes of *C. braarudii* both exhibited a prominent increase at the onset of summer (Figure 3.4)), ahead of an increase in SST (Figure 4.3), followed by a steady state in December, and reaching maximum abundance in mid-January, when SST reached a monthly average of 11.85^{o}C. Variations in SST were correlated either positively or negatively with all other parameters, which allowed the prediction of trends with regard to WI and DSL. Mean WI values also showed a seasonal pattern (Figure 4.4), with a maximum at the end of November, ahead of maximum SST, followed by a steady decline at the beginning of January.

WI derived from CA followed the trend of maximum coccolith length (DSL), consistent with results presented in previous chapters. During the seasonal interval studied, WI and DSL peaked in December 2004, and the lowest levels of DSL and WI were recorded in September 2003 (Figure 4.5).

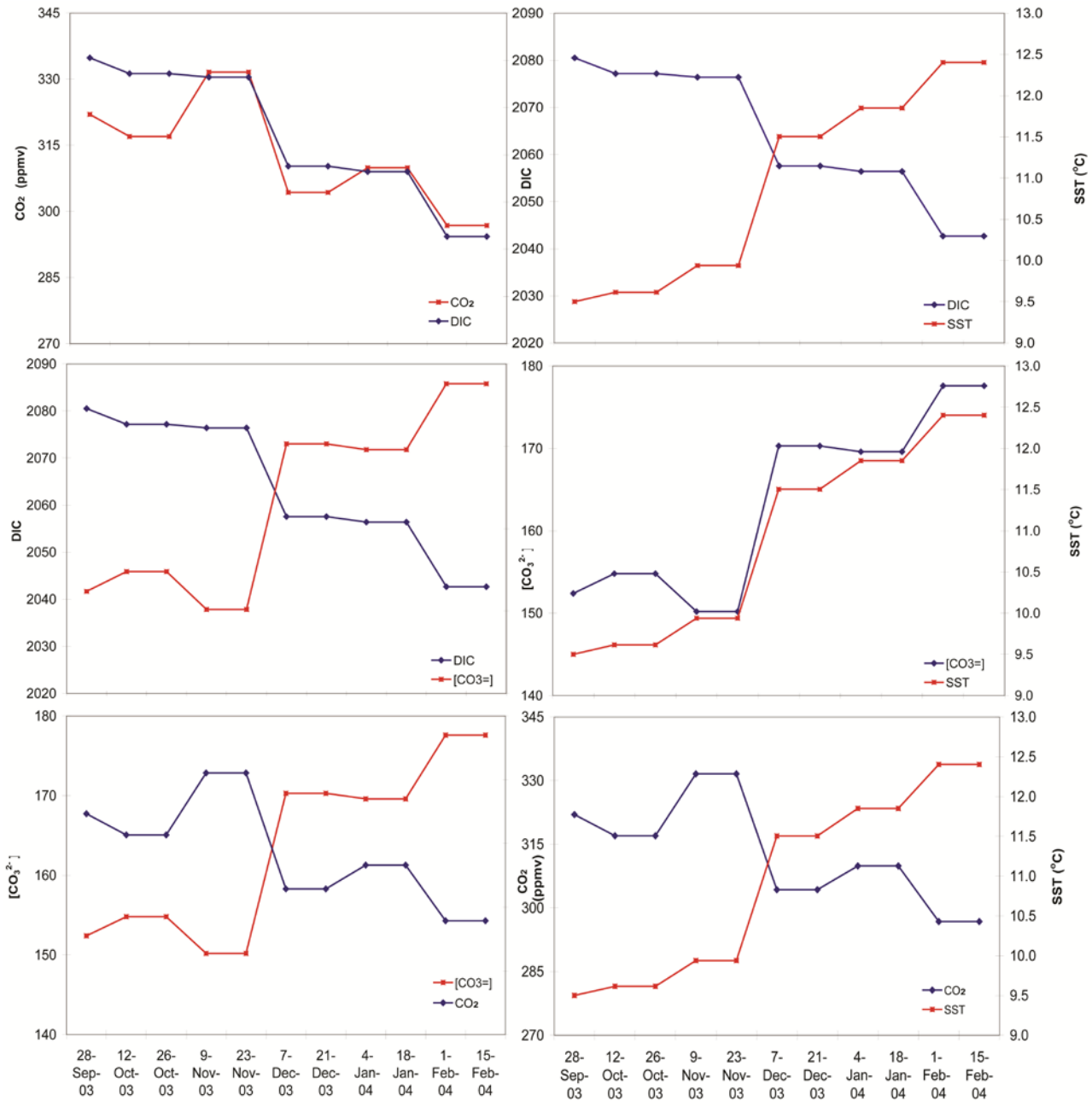

Figure 4.2. Seasonal trends of estimated environmental parameters and SST (°C) in the Southern Ocean, at sediment traps location. Carbonate parameters are dissolved inorganic carbon (DIC, in µM kg^{-1}), atmospheric CO_2 (ppmv) and carbonate ion concentrations ($[CO_3^{2-}]$ in µM kg^{-1}). Omega calcite and pH are directly related to DIC. Parameters are estimated from monthly oceanographic climatology following McNeil et al. (2007).

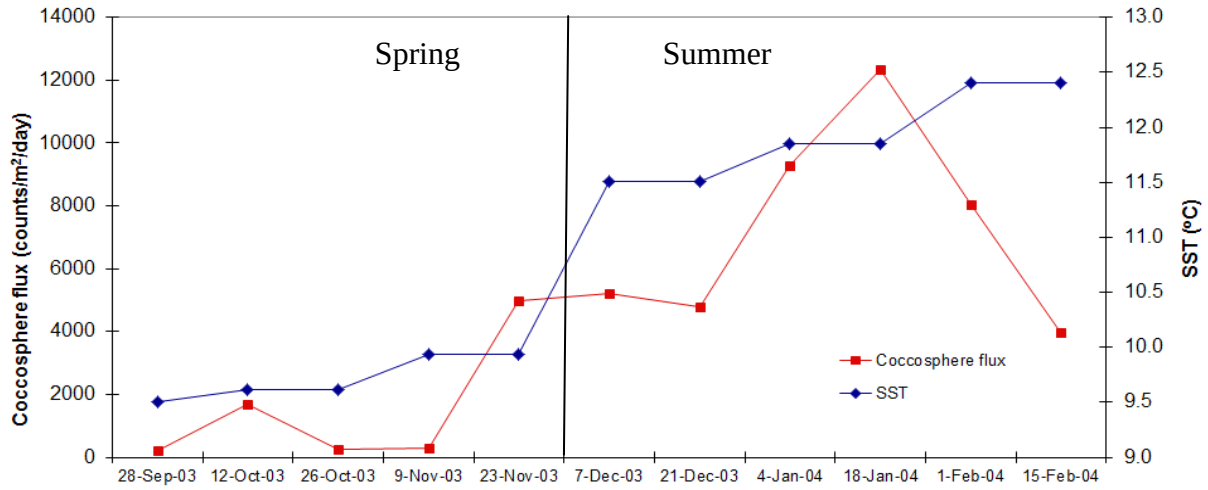

Figure 4.3. Seasonal variation of *in situ* sea surface temperature (SST, in ^{o}C) and coccosphere flux (counts/m^2/day), from fortnightly sediment trap samples during spring-summer 2003-2004. Dates indicate mid time of open cup.

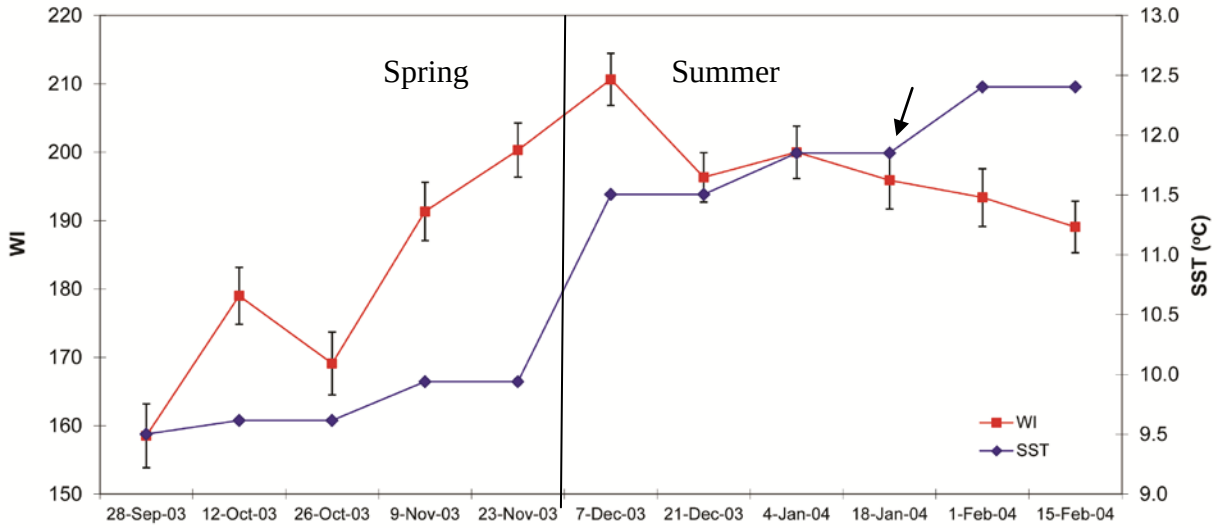

Figure 4.4. Seasonal trend of mean WI and *in situ* SST (^{o}C) during spring-summer 2003-2004. Black arrow indicates maximum abundance of *C. braarudii*. Error bars for WI are ± 1 s.e.

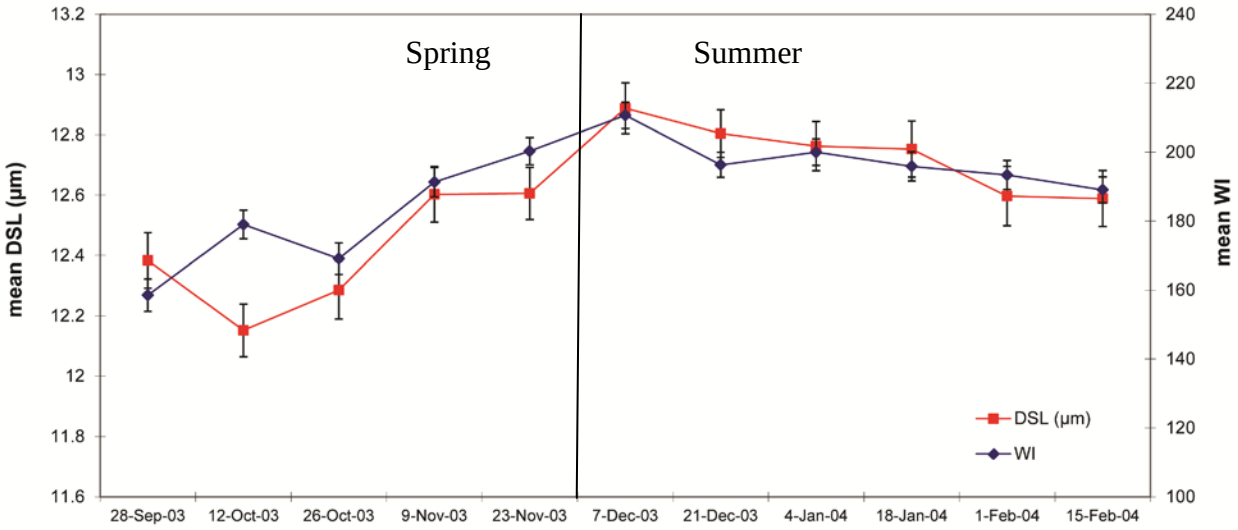

Figure 4.5. Seasonal trend of mean WI and mean DSL (µm) from sediment trap samples during spring-summer 2003-2004 (~ 300 specimens per samples). Dates indicate mid time of open cup. Error bars are ± 1 s.e.

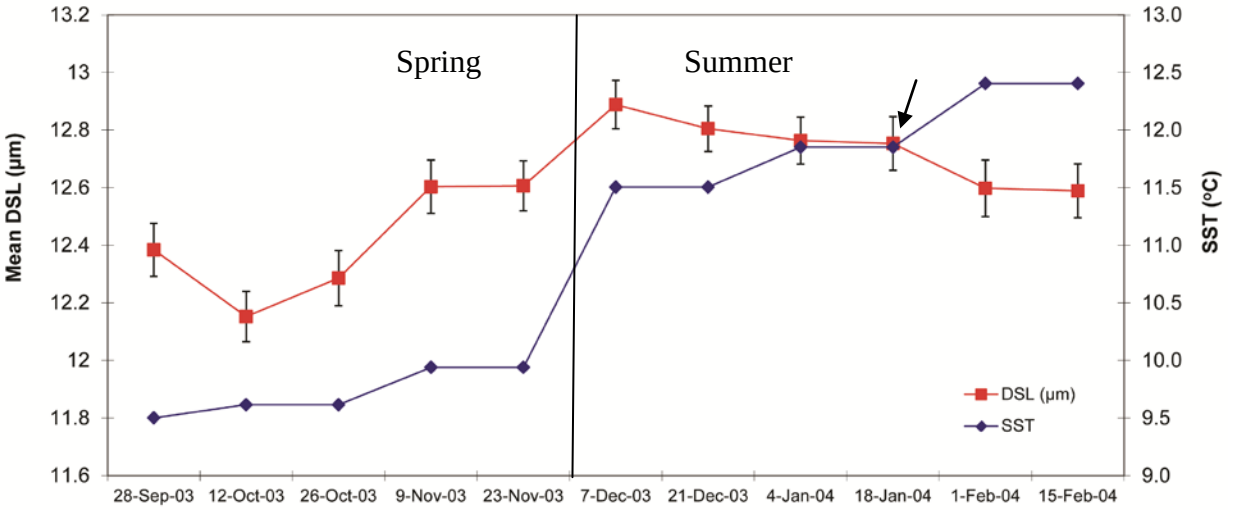

Figure 4.6. Seasonal trend of mean DSL (µm) and in situ SST (^{o}C) during spring-summer 2003-2004. Black arrow indicates maximum abundance of *C. braarudii*. Error bars for DSL are ± 1 s.e.

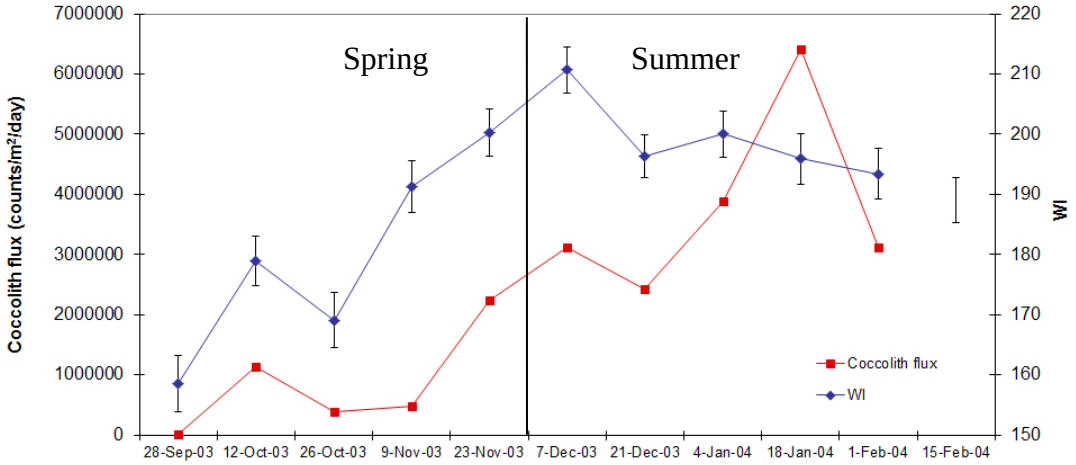

,,

Figure 4.7. Seasonal trend of mean WI and fortnightly coccolith flux (counts/m^2/day), from fortnightly sediment trap samples during spring-summer 2003-2004. Error bars for DSL are ± 1 s.e.

During the austral spring-summer season, spring showed a small population with on average lighter (Figure 4.7) and smaller coccoliths (Figure 4.5). An increase in WI and DSL at the beginning of November was followed a month later by an increase in coccosphere fluxes (~ 4.98 x 10^3 counts/m^2/day). WI and DSL reached a peak at the beginning of December, which coincided with a distinct increase in coccospheres fluxes (~ 12.32 x 10^3 counts/m^2/day) The maximum abundance in *C. braarudii* population occurred in January when both WI and DSL experienced a steady decline.

4.3.2.2 Chlorophyll *a*

Chlorophyll *a* (Chl *a*) showed a steady increase with SST, reaching a peak at the end of January, and then decreased during February (Figure 4.8). This decrease was consistent with coccolith and coccosphere fluxes, which peaked in mid-January and showed a marked decrease by February (Figure 3.4).

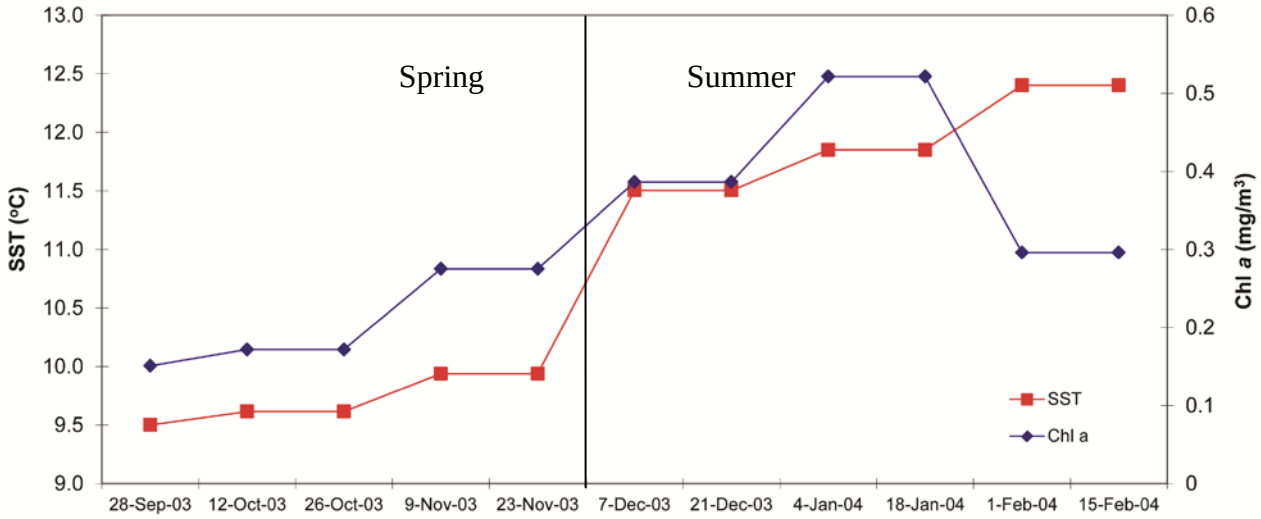

Figure 4.8. Chlorophyll *a* (Chl *a*) measurements (SeaWiFS, averages from the quadrats 46°S 47°S, 141°E 143°E) and mean SST (°C).

Seasonal trends of chlorophyll *a* were compared against DSL, WI, and central area of the coccolith (CAA, in µm^2), as well as coccosphere flux. Results showed a power-law correlation between Chl *a* and WI ($R^2 = 0.7$) (Figure 4.9a), and DSL ($R^2 = 0.79$) (Figure 4.9b). Hence, the CAA, from which WI is calculated, also showed a correlation with Chl *a* ($R^2 = 0.81$, Figure 4.9d). There was also a strong correlation between Chl *a* and coccosphere flux (m^2/day); ($R^2 = 0.75$, Figure 4.9c). Additionally correlations between Chl *a* and coccolith flux (Table 3.1) gave an R^2 value of 0.78.

Sample observations during coccolith and coccosphere counts at this particular trap location and time interval, at 2000 m depth, revealed that while other coccolithophores were present, such as *Emiliania huxleyi*, *Gephyrocapsa oceanica*, *Helicosphaera carteri* and *Calcidiscus* spp. and diatoms, were very rare, with low variability throughout the time series.

4.3.3 Morphological variations

Principal component analysis (PCA) was performed on all coccoliths parameters (distal shield area, DSA; proximal shield area, PSA; central area area, CAA; and central opening, COA), associated with SST in two categories; spring and summer (Figure 4.10). This distinction was valid for all other environmental parameters

(DIC, atmospheric CO_2, $[CO_3^{2-}]$), where major changes occurred at this time. There was a marked variation between spring and summer, however not matching observed morphological changes. DSA, CAA and WI were all main contributors to the variation along PC 1, while PSA and COA seemed to contribute negatively to the variation along PC 2. PC 1 and 2 contributed to 91% of the variation.

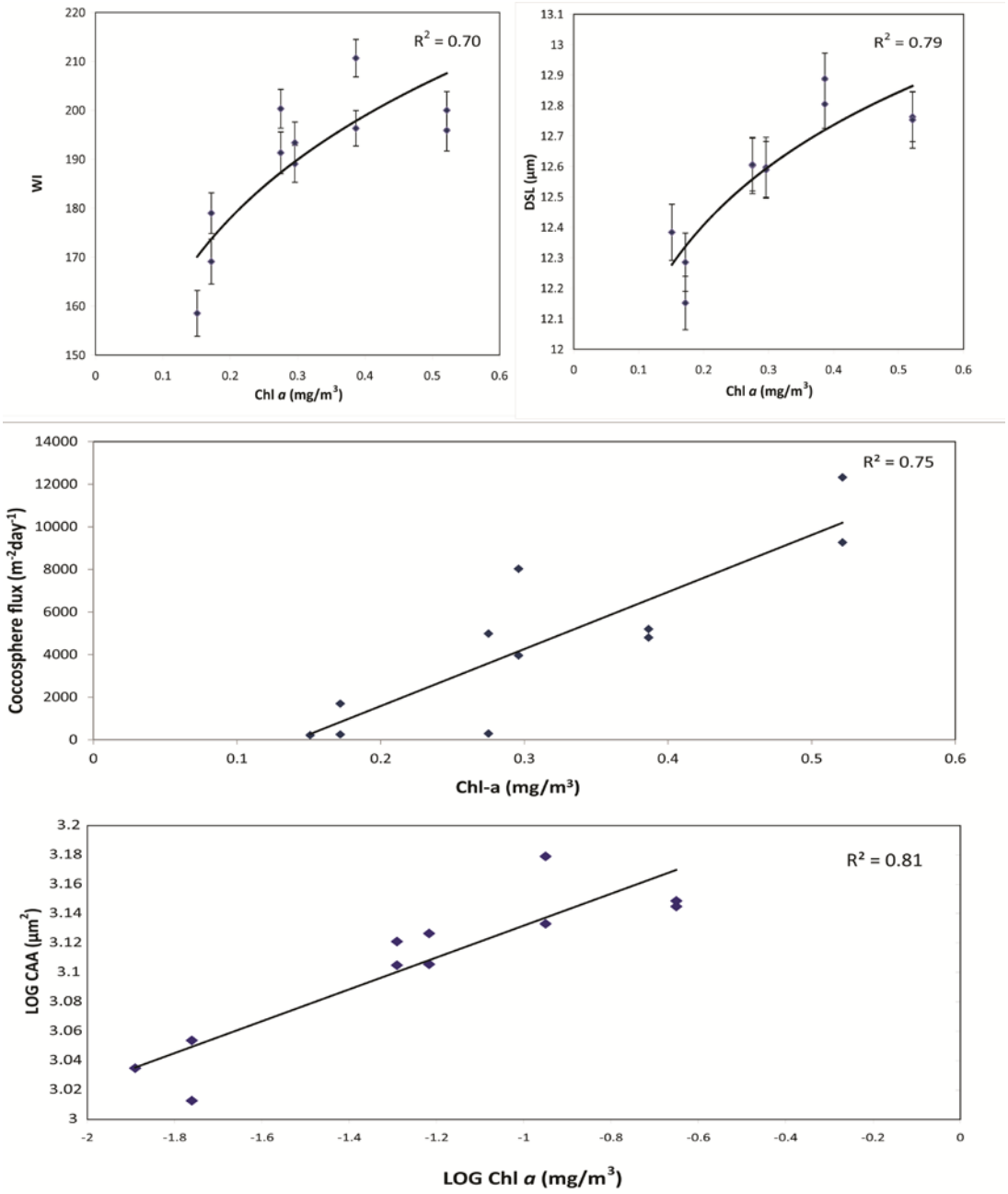

Figure 4.9. Correlations between chlorophyll *a* (Chl *a*, in mg/m^3) and morphological parameters, from sediment trap samples of spring-summer 2003-2004. (**a)** Weight index (WI); (**b)** Distal shield length (DSL, in µm); (**c)** Coccosphere flux (m^{-2}day^{-1}); (**d)** Central area area (CAA, µm^2). Error bars for WI and DSL are ± 1 s.e.

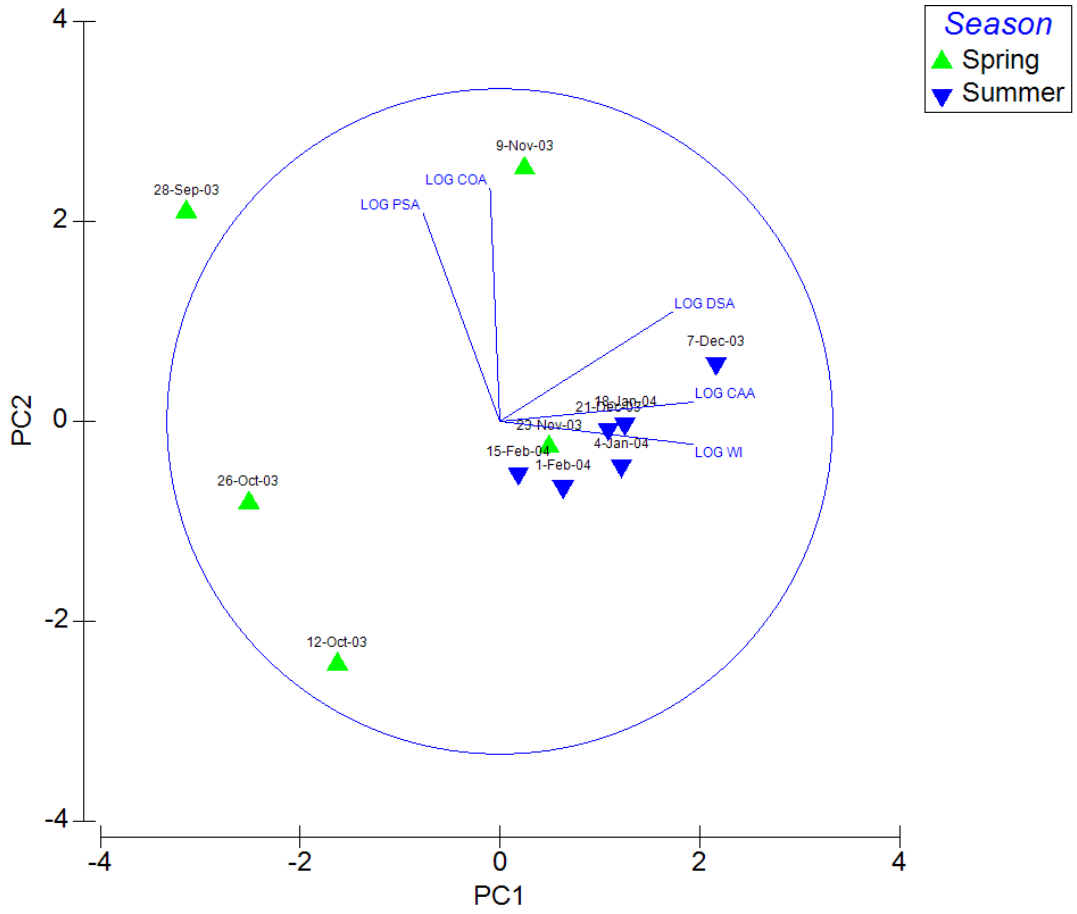

Figure 4.10. Principal component analysis (PCA) of morphological variations in relation to seasons. Seasons based on SST (<10^{o}C: spring; >10^{o}C: summer). Coccolith morphological parameters (except WI) are in areas, in µm^{2}; distal shield area, DSA; proximal shield area, PSA; central area area, CAA; and central opening, COA. Data transformed by natural logarithm.

Morphologically, early spring samples (Sep-Oct) were characterised for having a lower WI and DSA, while October and early November were characterised by having unusually large COA and PSA. This was also represented in the correlation between WI and DSL (Figure 4.11), where early spring showed the lowest DSL and WI, indicating an allometric relationship between these two parameters, whereby changes in size were associated with changes in weight. Early spring interval also showed the lowest levels of Chl *a* (Figure 4.9a, b), interpreted as the lowest levels of primary productivity.

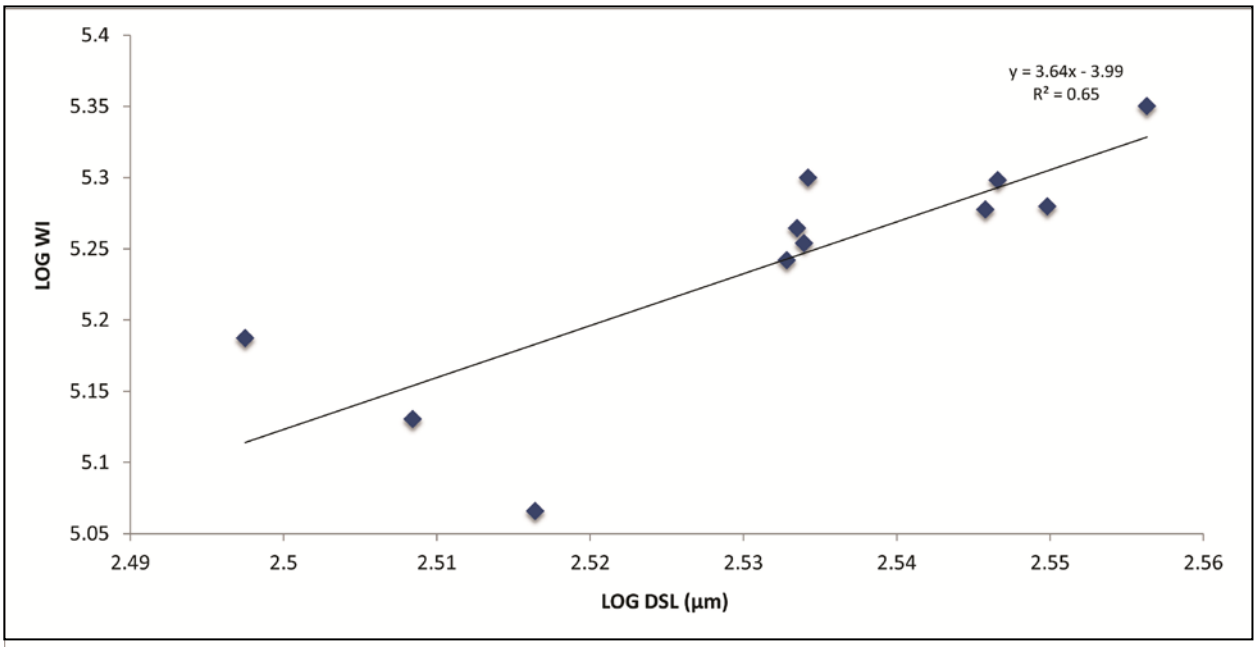

Figure 4.11. Seasonal correlation between WI (Log) and DSL (Log) during spring summer 2003-04.

A correlation matrix was created to test other parameters against morphology. Calcite saturation state (Ω_{cal}), and pH were included, derived using "CO_2SYS" (Pierrot et al., 2006), in addition to previously introduced carbonate measurement (4.2.2) . Nutrients such as phosphate, nitrate and silicate were also included, as well as salinity. Other morphological measurements were incorporated; distal shield rim (DSR = DSA – CAA), and GL_CA, which is the mean grey level (GL) measurements per coccolith from which WI was derived. The importance of the latter measurement lies in the fact that it provides an independent measure of mean thickness of the central area.

The correlation matrix summarises most results previously observed, such as correlations between cell concentration and DSL, WI, and SST. Correlations between Chl *a* and GL_CA/CAA, although relevant, are expected considering the correlation between WI and Chl *a*. This is also true for GL_CA/CAA and cell concentration. However there was a negative correlation between cell concentration and PSA, and no correlation between the latter parameter and Chl *a* or SST, which could have been expected if the allometry of coccoliths is assumed, where the whole shape of the lith varies with size in a proportional fashion. PSA also showed a weak negative correlation with Ω_{cal} and pH, whereas CAA showed a weak negative

correlation with DIC. There was no observable correlation between morphological characters and nutrients.

Table 4.1. Correlation matrix of environmental and morphological parameters. Correlation coefficients in bold are predicted correlation between morphological parameters and between environmental variables. Highlighted correlation coefficients in bold are significant correlations between environmental and morphological data. Morphological parameters, atmospheric CO_2, DIC and $[CO_3^{2-}]$ are in natural logarithm.

	LOG Chl-a (mg/m³)	LOG WI	LOG GL_CA	LOG DSL	LOG DSA	LOG PSA	LOG CAA	LOG COA	LOG DSR	LOG Coccolith flux ($m^{-2}day^{-1}$)	LOG Coccospheres flux ($m^{-2}day^{-1}$)	LOG $[CO_3^{-2}]$ (µM/kg)	LOG CO_2 (ppmv)	LOG DIC (µM/kg)	SST (°C)	Ω calcite	pH	Salinity (PSU)	Phosphate (µM/l)	Nitrate (µM/l)	Silicate (µM/l)
LOG Chl-a (mg/m³)	1																				
LOG WI	**0.83**	1																			
LOG GL_CA	**0.64**	**0.92**	1																		
LOG DSL	**0.89**	**0.80**	0.55	1																	
LOG DSA	**0.82**	**0.80**	0.58	**0.95**	1																
LOG PSA	-0.38	-0.43	-0.54	-0.06	0.03	1															
LOG CAA	**0.90**	**0.94**	**0.72**	**0.92**	**0.87**	-0.29	1														
LOG COA	-0.02	-0.17	-0.38	0.23	0.39	0.74	0.02	1													
LOG DSR	-0.48	-0.59	-0.50	-0.30	-0.13	0.64	-0.60	0.60	1												
LOG Coccolith flux ($m^{-2}day^{-1}$)	**0.76**	**0.87**	0.92	0.55	0.53	**-0.74**	**0.74**	-0.51	**-0.63**	1											
LOG Coccosphere flux ($m^{-2}day^{-1}$)	**0.80**	**0.80**	**0.68**	0.65	0.51	**-0.63**	**0.83**	-0.48	**-0.84**	**0.84**	1										
LOG $[CO_3^{-2}]$ (µM/kg)	**0.63**	0.48	0.31	0.56	0.43	-0.62	0.59	-0.20	-0.49	0.55	0.68	1									
LOG CO_2 (ppmv)	-0.41	-0.29	-0.16	-0.36	-0.22	0.64	-0.39	0.28	0.43	-0.41	-0.53	-0.96	1								
LOG DIC (µM/kg)	**-0.64**	-0.54	-0.38	-0.58	-0.49	0.59	**-0.63**	0.16	0.46	-0.58	-0.69	-0.97	0.90	1							
SST (°C)	**0.76**	**0.61**	0.42	**0.68**	0.59	-0.56	**0.72**	-0.12	-0.49	**0.63**	**0.76**	0.97	-0.85	**-0.98**	1						
Ω calcite	**0.63**	0.48	0.31	0.56	0.44	**-0.61**	0.59	-0.20	-0.48	0.54	0.68	1.00	-0.96	**-0.98**	**0.97**	1					
pH	0.41	0.29	0.16	0.36	0.21	**-0.64**	0.39	-0.28	-0.43	0.40	0.53	0.96	-1.00	**-0.90**	**0.85**	**0.95**	1				
Salinity (PSU)	0.27	0.04	-0.11	0.22	0.01	-0.45	0.18	-0.26	-0.35	0.16	0.31	0.63	-0.73	-0.45	0.45	**0.62**	**0.75**	1			
Phosphate (µM/l)	-0.50	-0.37	-0.15	-0.52	-0.42	0.38	-0.52	0.00	0.36	-0.34	-0.57	**-0.92**	0.87	**0.96**	**-0.93**	**-0.93**	**-0.86**	-0.40	1		
Nitrate (µM/l)	-0.43	-0.28	-0.14	-0.36	-0.22	0.63	-0.39	0.26	0.43	-0.40	-0.54	-0.96	1.00	**0.91**	**-0.87**	**-0.96**	**-1.00**	**-0.73**	**0.88**	1	
Silicate (µM/l)	-0.02	-0.06	0.06	-0.17	-0.12	0.23	-0.16	0.00	0.14	-0.03	-0.22	-0.71	0.78	**0.74**	**-0.63**	**-0.72**	**-0.77**	-0.31	**0.85**	**0.77**	1

4.4 Discussion

4.4.1 Morphological trends

C. braarudii's population south of the STF appeared well established from September to February, however the lack of data available for the remainder of the year means that predictions on the behaviour of this population cannot be easily made. Nevertheless, observations on the morphology of this species during this period of time can be related to environmental factors. The months of September and October had coccoliths with considerably smaller DSL and WI, when Chl *a* was at its lower level. This also coincided with a low cell concentration and low

temperature. Early spring samples did not show any sign of dissolution or malformation; hence these small, light coccoliths could be morphological variations belonging to a phenotype arising under conditions of low productivity, possibly remnants of a winter population. Between early and late spring there was an episode of growth, when the population increased tenfold, which coincided with an increase in productivity. This could imply the rise of a new population under more optimal conditions, producing larger, heavier phenotypes, i.e. a high productivity phenotype. This phenotypic variation could indicate that *C. braarudii* is responsive to the short term physical variability intrinsic to seasonality such as SST, which agrees with previous studies where morphotype variations and abundance in *C. leptoporus* (Northern Hemisphere tropical and subtropical zone) were related to environmental factors, mainly SST (Renaud et al., 2002). However, these authors found relative abundance to correlate with nutrient composition, which was not the case in the present study. Also, the pick of *C. leptoporus* flux was during spring, decreasing drastically in summer in their subtropical site. Hence, it is still possible that *C. braarudii* may respond differently to changes in the chemical composition of the ocean.

It is evident that plankton productivity cannot be the direct driver of phenotypic variations such as WI and DSL, as high or low productivity in a community are not known to affect the morphological nature of a given population within that community. However it is likely that the parameters that provide the conditions under which primary production thrives are the same that will provide optimal conditions for coccolith calcification. In studies by Renaud and Klaas (2001) on the seasonality of *C. leptoporus* off Bermuda, these authors not only found high seasonal variability in abundance, but also distinctive variations in morphology - with at least two morphotypes contributing to and alternating within the populations. Similar to this study, these authors recorded maximum abundance during late spring/summer, declining in late summer. In the present study, morphological variations were partially correlated with abundance, and some parameters were highly correlated with Chl *a*, such as CAA. The CAA was also slightly correlated with DIC. The central area delineates the location of the protococcolith ring, where coccolith biomineralization starts, and therefore this correlation could indicate that coccolithogenesis behaves in a seasonal manner and responds in line with the

general conditions of optimal primary production in the Southern Ocean. This is congruent with Renaud and Klaas (2001) which concluded that morphological plasticity could be linked with seasonality and environmental parameters such as temperature. However, there was no strong evidence to propose that the size of the CAA, and biomineralization, were related to changes in DIC.

4.4.2 Seasonal trends

The coccolith morphology of *Coccolithus braarudii* in the Southern Ocean sector South of Tasmania, presented marked seasonal trends during spring 2003 - summer 2004, south of the STF, with maximum abundance in mid-summer and a decrease in late summer. This happened later, on a seasonal basis, than in the Northern Hemisphere, where peaks have been recorded either in early or late summer (Andruleit, 1997; Haidar et al., 2000; Malinverno et al., 2009) but, nevertheless, during periods of high productivity, which agrees with previous studies. These variations were only partly correlated with physical oceanographic parameters and the biochemical conditions of the area. Furthermore, there was no evidence for upwelling in the area of the SAZ - instead this occurs mostly south of the PF (Findlay and Giraudeau, 2000; Anderson et al., 2009) indicating that a seasonal trend in the plankton community is not a result of this factor. The variation presented by WI and DSL seemed not related to seawater carbonate chemistry, and only partially related to SST. There were overall no correlations between morphological patterns of *C. braarudii* and seasonal changes in the chemical composition of the SAZ. This might be another indicator that this species is insensitive to such short-term biochemical changes, as was observed in culture experiments (Langer et al., 2006).

Population averages showed maximum abundance in mid-summer, along with Chl *a*, which did not coincide with peaks in other environmental parameters. However, this might indicate optimal conditions for this species. *C. braarudii* populations were in line with the primary productivity in the SAZ and the abundance patterns of this species agreed with Howard et al. (2011)'s pteropod concentration for the same period of time. More observations are needed in order to estimate exactly how much of the total primary productivity coccolithophores are responsible for. For mass flux

components recorded in the area of the SAZ, SAF and PFZ, in sediments trap samples (1997-1998), Trull et al. (2001c) found that particulate inorganic carbon (PIC), in the form of $CaCO_3$, was almost double the amount of biogenic silica in the SAZ up to 54^{o}S, where it is replaced by silica fluxes in the PFZ. Balch et al. (2011) also claimed high concentrations of PIC near the SAF, and Wight et al (2010) associated pigments with diatoms in the area of the sea ice, south of the PF. This could be further indication of a more substantial contribution of non-blooming coccolithophores in the carbonate budget estimate, as previously argued by Sarmiento et al. (2002). This has also been recorded by Baumann (2004), who claimed the percentage of small dominant species in the assemblage tends to overestimate their mass flux.

No correlations were found between nutrients and any of our coccolith morphological parameters. Other studies have suggested that phytoplankton growth in the Southern Ocean is not limited by the availability of major nutrients such as silicate, phosphate and nitrate (Lourey and Trull, 2001). Our results seem to point to the same direction regarding coccolithophores in the Southern Ocean.

Even though the specific factors affecting coccolith morphology remain elusive, there was clear evidence an allometric relationship between coccolith size and weight. The observed seasonal variability in coccolith morphology mostly co-varies with SST, indicative of some morphological plasticity in the short-term patterns of this species. Figure 2.8 and Chapter 2 provide a preliminary insight in the allometric behaviour of coccolith size and weight on a geological time scale, where subtle but significant changes in morphology were documented. Therefore it is important to investigate how morphological changes take place at a geological time scale, by studying coccolith allometric characteristics in the long term.

4.5 Conclusions

The Southern Ocean South of Tasmania, and more precisely the SAZ, hosted a population of *C. braarudii* during early spring 2003 to late summer 2004, which varied phenotypically with seasons. Throughout time the overall condition of

coccoliths and coccospheres was good, with presence of central bridge and not serrated edges. Even though this study cannot account for a winter population, results imply that there could be a small (perhaps dormant) population throughout winter and that the smaller, lighter phenotypes seen in early spring were remnants of this population.

C. braarudii concentrations varied together with chlorophyll *a*. These findings call for more research into the real contribution of coccolithophores in the primary productivity of the SAZ, particularly those holding large coccoliths such as *C. braarudii* and *Calcidiscus* ssp.

Coccolith and coccosphere concentrations were also correlated with WI and DSL, defining the combination of WI and morphometry as a proxy for seasonal physiological and morphological behaviour in coccolithophores. At a seasonal level, there appeared to be a constant allometric relationship between size and weight, and more research on the geological record may provide further insight the nature of this relationship at an evolutionary level, and in the biomineralization patterns of this species in the Southern Ocean.

Chapter 5 *Coccolithus braarudii* [(Gaarder, 1962) Baumann et al., 2003] during the late Quaternary: Calcification patterns from the Last Glacial Maximum to the present

Abstract

Fossil material from Tasman Sea Core MD972106 and sediment trap samples were examined for variations in the coccolith weight index (WI) and size of *Coccolithus braarudii* in order to reconstruct changes in calcification during the late Quaternary. Four discrete time intervals were assessed: the Last Glacial Maximum (LGM, 20.1-19.9 ka), deglaciation (16.2 - 15.6 ka), Holocene (4.2 - 3.1ka) and present (sediment trap samples, September, 2003-February, 2004). We compare these morphological data with independent proxies for ocean chemistry and temperature, in order to create chronological correlations. Results showed lighter, larger coccoliths during the LGM, which could imply an adaptation to glacial conditions. Holocene samples contained a smaller, but heavier phenotype, while a larger, heavier phenotype was predominant in the contemporary Tasman Sea. Sediment traps indicate that the allometry between coccolith size and weight in *C. braarudii* is not constant throughout time, but the shape of the coccoliths has undergone subtle changes. While variations in distal shield length (DSL) were correlated with environmental parameters such as SST, atmospheric CO_2 and [CO_3^{2-}], weight index (WI) was not related to any of these parameters. However, a calculation of shape based on a cubic relationship between WI and DSL (WI/DSL^3) produced correlations with SST and to a lesser extent to CO_2 and [CO_3^{2-}]. This provides evidence for phenotypic variation within coccoliths through time, and needs to be addressed when looking at intra-specific responses in coccolithophores.

5.1 Introduction

5.1.1 Historical carbon trends

The late Quaternary has seen major changes in global temperature, CO_2 levels and carbon species partitioning in the global oceans, with strong glacial-interglacial cycles for the past 100,000 years. The last glaciation reached its peak around 20,000 years ago (~ 20 ka), when atmospheric CO_2 was low with values around 190-200 ppm (Figure 5.1). During the period of deglaciation, CO_2 levels gradually rose with temperature to ~ 200 to 266 ppm, remaining relatively constant during the Holocene, reaching 283 ppm around 1000 years ago. Pre-industrial levels were around 270 ppm. Today, levels of CO_2 have reached ~ 390 ppmv. The bulk of the CO_2 will eventually be neutralized by carbonate ($CaCO_3$) dissolution in the deep marine environment. This is, however, a relatively slow process that operates on the time scale of ocean circulation (ca. 1000 yrs) and is therefore causing accumulation of CO_2 in the atmosphere (Erez, 2003). This rapid increase in atmospheric CO_2, and hence an increase in absorption into the ocean, has led to a shift in seawater pH, reducing carbonate ions and the calcite saturation state (Ω_{cal}) and its availability to marine calcifiers. Anthropogenic CO_2 enrichment of ~ 60 μmol kg^{-1} as dissolved inorganic carbon (DIC) in the subantarctic Southern Ocean corresponds to a carbonate ion concentration ($[CO_3^{2-}]$) decrease of ~ 36 μmol kg^{-1}, equivalent to a decrease in pH of 0.14 (Moy et al., 2009).

Recognition of the phenomenon of lowered ocean pH due to the oceanic uptake of excess atmospheric CO_2 (Caldeira and Wickett, 2003; Doney et al., 2009; The Royal Society, 2005), has stimulated widespread research aimed at understanding its impact on calcifying marine biota. Specific attention has been given to corals (Langdon and Atkinson, 2005; Tribollet et al., 2009), foraminifera (Dissard et al., 2010; Moy et al., 2009), and coccolithophores (Riebesell et al., 2000; Delille et al., 2005; Langer et al., 2006; Beaufort et al., 2011). One major outcome is the recognition of significant species-specific, as well as strain-specific (e.g. Langer et al., 2009), responses within taxonomic groups and between groups of organisms (Ries et al., 2009), preventing straightforward extrapolations of documented responses to future scenarios of climatic change. Ultimately, it is crucial for such

predictions to understand the effects of ocean acidification on entire biological communities (Riebesell et al., 2008; Ries et al., 2009).

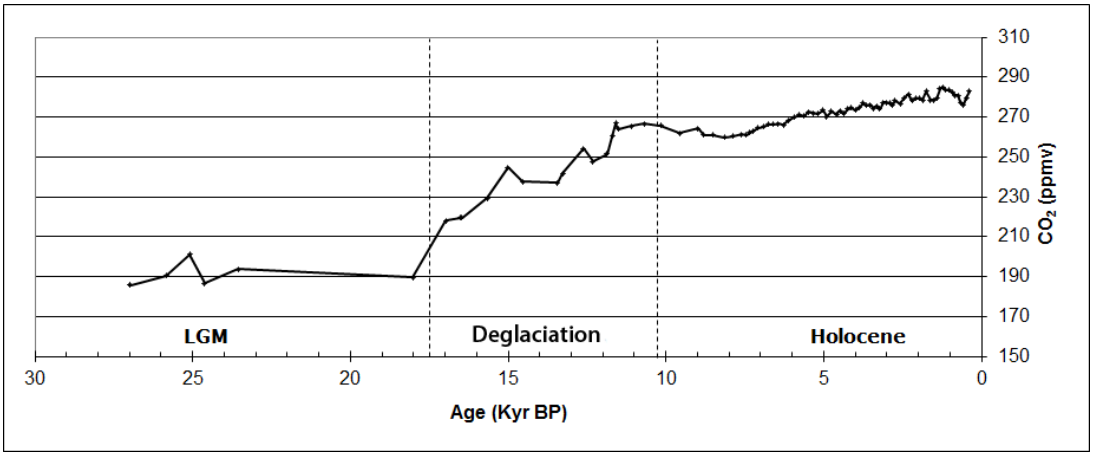

Figure 5.1. Atmospheric CO_2 (ppmv) reconstruction of the past 27 ka, from Taylor Dome records, plotted against air age, Antarctica. Data combined from (Indermuhle et al. (1999); (Smith et al., 1999)).

5.1.2 Nannoplankton-based paleoceanography in the Southern Ocean

The biogeography and floral composition of calcareous nannoplankton, which reflect the environmental signatures of surface waters, are an ideal proxy for the study of paleoceanography and paleoclimate in the Southern Ocean (Findlay and Flores, 2000). Nannoplankton assemblages have extensively been studied in this area of the Southern Ocean (Burns, 1975; Hiramatsu and DeDeckker, 1996, 1997a; Findlay and Giraudeau, 2000, 2002). Hiramatsu and DeDeckker (1997b) looked at assemblages in three cores located in the Tasman Sea. They observed that nannoplankton assemblages near the STF could be interpreted as a southern incursion of the STF during interglacial periods.

High coccolith concentrations in sediments may be the result of high coccolithophore productivity in surface waters, or due to low coccolith dissolution in water or at sediment/water interface, or both. Conversely, low coccolith accumulation may result from low surface-water productivity or high dissolution (Flores et al., 2003). Additionally, glacial-interglacial climate changes are documented by complementary climate records largely derived from deep sea sediments, continental deposits of flora, fauna and loess, and ice cores (Petit et al., 1999). Combined records of nannoplankton and past climatic variation are

important tools, and enable us to test hypotheses of biological strategies of adaptation in calcifying nannoplankton, which in turn can improve the understanding of present morphologies and help predict responses to future climatic change.

5.1.3 Purpose of this study

In this study, we examined the fossil record of the weight and morphometry of the coccolithophore *Coccolithus braarudii* [(Gaarder, 1962) Baumann et al., 2003], from Core MD972106 located on the South Tasman Rise (STR) (45^{o} 08.89'S; 146^{o} 17.12'E, 2334 m water depth), and compare this with extant populations recorded by sediment trap samples gathered in spring/summer 2003-2004, at 46^{o} 49.47'S, 141^{o} 38.73'E (SAZ Project, ACE CRC). Three discrete time intervals were analysed, the last glacial maximum (LGM), deglaciation, and late Holocene (core sediment), plus a fourth time interval comprising the period between September, 2003 to February, 2004 (sediment trap samples). These intervals were chosen because they cover substantial fluctuations in carbonate chemistry and temperature, among other environmental factors. In particular, late Holocene was chosen as an interval in which atmospheric and ocean carbonate chemistry was close to preindustrial values, but as far from maximum glacial values as possible. The scope of these samples also reflect the maximum preindustrial range (from Last Glacial Maximum to Holocene) of *Globigerina bolloides* (Moy et al., 2009), useful for later comparison. Additionally, we use environmental proxy data from planktonic foraminifera (Moy et al., 2009), and additional atmospheric CO_2 reconstruction from Taylor Dome, Antarctica, to create the recent history of calcification of *C. braarudii*, in order to relate response to past and present environmental conditions.

5.2 Materials and methods

5.2.1 Core sediment

Core MD972106 is located north of the STF, on the STR (45^{o} 09'S, 146^{o} 16'E, 3310 m water depth, Figure 1.6). MD972106 is a 32 m long piston core collected using

the CALYPSO Kullenberg corer on board the *Marion Dufresne* in 1997. The average sedimentation rate of the core was estimated at ~ 9.3 cm kyr^{-1} (Moy et al., 2006). The core was sampled every 5 cm at the Geoscience Australia core repository (Canberra). Raw sediment was weighed before and after oven-drying at 60^{o}C, and disaggregated with distilled water. Water saturated sediment samples were wet-sieved through a 150-μm mesh. The fine fraction (<150μm) samples were settled and oven dried (Moy et al., 2006). For full details on the stratigraphy, chronology and stable isotopic composition of the core, refer to Moy et al. (2006).

Three discrete intervals within the core were sampled, namely the end of the last glaciation, mid deglaciation period and mid to late Holocene (Table 5.1). For each interval, three depths were sampled with three replicates each, resulting in a total of 27 analysed samples. Smear slides were prepared with semi-dry sediment, by mixing a small amount with MQ water (pH 8.1) until a thick, homogenised paste was formed. This paste was thinly spread on the slide with the aid of a toothpick and immediately placed on a hotplate to dry. Slides were fixed with a drop of Eukitt® (Fluka Analytical) and a coverslip pressed firmly onto the slide, to ensure a single thin layer of material.

5.2.2 Sediment traps

Sediment trap samples prepared for morphometric analysis (Chapter 3) were also used in this study. These samples were collected from September 2003 to February 2004, 11 samples in total, with three replicates per sample. Refer to Chapter 3 for details on mooring and sample preparation for light microscopy (LM). Over 3000 individual coccoliths were measured. For statistical analysis, a subset of 900 randomly selected specimens was used, to allow for natural variations to be taken into account when comparing past and present samples, without the bias of a seasonal factor. For chronological analysis, samples were separated in three seasons, following results in Chapter 4.

5.2.3 **Estimate weight by birefringence**

Images were gathered with a Leica DM6000 cross-polarised microscope (LM) using

a 100x oil immersion objective lens with a Leica DFC420C colour camera. For each replicate, 100 images of individual coccoliths were gathered randomly, giving a total of 300 specimens per sample (N = ~ 300). Each coccolith was photographed both in cross-polars (POL) and brightfield (BF) modes. The modified method of birefringence was applied to images in POL (see Chapter 2). Calcification therefore is estimated as a weight index (WI).

5.2.4 Morphometric Measurements

Images in BF were used for morphometric measurements. Eight measurements were taken for each coccolith (100 specimens), using the software Image J; the length and width of the distal shield (DS), proximal shield (PS), central area (CA), and central opening (CO). From this measurement, whole area was calculated using the standard ellipse formula ($A= L/2 * W/2 * \pi$), resulting in DS area (DSA), PS area (PSA), CA area (CAA) and CO area (COA). Distal shield length (DSL) was consistently compared to WI following a combined approach of WI and morphometry.

Table 5.1**.** Sample depths (in cm) within Core MD972106, and corresponding age estimates (in ka).

Core MD972106	Core depth (cm)	Age (ka)
Late Holocene	13	3.1
	18	3.6
	23	4.2
Deglaciation	153	15.6
	158	15.9
	163	16.2
Last Glacial Maximum (LGM)	213	19.9
	218	20.7
	223	21.6

5.2.5 Environmental proxy data

Carbonate ions concentrations [CO_3^{2-}] were reconstructed from LGM and Holocene shell weight the foraminifers *G. inflata* and *G. bulloides* from Core MD972106, through linear regressions (Moy, 2005). Atmospheric CO_2 was reconstructed from isotopic composition at Taylor Dome, Antarctica (77^o 48'S, 158^o 43' E; 2374 m above sea level; accumulation rate, 7 cm ice equivalent per year) (Indermuhle et

al., 1999). Sea surface temperature was sourced from alkelone estimates (E. Calvo, unpublished data).

5.2.6 Statistical Analysis

Changes in calcification (as estimated by WI) and morphological parameters through time were analysed as a nested mixed model with the SAS System, which consisted of pair-wise comparison of time intervals for all parameters. The model was applied to all replicates within samples for the whole data set. The Tukey-Kramer test was used for test of significance. Primer 6 was used for Principal Component Analysis (PCA). Pair-wise linear regression models between morphological parameters and their correlations were produced in Excel 2010 and SPSS. Morphological data was transformed prior to analysis using the natural logarithm so that any non-linear, power-law allometry could be accommodated in log-linear regression models (Equation 4.1 and 4.2; see details in Chapter 4).

5.3 Results and interpretation

5.3.1 Changes in calcification and size

Statistical analysis showed no significant variation in DSL throughout the late Quaternary, but showed a significant change in DSL from Holocene to the present (Table 5.2). WI showed a significant change from LGM to present and from Holocene to present.

Table 5.2. Pair-wise comparison of distal shield length (DSL) and weight index (WI) between time intervals. Values in bold indicate a significant difference in either parameter between tested intervals, at $p<0.05$ (*) by Tukey-kramer test.

Time intervals pair-wise comparisons	**DSL**	**WI**
Holocene- LGM	0.16	0.98
Holocene- Present	**0.02***	**0.03***
Holocene-Trans	0.35	0.42
LGM-Present	0.58	**0.02***
LGM-Trans	0.28	0.28
Present-Trans	0.92	0.3

Chronological series (Figure 5.2a) and cross plots of mean WI and mean DSL (Figure 5.2b) showed that whilst coccoliths were largest during the onset of the LGM, their weight was significantly lower. During the mid and late LGM, mean coccolith DSL decreased. The deglaciation period between LGM and the Holocene also experienced an increase in size, followed by a steep drop at the beginning of the Holocene, when coccolith size remained relatively stable. During the LGM large coccoliths were associated with low WI, however for the remainder of the studied time series DSL was highly associated with WI (Figure 5.2a). From Holocene to present there was a significant increase in WI and DSL. Although the trend indicated that significant variations were driven by summer samples, a random subset of sediment trap samples (N = 900) (Table 5.2) implied that statistically significant variations from the past to the present were not the result of seasonality.

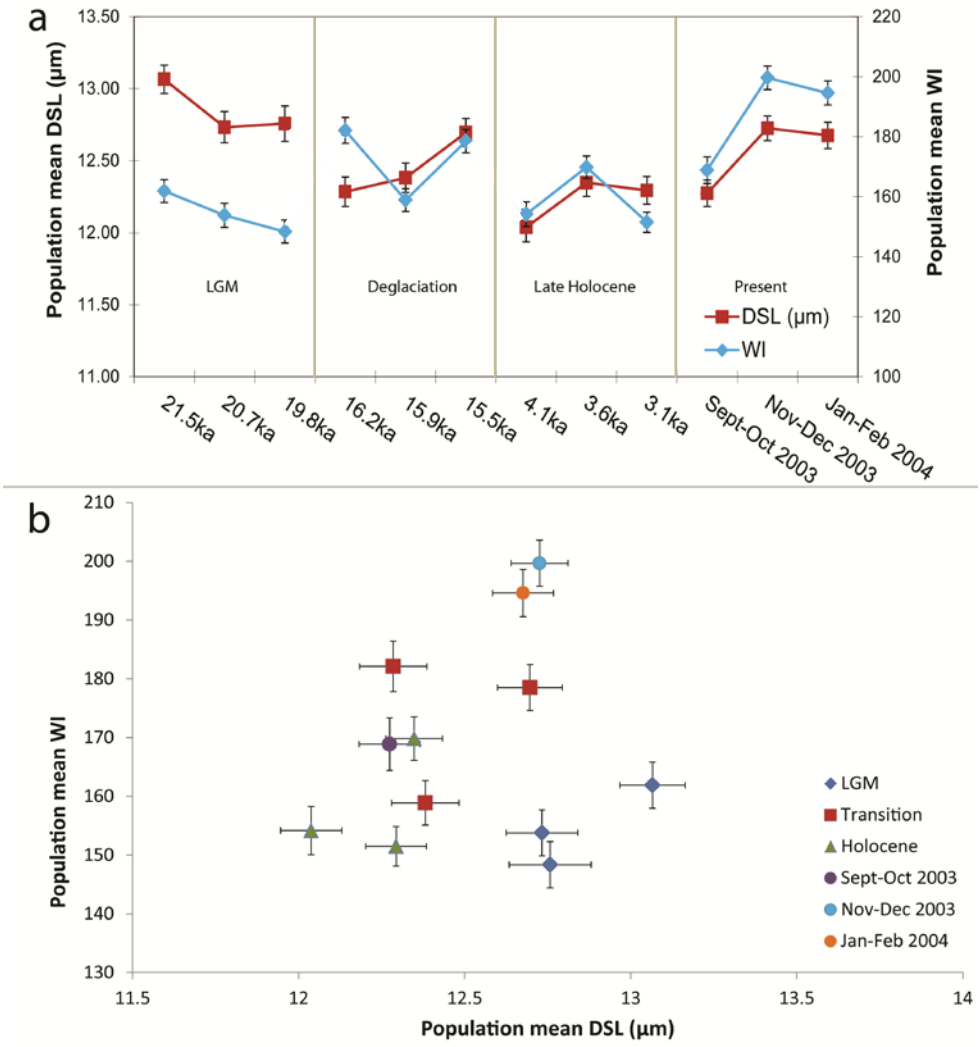

Figure 5.2. **(a)** Time series of *Coccolithus braarudii* mean weight index (WI) and mean distal shield length (DSL) (µm) from the onset of the LGM to the late Holocene, and from September 2003 to February 2004, grouped in seasonal populations. **(b)** Cross plot of population mean WI and population mean DSL. Error bars for WI and DSL are ± 1 s.e.

5.3.2 Overall morphometric variability

Coccolith area was calculated from lengths and widths of all coccolith features, in order to look at general morphological variability. Pair-wise comparisons of time intervals (Table 5.3) showed an overall significant variability in DSA, PSA, CAA and WI. There was no significant variability in DSA from fossil material to modern one, in contrast to the variability in DSL (Table 5.2). PSA and CAA remained statistically constant throughout the Quaternary, with their overall significant variation exclusively driven by significant changes from geological times to present. WI also showed a significant change from LGM and Holocene to present.

Table 5.3. Pair-wise comparison of distal shield area (DSA), proximal shield area (PSA), central area area (CAA), central opening area (COA) and weight index (WI), between time intervals. Values in bold indicate significance at p<0.05(*), and at p<0.001 (**) by Tukey-Kramer test.

Time intervals pair-wise comparisons	DSA	PSA	CAA	COA	WI
Overall p	**0.02***	**0.0005****	**0.01***	0.21	**0.01***
Holocene- LGM	**0.01**	0.83	0.56	0.99	0.98
Holocene- Present	0.14	**0.001****	**0.01***	0.95	**0.03***
Holocene-Trans	0.65	0.53	0.45	0.27	0.42
LGM-Present	0.42	**0.0006****	**0.06***	0.87	**0.02**
LGM-Trans	**0.08***	0.19	0.99	0.21	0.28
Present-Trans	0.62	**0.007****	**0.08***	0.46	0.3

Results are synthesised in Figure 5.3, where sediment samples have been merged into one data point. Figure 5.3 shows the heaviest coccoliths happening at the highest levels of atmospheric CO_2, in present time. There is overall high variability in WI between samples among ages, with the deglaciation period showing the highest variability.

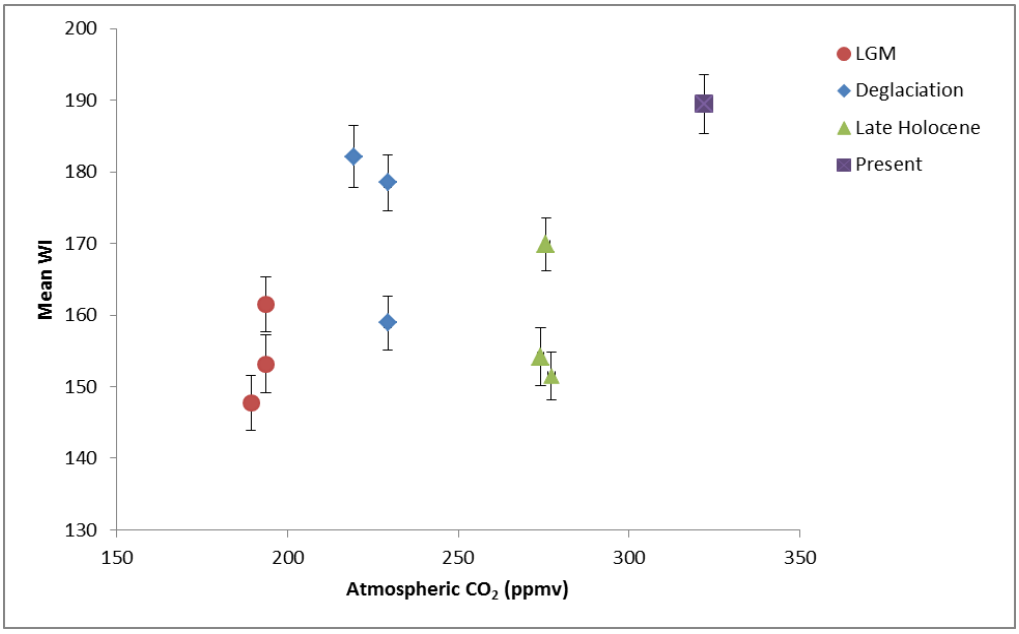

Figure 5.3. Correlation between mean WI and atmospheric CO_2 (ppmv) from the last glacial maximum (LGM) to the present. Sediment trap samples have been merged into one data point for comparison.

Principal component analysis (PCA) of mean variability among time intervals is shown in Figure 5.4. PC 1 and 2 together contributed to 84% of the variability. The bulk of the variation ran along PC 1 (64%) with CAA and WI as major contributors. The heaviest coccoliths (high WI) had large CAA, and were observed in trap

samples during summer. The LGM and Holocene populations had similar loadings on PC 1, grouping at lighter WI and smaller CAA. This is consistent with the pair-wise comparisons (Table 5.3), where these time intervals differed only in DSA, which only contributed in the variation along PC 3. Although COA showed no significant variability, it contributed mainly to PC 2 along with PSA, showing that COA was at its smallest during the transition between late winter/early spring populations, while PSA was at its smallest in sediment trap samples, explaining its significant differences from the late Quaternary to the present in Table 5.3.

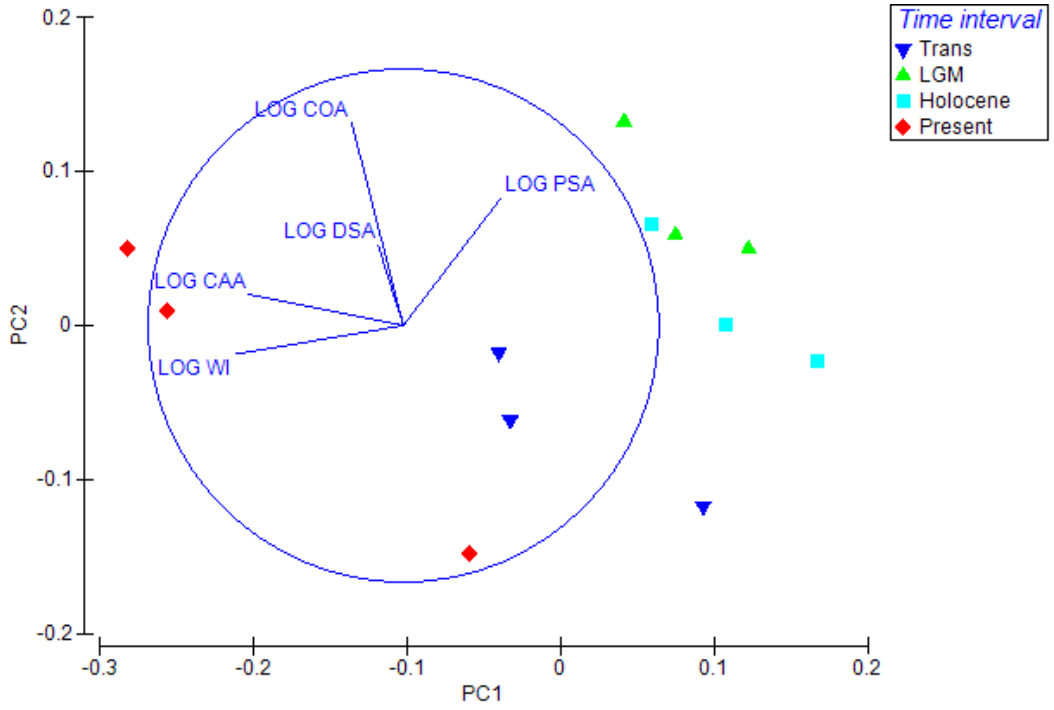

Figure 5.4. Principal component analysis (PCA) of mean morphometrical parameters for different time intervals; 82.9% of the morphological variation is explained by PCA 1 and 2. Data have been transformed by natural logarithm.

5.3.3 Size determined variability

Percentile values were calculated in each sample for DSL, WI, DSA, PSA, CAA and COA, in order to depict size-determined variations among coccoliths, i.e. to test whether coccoliths of different sizes might display different phenotypic responses through time. Cross plots between WI and DSL for each percentile (Figure 5.5) all showed a similar pattern as for population mean values (Figure 5.2b), with lightly

calcified coccoliths during the LGM, but at similar DSL to that of present-day coccoliths - no matter whether coccoliths were large or small, there was a significant offset in weight between these time intervals. There was also a clear difference between early spring and summer populations in the sediment traps, in both WI and DSL, although not as marked for the larger and heavier coccoliths (as depicted by the 95th percentile).

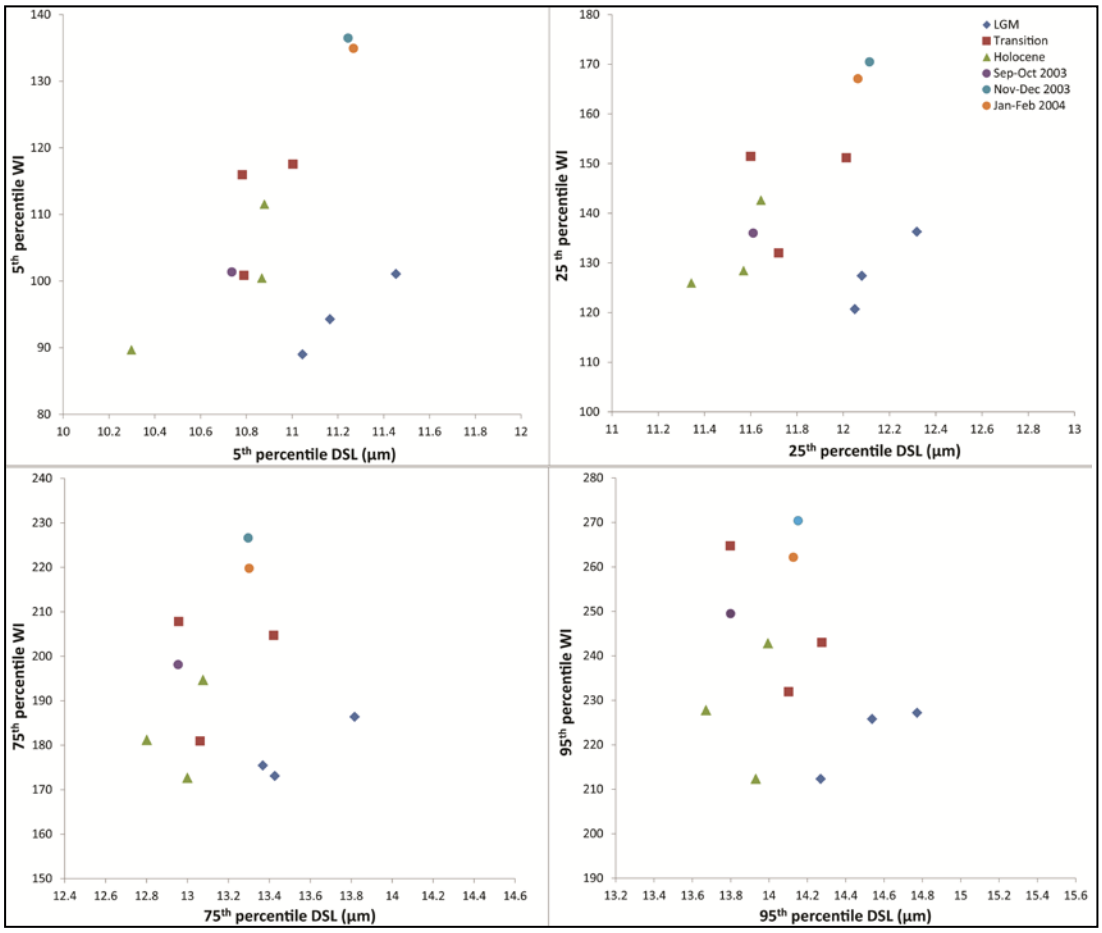

Figure 5.5. Cross plots of WI and DSL (µm), for the 5th, 25th, 75th and 95th percentiles of each parameter for the four time intervals. Sediment trap samples are separated into three seasonal sub-samples, following previous observations (Chapter 4).

The deglaciation period tended to have intermediate values of those of late Holocene and sediment trap samples. In summary, the smaller size fraction showed a more distinctive signal of variation, and in this case it could drive the population's mean up (or down). The most obvious signal however lies in the consistent difference between Holocene and LGM specimens driven by both DSL and WI.

PCAs were performed for each percentile of each morphological parameter (Figure 5.6). Overall, percentiles varied consistently through time. The 5th percentile revealed a weak variation running along PC 2. For the 25th percentile value, there was a clear variation between the morphology of coccoliths in the LGM and late Holocene running along PC 1. PC1 and 2 explained 82% of the variation, while 11% of the variation was explained by COA in PC 3.

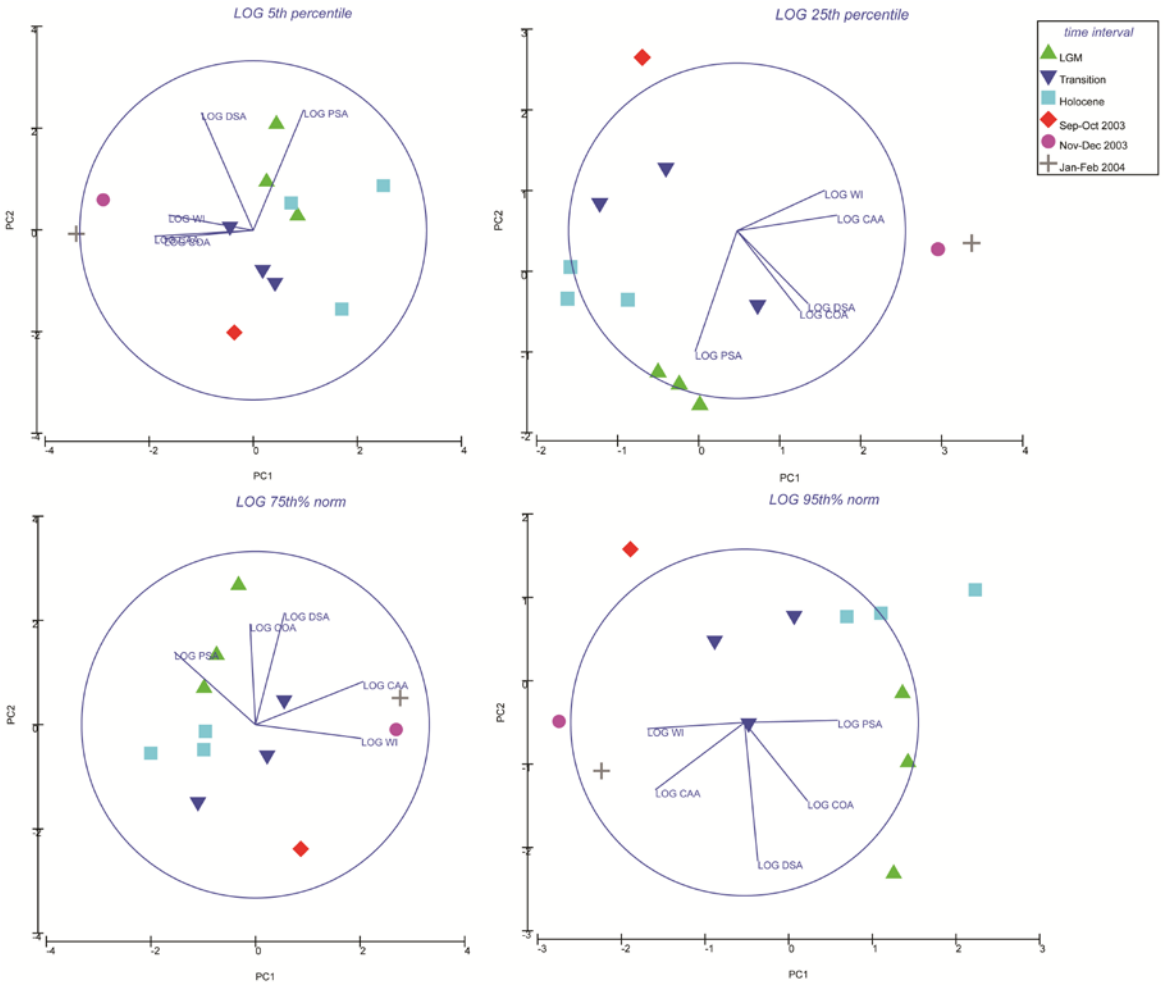

Figure 5.6. PCAs of percentiles of morphological parameters, from the late Quaternary to the present. Results are in natural logarithm.

Variations in morphology of the 75th and the 95th percentile ran along PC 2. WI and CAA had scores in PC 1, DSA contributes mainly along PC 2, and COA along PC 3. There was 79% cumulative variation for PC 1and 2 in the 75th percentile and 78% of cumulative variation for PC 1 and 2 in the 95th percentile. The overall spread of the percentiles revealed that small-sized coccoliths belonged to a more stable

phenotypic population within the time intervals, while the largest size coccolith showed the largest variation within populations.

It is important to note that this consistency between percentiles and the population means indicates that the whole population varied across time intervals. Trends observed in PCA were congruent with statistical comparison (Table 5.3) with WI being the main driver of the variation. Significant variations in DSA and PSA were also present in Figure 5.6. COA became consistently smaller during the peak of the deglaciation period and the end of the Holocene. However these variations were not statistically significant (Table 5.3).

5.3.4 Environmental variability

Proxy environmental parameters are displayed in a chronological time series (Figure 5.6). SST sourced from alkenone estimates (E. Calvo, unplublished data) was ~ 8 ^{o}C during the LGM increasing to 9.7 ^{o}C at the end of this period (for details in proxy SST refer to Moy et al. (2009)). During the deglaciation, SST remained stable at ~ 12 ^{o}C, and ~ 13 ^{o}C during the Holocene. During early spring 2003, SST was 9.5 ^{o}C, increasing to 10.7 ^{o}C in early summer and to 12 ^{o}C in late summer (Figure 5.7). Levels of atmospheric CO_2 were relatively stable within geological time intervals, from ~ 193 ppmv during the LGM to ~ 270 ppmv during the Holocene (Indermuhle et al., 1999; Smith et al., 1999). There has been an increase of ~ 13% in atmospheric CO_2 from the Holocene to the present, with seasonal fluctuations ranging from ~ 300 to ~ 318 ppmv. Reconstructed [CO_3^{2-}] was also stable, with a steady decline from ~ 290 μM kg^{-1} during the LGM, to ~ 220 μM kg^{-1} during the late Holocene. At present there has been an overall ~ 30% decline in [CO_3^{2-}]; during the seasonal interval, [CO_3^{2-}] increased by ~ 11 % from early spring to summer ranging from ~ 154 to ~ 173 μM kg^{-1}.

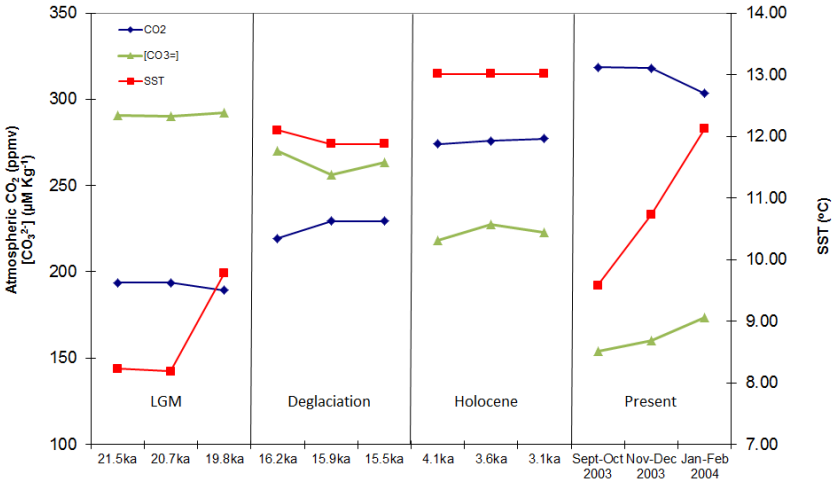

Figure 5.7. Chronology of CO_3^{2-} concentrations ([CO_3^{2-}] in µM kg^{-1}), atmospheric CO_2 (ppmv) and SST (^oC) (proxy and *in situ* for core sediment and sediment trap samples, respectively) for discrete time intervals: LGM, deglaciation, Holocene and spring - summer 2003-2004.

A correlation matrix (Table 5.4) between morphometric parameters and environmental data throughout time intervals showed that changes in mean DSL were highly correlated with SST, followed by [CO_3^{2-}] and atmospheric CO_2, and that it did not correlate with DIC. There was no correlation between WI and any environmental variables, including carbon species. In terms of morphological correlations, there was no correlation between WI and DSL, or any other size parameter - confirming that shape has changed between the studied populations. This finding implies that the allometry between coccolith size and weight was not constant for *C. braarudii* due to differences in the degree of calcification. There was however a negative correlation between COA and DIC.

Table 5.4. Correlation matrix of environmental and morphological parameters. Bold correlation coefficients are predicted correlation, highlighted correlation coefficients are significant correlations between environment and morphological variable. Morphological parameters, atmospheric CO_2, DIC and $[CO_3^{2-}]$ are in natural logarithm.

	LOG WI	LOG GL_CA	LOG DSL	LOG DSA	LOG PSA	LOG CAA	LOG COA	LOG $[CO_3^{2-}]$ ($\mu M\ kg^{-1}$)	LOG CO_2 (ppmv)	SST (°C)
LOG WI	1									
LOG GL_CA	0.40	1								
LOG DSL	-0.11	-0.05	1							
LOG DSA	-0.15	0.00	**0.99**	1						
LOG PSA	-0.19	-0.01	**0.61**	**0.66**	1					
LOG CAA	0.47	0.05	0.54	0.53	0.15	1				
LOG COA	-0.18	-0.42	0.10	0.17	0.34	-0.04	1			
LOG $[CO_3^{2-}]$ ($\mu M\ kg^{-1}$)	0.05	-0.22	**0.86**	**0.82**	0.19	**0.65**	0.06	1		
LOG CO_2 (ppmv)	0.07	0.31	**-0.85**	**-0.81**	-0.19	-0.61	-0.08	**-0.99**	1	
SST (°C)	0.25	0.29	**-0.90**	**-0.91**	-0.49	-0.49	-0.30	**-0.87**	**0.90**	1

Correlations between WI and DSL with the most relevant parameters expressed in Table 5.4 (SST, $[CO_3^{2-}]$ and atmospheric CO_2) are represented in cross plots, in addition to age (ka). DSL correlated with all parameters (Figure 5.8). In contrast, there was no correlation between WI and environmental parameters, including age (Figure 5.9).

Amid these results, it was crucial to record how whole coccolith shape varied in response to carbon chemistry and temperature. Coccolith shape could be calculated in the form of a calcification index (CI) through the following equation (Young, 2011, pers. comm.):

$$CI = WI/DSL^3 \qquad \text{Equation 5.1}$$

The cubic fit will add an estimation of how the allometric relationship between WI and DSL responded to environmental changes.

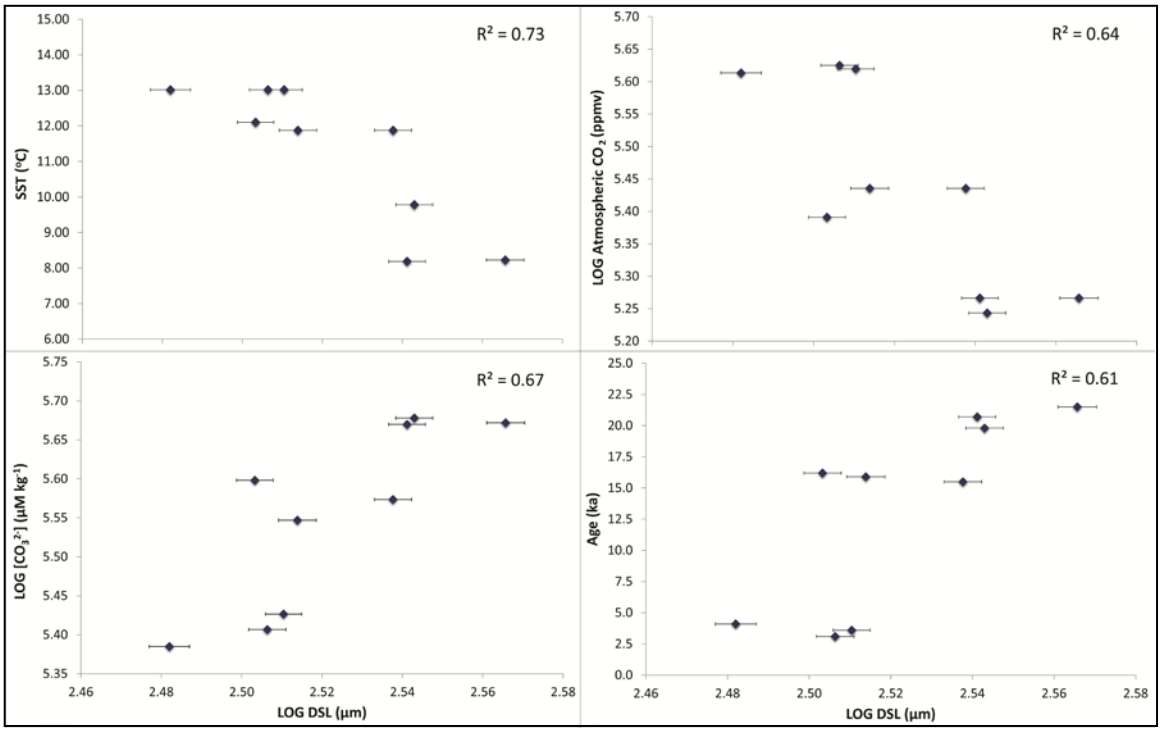

Figure 5.8. DSL response to SST (°C), atmospheric CO_2 (ppmv), CO_3^{2-} concentrations ($[CO_3^{2-}]$ in µM kg^{-1}), and age (ka) through LGM, deglaciation and Holocene (three samples per time interval, N= ~ 300 per sample). DSL, SST, atmospheric CO_2 and $[CO_3^{2-}]$ have been transformed by natural logarithm. Environmental variables are available for each data point only, therefore no error bars are available. Error bars for DSL are ± 1 s.e.

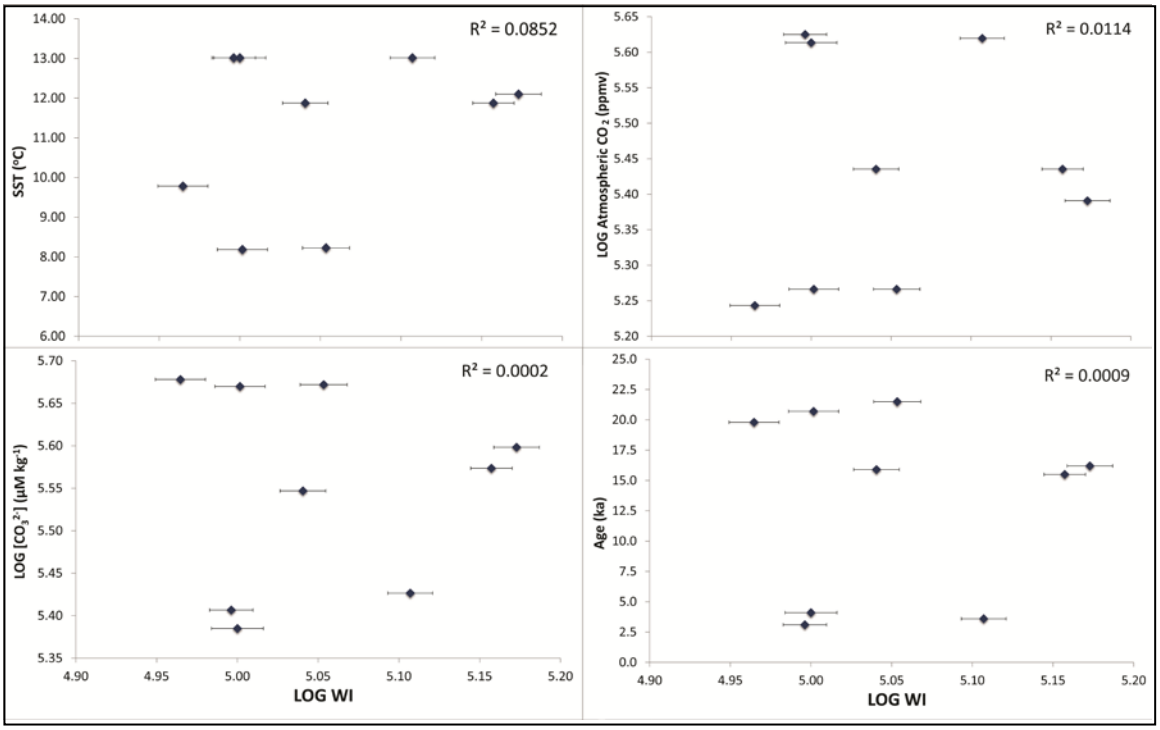

Figure 5.9. WI response to SST (°C), atmospheric CO_2 (ppmv), CO_3^{2-} concentrations ($[CO_3^{2-}]$ in µM kg^{-1}), and age (ka) through LGM, deglaciation and Holocene (three samples per time interval, N= ~ 300 per sample). WI, SST, atmospheric CO_2 and $[CO_3^{2-}]$ have been transformed by natural logarithm. Environmental variables are available for each data point only, therefore no error bars are available. Error bars for WI are ± 1 s.e.

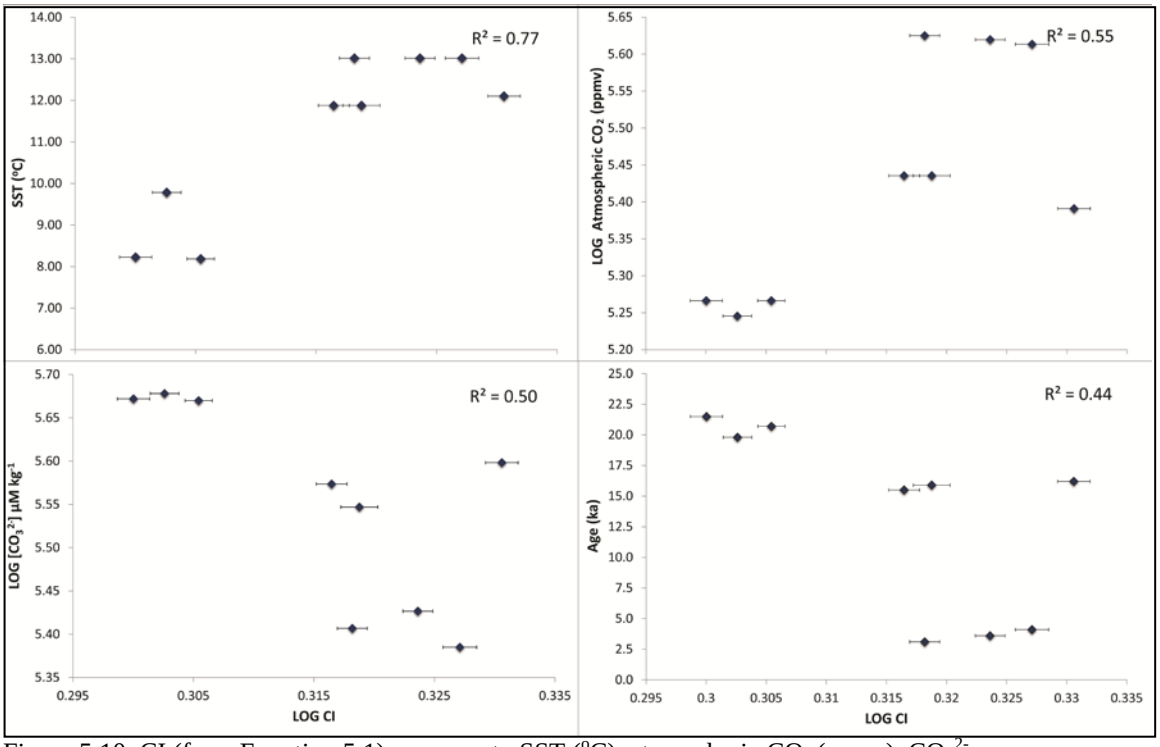

Figure 5.10. CI (from Equation 5.1) response to SST (°C), atmospheric CO_2 (ppmv), CO_3^{2-} concentrations ($[CO_3^{2-}]$ in µM kg^{-1}), and age (ka) through LGM, deglaciation and late Holocene (three samples per time interval, N= ~ 300 per sample). CI, SST, atmospheric CO_2 and $[CO_3^{2-}]$ have been transformed by natural logarithm. Environmental variables are available for each data point only, therefore no error bars are available. Error bars for CI are ± 1 s.e.

The lowest CI was recorded during the LGM, and the highest during the late Holocene, congruent with estimation of weight by WI (Figure 5.10). A positive correlation between shape and SST was recorded ($R^2 = 0.77$), where low CI was associated with low temperature. There was a slight positive correlation with atmospheric CO_2 ($R^2 = 0.55$), with low CI during the LGM, when atmospheric CO_2 was at its lowest. $[CO_3^{2-}]$ recorded a slight negative correlation ($R^2 = 0.5$), with high concentrations associated with low CI. These relationships may indicate that allometric relationships between WI and DSL might be responsive to change in carbon chemistry and SST.

5.4 Discussion

5.4.1 Assessment of comparative analysis

Before comparing data derived from fossil and extant material, a number of issues

need to be considered. The time period of collection of sediment trap samples represented only a snap shot compared with several years of deposition of fossil nannoplankton (e.g. Hiramatsu and DeDeckker, 1996). Sedimentation rates and bioturbation (mixing of sediment by borrowing benthos) determine the temporal resolution of sediment cores, influencing the number of integrated years represented in morphological studies, particularly in studies using highly sensitive methodology such as the one used here. Additionally, it is difficult to distinguish between the original calcification responses to chemical changes in the surface ocean and post-mortem conditions at the sea floor (Honisch et al., 2012) due to (partial) dissolution resulting from sedimentation. As observed in Chapter 2, SEM observations throughout the core sediment samples can confirm that dissolution was highly unlikely, and this should be expected when taking into account the location of the core above the calcite saturation horizon, estimated in this area at ~ 4030 m.

An additional problem arises when trying to compare environmental proxy data with biological observations. The lack of resolution of the environmental proxy data does not account for all biological data collected in this study. Furthermore, changes in the physical and chemical systems range from season to thousands of years, whereas the adaptation time of quantifiable aspects of the biosphere (biomass, productivity, abundance) may range from the ecological time-scale of days to the evolutionary time scale of millions of years (Thierstein et al., 2004). Therefore, establishing environmental correlations at discrete points at the geological levels need to be interpreted with care. Nevertheless, the reliability of the biological data lies in the number of observations, which will inevitably decrease the error. Ultimately, this is the first study to document comparative analyses based on fossil material and sediment trap samples in the Southern Ocean and offers some first valuable insights into the intra-specific calcification responses of *C. braarudii* at multiple time scales and in natural settings.

5.4.2 Morphological changes in C. braarudii *over the past 20,000 years*

Calcification (WI) of modern *C. braarudii* coccoliths has significantly increased (not decreased) since the late Holocene, and so has DSL. As in the modern samples, DSL followed the trend of WI except for a marked discrepancy in the LGM

populations, when low mean WI (~ 155 - 160) coincided with large mean DSL (~ 12.7 - 13µm), similar to DSL seen in sediment trap samples (Figure 5.2), indicating that the allometric relationship between WI and DSL was not constant throughout all time intervals. Lighter, larger coccoliths during the LGM may be the result of a morphological strategy by which low calcification acts as a trade-off for larger coccoliths, in order to achieve optimum adaptation to the prevailing conditions. During the Holocene, when most environmental conditions were opposite to those of the LGM, i.e., higher SST, lower [CO_3^{2-}], higher atmospheric CO_2, morphological changes showed that another phenotype may have arisen, with smaller, but heavier coccoliths, compared to LGM coccoliths. Even though there were significant variations among the three examined time intervals, DSA did not vary from the late Holocene to present-day ($p = 0.14$), while WI showed a significant increase from the LGM and from late Holocene to present ($p<0.05$).

Additionally, there was a significant decrease in PSA from geological times to present (Table 5.3), while there was an increase in DSL and relatively stable DSA across the time intervals. This was a further indication that coccolith morphology does not vary proportionally through time and that each parameter could be adapting independently to fulfil different roles.

Percentile variations showed that although the most stable within percentiles, the small size fraction (5^{th} percentile) is the source of most variation compared with the remainder percentiles (Figure 5.5), and that small-sized coccoliths might be in this case putting a bias on the mean. This is an issue that needs to be taken into consideration when looking at coccolith mean variation. Therefore percentile analysis is strongly recommended for this type of biometric investigations.

5.4.3 **C. braarudii** *in response to carbon chemistry*

While DSL appears highly correlated to changes in SST, CO_2 and [CO_3^{2-}] (Table 5.4), WI did not correlate to these or any particular environmental factor (Figure 5.9), however present-day coccoliths do show an overall increase in size and weight, and the highest WI of *C. braarudii* coincides with the highest levels of atmospheric CO_2 since the LGM (Figure 5.3). In agreement with laboratory studies which showed that *C. braarudii* was not responsive to carbon chemistry compared with other

species such as *Calcidiscus* spp. (Langer et al., 2006), the present field study indicated that coccolith weight, and thus net calcification, was not responsive to changes in carbon chemistry, and that variations in WI must be induced by a combination of factors. At the present conditions of high atmospheric CO_2, high temperature and low [CO_3^{2-}], which are unprecedented for at least the past ~ 20,000 years, it would appear that a phenotype has arisen that is heavier and larger, which might enable the cell to thrive under the present conditions.

DSA did not vary from the late Holocene to present-day ($p = 0.14$), yet DSL significantly increased ($p<0.05$), and WI recorded a significant increase from the LGM and from late Holocene to present ($p<0.05$). Allometric relationships need to be taken into account when studying responses in morphology, particularly at a geological scale. The decoupling between WI and DSL has contributed to the conclusion that allometry between morphological parameters can vary through time (see Figure 2.8). Furthermore, it has provided a powerful tool to demonstrate how shape, in the form of calcification index (CI; Young, 2011, pers. comm.) may be influenced by environmental parameters. Low CI values are associated with low levels of CO_2, high [CO_3^{2-}] and low SST during the LGM, whilst a high CI was associated with opposite conditions during the late Holocene, even though this time interval was associated with small coccolith size. This could imply that coccolith formation in *C. braarudii* does respond to particular environmental conditions, whereby coccolithophores have the ability to vary the shape of their coccolith by decoupling size and weight, allowing this species to tolerate various conditions through time.

5.5 Conclusions

Coccolith weight (WI) in *C. braarudii* in the Southern Ocean, south of Tasmania, has significantly increased from the late Quaternary to the present, but showed no significant correlations with environmental proxy data. This result appears consistent with previous research stating that the *Coccolithus* genus might be more insensitive to changes in carbon chemistry composition in the ocean, compared with other coccolithophores. Results showed that larger, lighter coccoliths dominated the

LGM, which might have been an adaptation to glacial conditions. These were replaced by smaller, yet heavier coccoliths during the late Holocene, when opposite conditions prevailed to those seen in the LGM, in terms of temperature, atmospheric CO_2 and $[CO_3^{2-}]$.

Allometric relationships have proven to be non-constant in a geological time scale (the past 20,000 years), and consideration needs to be given to morphological parameters independently in order to fully understand the morphological plasticity of this species.

Finally, the quantification of coccolith shape through the calculation of CI could be a useful tool to reconstruct the morphometry of coccoliths, combining WI and DSL in order to depict real signals in morphometric variability of coccolithophores in response to environmental changes through time.

Further research is crucial for extrapolation of these results to other areas of the Southern Ocean as well as proper extrapolation of morphological responses by other coccolithophore species.

Chapter 6 General conclusions

Coccolithophores are a crucial component in the primary productivity of oceans and the consequences of increased CO_2 intake and ocean acidification are yet to be clarified among different coccolithophore species. Hence, the debate on the methodologies used to estimate the calcification of coccolithophores in the fossil record and extant sampling material remains current.

The use of calcite birefringence of the central area (CA) as a weight reference in *Coccolithus pelagicus* (*sensu lato*) provides a useful tool for a range of sampling sources, including down-core sediments, sediment traps and culture material. It is a consistent weight reference which allows for comparison of coccolith calcification to carbonate chemistry from proxy estimates as well as in culture and *in situ*. Most importantly, the decoupling of coccolith length from weight, provided by the estimation of WI, will allow recognition of how each morphological parameter of coccoliths are most affected by changes in carbonate chemistry and other environmental variables, thus unravelling intra-specific phenotypic variability in ancient and modern coccolithophores.

Recently, Lohbeck et al. (2012) found that *E. huxleyi*, previously presumed to be vulnerable to changes in oceanic pH in the short term, responded positively to long-term changes in carbon chemistry. Yet again, response of *E. huxleyi* to carbon chemistry should not be extrapolated to other species. Therefore, a pressing issue is the lack of comparative analysis with other large coccolithophore taxa, namely of *Calcidiscus* species present in the core and in sediment trap samples, which could not be undertaken in the framework of this thesis. If WIs of *Calcidiscus* are calculated, this would certify the consistency of this methodology. Such a parallel study would also deliver some clues, by comparing morphological variations and adaptive strategies of species which have evolved under different carbonate conditions, as suggested by Henderiks and Rickaby (2007).

Having achieved a consistent method of assessment, urgent focus needed to be allocated to the confirmation of presence and identification of *Coccoliths* species in

the Southern Ocean, before tackling its geological history, in consideration to past contradicting observations. For this, recent sediment trap samples were used, and results concluded that the Southern Ocean, south of Tasmania, hosted a population of the now recognised *C. braarudii* (Gaarder, 1962) Baumann et al., 2003, during early spring 2003 to late summer 2004, based on sediment trap data.

These sediment trap samples also provided a crucial opportunity to study the seasonality and morphological variability of *C. braarudii* throughout a continuous period of time. The population observed from early spring 2003 to late summer 2004, varied phenotypically throughout this time series, with smaller, lighter phenotypes seen in early spring, and larger, heavier phenotypes in late spring and summer.

Cell concentrations varied together with *in situ* chlorophyll *a* during this period, also correlating with WI and DSL. This finding further endorses WI and morphometry as a combined proxy for seasonal, physiological and morphological behaviour in coccolithophores.

The recent geological history of the genus C*occolithus* was next addressed, and results were compared with those observed in the sediment trap samples. Coccolith weight (WI) in *C. braarudii* in the Southern Ocean, south of Tasmania, has significantly increased (not decreased) from the late Quaternary to the present. However, WI does not respond to changes in carbonate chemistry, further confirming that this genus could be insensitive to changes in ocean chemistry composition.

In the studied core, larger, yet lighter coccoliths dominated during the LGM, presumably as a response to tolerate glacial conditions. The rise of smaller, yet heavier coccoliths during the Holocene might therefore confirm that this species expresses mechanisms of adaptation to tolerate conditions opposite to the ones seen in the LGM, in terms of SST, atmospheric CO_2 and $[CO_3^{2-}]$.

Allometric relationships, i.e. variations in size with shape, were deemed relevant and therefore analysed in this study. At a seasonal level, there seemed to be constant allometry between size and weight. However the allometry of this species throughout geological time scale was found to be non-constant, where shape varied irregularly with size on three specific time intervals. This further stresses the

need to study coccolith morphological parameters independently in order to fully understand the plasticity of this species.

Additionally, the concept of shape through the calculation of calcification index (CI) in *C. braarudii* can serve as a useful tool to reconstruct coccolith morphometry, combining WI and DSL in order to depict morphometric variability of coccolithophores in response to environmental changes through time.

This study only tackles the morphology of this species during three time intervals over the past 20 ka; however we provide the necessary tools to look at the whole morphological history of this species and unravel the mechanisms of its survival since its evolution during the Palaeocene (Haq and Lohmann, 1976), as the present findings give us some clues in order to explain the success of this species for the last 63 Ma. It will also be crucial to investigate changes in morphology, with the same methodology, in other geographical settings. More cores in various locations throughout the Southern Ocean would be ideal to put this methodology to the test and improve our knowledge of the evolution of *C. braarudii* and the whole coccolithophore community in the Southern Ocean. Additionally, annual sediment trap samples of several years would be optimal to depict further seasonal and inter-annual variability in WI, DSL and fluxes. This would enable us to see if the variability observed in the core is due to real evolutionary changes or seasonal changes within the time intervals. Additionally, more explicit data of other parameters such as nutrient composition would help clarify what are the parameters, or combination of parameters, are the drivers of *C. braarudii*'s morphological evolution.

Chapter 7 References

Anderson, R.F., Ali, S., Bradtmiller, L.I., Nielsen, S.H.H., Fleisher, M.Q., Anderson, B.E., Burckle, L.H., 2009. Wind-Driven Upwelling in the Southern Ocean and the Deglacial Rise in Atmospheric CO(2). Science 323, 1443-1448.

Andruleit, H., 1997. Coccolithophore fluxes in the Norwegian-Greenland Sea: Seasonality and assemblage alterations. Marine Micropaleontology 31, 45-64.

Archer, D., Winguth, A., Lea, D., Mahowald, N., 2000. What caused the glacial/interglacial atmospheric pCO(2) cycles? Reviews of Geophysics 38, 159-189.

Aubry, M.P., 2007. A major Pliocene coccolithophore turnover: Change in morphological strategy in the photic zone, in: Monechi, S., Coccioni, R., Rampino, M. (Eds.), Large Ecosystem Perturbations: Causes and Consequences. Geological Soc Amer Inc, Boulder, pp. 25-51.

Balch, W.M., Drapeau, D.T., Bowler, B.C., Lyczskowski, E., Booth, E.S., Alley, D., 2011. The contribution of coccolithophores to the optical and inorganic carbon budgets during the Southern Ocean Gas Exchange Experiment: New evidence in support of the "Great Calcite Belt" hypothesis. Journal of Geophysical Research-Oceans 116.

Baumann, K.-H., Freitag, T., 2004. Pleistocene fluctuations in the northern Benguela Current system as revealed by coccolith assemblages. Marine Micropaleontology 52, 195-215.

Baumann, K.H., 2004. Importance of size measurements for coccolith carbonate flux estimates. Micropaleontology 50, 35-43.

Baumann, K.H., Andruleit, H.A., Samtleben, C., 2000. Coccolithophores in the Nordic Seas: comparison of living communities with surface sediment assemblages. Deep-Sea Research Part Ii-Topical Studies in Oceanography 47, 1743-1772.

Beaufort, L., 2005. Weight estimates of coccoliths using the optical properties (birefringence) of calcite. Micropaleontology 51, 289-297.

Beaufort, L., Dollfus, D., 2004. Automatic recognition of coccoliths by dynamical neural networks. Marine Micropaleontology 51, 57-73.

Beaufort, L., Heussner, S., 1999. Coccolithophorids on the continental slope of the Bay of Biscay - production, transport and contribution to mass fluxes. Deep-Sea Research Part Ii-Topical Studies in Oceanography 46, 2147-2174.

Beaufort, L., Probert, I., de Garidel-Thoron, T., Bendif, E.M., Ruiz-Pino, D., Metzl, N., Goyet, C., Buchet, N., Coupel, P., Grelaud, M., Rost, B., Rickaby, R.E.M., de Vargas, C., 2011. Sensitivity of coccolithophores to carbonate chemistry and ocean acidification. Nature, DOI 10.1038/nature10295, in press.

Belkin, I.M., Gordon, A.L., 1996. Southern Ocean fronts from the Greenwich meridian to Tasmania. Journal of Geophysical Research-Oceans 101, 3675-3696.

Boeckel, B., Baumann, K.H., 2004. Distribution of coccoliths in surface sediments of the south-eastern South Atlantic Ocean: ecology, preservation and carbonate contribution. Marine Micropaleontology 51, 301-320.

Bollmann, J., 1997. Morphology and biogeography of Gephyrocapsa coccoliths in Holocene sediments. Marine Micropaleontology 29, 319-350.

Borges, A.V., Tilbrook, B., Metzl, N., Lenton, A., Delille, B., 2008. Inter-annual variability of the carbon dioxide oceanic sink south of Tasmania. Biogeosciences 5, 141-155.

Bown, P.R., 2005. Calcareous nannoplankton evolution: a tale of two oceans. Micropaleontology 51, 299-308.

Bown, P.R., Lees, J.A., Young, J.R., 2004. Calcareous nannoplankton evolution and diversity through time, in: Thierstein, H.R., Young, J.R. (Eds.), Coccolithophores: From Molecular Processes to Global Impact. Springer, London, p. 565.

Bown, P.R., Young, J.R., 1998. Introduction, in: Bown, P.R. (Ed.), Calcareous nannofossil biostratigraphy. Chapman and Hall, London, pp. 1-15.

Boyd, P.W., Trull, T.W., 2007. Understanding the export of biogenic particles in oceanic waters: Is there consensus? Progress in Oceanography 72, 276-312.

Broecker, W.S., 1997. Thermohaline circulation, the Achilles heel of our climate system: Will man-made CO2 upset the current balance? Science 278, 1582-1588.

Broerse, A.T.C., Brummer, G.J.A., Van Hinte, J.E., 2000a. Coccolithophore export production in response to monsoonal upwelling off Somalia (northwestern Indian Ocean). Deep-Sea Research Part Ii-Topical Studies in Oceanography 47, 2179-2205.

Broerse, A.T.C., Ziveri, P., Honjo, S., 2000b. Coccolithophore (-CaCO(3)) flux in the Sea of Okhotsk: seasonality, settling and alteration processes. Marine Micropaleontology 39, 179-200.

Broerse, A.T.C., Ziveri, P., van Hinte, J.E., Honjo, S., 2000c. Coccolithophore export production, species composition, and coccolith-CaCO3 fluxes in the NE Atlantic (34 degrees N 21 degrees W and 48 degrees N 21 degrees W). Deep-Sea Research Part Ii-Topical Studies in Oceanography 47, 1877-1905.

Brovkin, V., Ganopolski, A., Archer, D., Munhoven, G., 2012. Glacial CO2 cycle as a succession of key physical and biogeochemical processes. Climate of the Past 8, 251-264.

Brownlee, C., Taylor, A., 2004. Calcification in Coccolithophores: A cellular perspective in: Thierstein, H.R., Young, J.R. (Eds.), Coccolithophores: From Molecular processes to Global Impact. Springer, London, p. 565.

Burns, D.A., 1975. Abundance and Species Composition of Nannofossil Assemblages in Sediments from Continental-Shelf to Offshore Basin, Western Tasman Sea. Deep-Sea Research 22, 425-431.

Cachao, M., Moita, M.T., 2000. Coccolithus pelagicus, a productivity proxy related to moderate fronts off Western Iberia. Marine Micropaleontology 39, 131-155.

Caldeira, K., Wickett, M.E., 2003. Anthropogenic carbon and ocean pH. Nature 425, 365-365.

Cassar, N., DiFiore, P.J., Barnett, B.A., Bender, M.L., Bowie, A.R., Tilbrook, B., Petrou, K., Westwood, K.J., Wright, S.W., Lefevre, D., 2011. The influence of iron and light on net community production in the Subantarctic and Polar Frontal Zones. Biogeosciences 8, 227-237.

Cefarelli, A.O., Ferrario, M.E., Almandoz, G.O., Atencio, A.G., Akselman, R., Vernet, M., 2010. Diversity of the diatom genus *Fragilariopsis* in the Argentine Sea and Antarctic waters: morphology, distribution and abundance. Polar Biology 33, 1463-1484.

Cook, S.S., Whittock, L., Wright, S.W., Hallegraeff, G.M., 2011. Photosynthetic pigment and genetic differences between two Southern Ocean morphotypes of *Emiliana Huxleyi (Haptophyta)*. Journal of Phycology 47, 2-12.

Cubillos, J.C., Wright, S.W., Nash, G., de Salas, M.F., Griffiths, B., Tilbrook, B., Poisson, A., Hallegraeff, G.M., 2007. Calcification morphotypes of the coccolithophorid *Emiliania huxleyi* in the Southern Ocean: changes in 2001 to 2006 compared with historical data. . Marine Ecology Progress Series 348, 47-54.

De Vargas, C., Aubry, M., Probert, I., Young, J.R., 2007. Origin and Evolution of Coccolithophres: From Coastal Hunters to Oceanic Farmers, in: Falkowski, P.G., Knoll, A.H. (Eds.), Evolution of primary producers in the Sea. Elsevier Inc., London, p. 441.

De Vargas, C., Probert, I., 2004. New keys to the past: Current and future DNA studies in coccolithophores. Micropaleontology 50, 45-54.

Delille, B., Harlay, J., Zondervan, I., Jacquet, S., Chou, L., Wollast, R., Bellerby, R.G.J., Frankignoulle, M., Borges, A.V., Riebesell, U., Gattuso, J.P., 2005. Response of primary production and calcification to changes of pCO_2 during experimental blooms of the coccolithophorid *Emiliania huxleyi*. Global Biogeochemical Cycles 19, GB2023, DOI: 10.1029/2004GB002318.

Deuser, W.G., Mullerkarger, F.E., Hemleben, C., 1988. Temporal variation of particle fulxes in the deep Sub-Tropical and Tropical North-Atlantic -

Eulerian versus Lagrangian effects. Journal of Geophysical Research-Oceans 93, 6857-6862.

Dickson, A.G., Millero, F.J., 1987. A comparison of the equilibrium constants for the dissociation of Carbonic Acid in seawater media. Deep-Sea Research Part A. Oceanographic reasearch papers. 34, 1733-1743.

Dissard, D., Nehrke, G., Reichart, G.J., J., B., 2010. Impact of seawater pCO_2 on calcification and Mg/Ca and Sr/Ca ratios in benthic foraminifera calcite:results from culturing experiments with *Ammonia tepida*. Biogeosciences 7, 81-93.

Doney, S.C., Fabry, V.J., Feely, R.A., Kleypas, J.A., 2009. Ocean Acidification: The Other CO_2 Problem. Annual Review of Marine Science 1, 169-192.

Erez, J., 2003. The source of Ions for Biomineralization in Foraminifera and their Implications for Paleoceanographic Proxies, in: Dove, P.M., De Yoreo, J.J., S., W. (Eds.), Biomineralization. The mineralogical Society of America, Washington, p. 381.

Feely, R.A., Sabine, C.L., Lee, K., Berelson, W., Kleypas, J., Fabry, V.J., Millero, F.J., 2004. Impact of anthropogenic CO2 on the CaCO3 system in the oceans. Science 305, 362-366.

Findlay, C.S., Flores, J.A., 2000. Subtropical front fluctuations south of Australia (45^{o}09'S, 146^{o}17'E) for the last 130 ka years based on calcareous nannoplankton. Marine Micropaleontology 40, 403-416.

Findlay, C.S., Giraudeau, J., 2000. Extant calcareous nannoplankton in the Australian Sector of the Southern Ocean (austral summers 1994 and 1995. Marine Micropaleontology 40, 417-439.

Findlay, C.S., Giraudeau, J., 2002. Movement of Oceanic fronts south of Australia during the last 10 ka: interpretation of calcareous nannoplankton in surface sediments from the Southern Ocean. Marine Micropaleontology 46, 431-444.

Flores, J.A., Gersonde, R., Sierro, F.J., 1999. Pleistocene fluctuations in the Agulhas Current Retroflection based on the calcareous plankton record. Marine Micropaleontology 37, 1-22.

Flores, J.A., Marino, M., Sierro, F.J., Hodell, D.A., Charles, C.D., 2003. Calcareous plankton dissolution pattern and coccolithophore assemblages during the last 600 kyr at ODP Site 1089 (Cape Basin, South Atlantic): paleoceanographic implications. Palaeogeography Palaeoclimatology Palaeoecology 196, 409-426.

Geisen, M., Billard, C., Broerse, A.T.C., Cros, L., Probert, I., Young, J.R., 2002. Life-cycle associations involving pairs of holococcolithophorid species: intra-specific variation or cryptic speciation? European Journal of Phycology 37, 531-550.

Geisen, M., Young, J.R., Probert, I., Saez, A.G., KH., B., Sprengel, C., Bollmann, J., Cros, L., De Vargas, C., Medlin, L., 2004. Species level variation in Coccolithophores, in: Thierstein, H.R., Young, J.R. (Eds.), Coccolithophores: From Molecular Processes to Global Impact. Springer, London, pp. 327-366.

Giraudeau, J., Bailey, G.W., 1995. SPATIAL DYNAMICS OF COCCOLITHOPHORE COMMUNITIES DURING AN UPWELLING EVENT IN THE SOUTHERN BENGUELA SYSTEM. Continental Shelf Research 15, 1825-&.

Giraudeau, J., Monteiro, P.M.S., Nikodemus, K., 1993. Distribution and malformation of living coccolithophores in the northern Benguela upwelling system off Namibia. Marine Micropaleontology 22, 93-110.

Griffith, E.M., Paytan, A., Caldeira, K., Bullen, T.D., Thomas, E., 2008. A Dynamic Marine Calcium Cycle During the Past 28 Million Years. Science 322, 1671-1674.

Gruber, N., Gloor, M., Fletcher, S.E.M., Doney, S.C., Dutkiewicz, S., Follows, M.J., Gerber, M., Jacobson, A.R., Joos, F., Lindsay, K., Menemenlis, D., Mouchet, A., Muller, S.A., Sarmiento, J.L., Takahashi, T., 2009. Oceanic sources, sinks, and transport of atmospheric CO(2). Global Biogeochemical Cycles 23.

Haidar, A.T., Thierstein, H.R., 2001. Coccolithophore dynamics off Bermuda (N. Atlantic). Deep-Sea Research Part Ii-Topical Studies in Oceanography 48, 1925-1956.

Haidar, A.T., Thierstein, H.R., Deuser, W.G., 2000. Calcareous phytoplankton standing stocks, fluxes and accumulation in Holocene sediments off Bermuda (N. Atlantic). Deep-Sea Research Part Ii-Topical Studies in Oceanography 47, 1907-1938.

Hallegraeff, G.M., 1984. Coccolithophorids (Calcareous Nanoplankton) from Australian Waters. Botanica marina 27, 229-247.

Halloran, P.R., Hall, I.R., Colmenero-Hidalgo, E., Rickaby, R.E.M., 2008. Evidence for a multi-species coccolith volume change over the past two centuries: understanding a potential ocean acidification response. Biogeosciences 5, 1651-1655.

Haq, B.U., Lohmann, G.P., 1976. Early Cenozoic Calcareous Nannoplankton Biogeography of Atlantic Ocean. Marine Micropaleontology 1, 119-194.

Hasle, G.H., 1960. Plankton Coccolithophorids from the Subantarctic and Equatorial Pacific Norwegian Journal of Botany 8, 77-88.

Henderiks, J., 2008. Coccolithophore size rules - Reconstructing ancient cell geometry and cellular calcite quota from fossil coccoliths. Marine Micropaleontology 67, 143-154.

Henderiks, J., Rickaby, E.M., 2007. A coccolithophore concept for constraining the Cenozoic carbon cycle. Biogeosciences 4, 323-329.

Henderiks, J., Winter, A., Elbrachter, M., Feistel, R., van der Plas, A., Nausch, G., Barlow, R., 2012. Environmental controls on *Emiliania huxleyi* morphotypes in the Benguela coastal upwelling system (SE Atlantic). Marine Ecology Progress Series 448, 51-66.

Henriksen, K., Stipp, S.L.S., Young, J.R., Bown, P.R., 2003. Tailoring calcite: Nanoscale AFM of coccolith biocrystals. American Mineralogist 88, 2040-2044.

Henriksen, K., Stipp, S.L.S., Young, J.R., Marsh, M.E., 2004a. Biological control on calcite crystallization: AFM investigation of coccolith polysaccharide function. American Mineralogist 89, 1709-1716.

Henriksen, K., Young, J.R., Bown, P.R., Stipp, S.L.S., 2004b. Coccolith biomineralisation studied with atomic force microscopy. Palaeontology 47, 725-743.

Henriksen, K., Young, J.R., Bown, P.R., Stipp, S.L.S., 2004c. Coccolith biomineralization studied with atomic force microscopy. Palaeontology 47, 725-743.

Hiramatsu, C., DeDeckker, P., 1996. Distribution of calcareous nannoplankton near the Subtropical Convergence, south of Tasmania, Australia. Marine and Freshwater Research 47, 707-713.

Hiramatsu, C., DeDeckker, P., 1997a. The calcareous nannoplankton assemblages of surface sediments in the Tasman and Coral Seas. Palaeogeography Palaeoclimatology Palaeoecology 131, 257-285.

Hiramatsu, C., DeDeckker, P., 1997b. The late Quaternary calcareous nannoplankton assemblages from three cores from the Tasman Sea. Palaeogeography Palaeoclimatology Palaeoecology 131, 391-412.

Honisch, B., Ridgwell, A., Schmidt, D.N., Thomas, E., Gibbs, S.J., Sluijs, A., Zeebe, R., Kump, L., Martindale, R.C., Greene, S.E., Kiessling, W., Ries, J., Zachos, J.C., Royer, D.L., Barker, S., Marchitto, T.M., Moyer, R., Pelejero, C., Ziveri, P., Foster, G.L., Williams, B., 2012. The Geological Record of Ocean Acidification. Science 335, 1058-1063.

Howard, W.R., Roberts, D., Moy, A.D., Lindsay, M.C.M., Hopcroft, R.R., Trull, T.W., Bray, S.G., 2011. Distribution, abundance and seasonal flux of pteropods in the Sub-Antarctic Zone. Deep-Sea Research Part Ii-Topical Studies in Oceanography 58, 2293-2300.

Iglesias-Rodriguez, M.D., Halloran, P.R., Rickaby, R.E.M., Hall, I.R., Colmenero-Hidalgo, E., Gittins, J.R., Green, D.R.H., Tyrrell, T., Gibbs, S.J., von Dassow, P., Rehm, E., Armbrust, E.V., Boessenkool, K.P., 2008. Phytoplankton Calcification in a high- CO2 world. Science 320, 336-340.

Indermuhle, A., Stocker, T.F., Joos, F., Fischer, H., Smith, H.J., Wahlen, M., Deck, B., Mastroianni, D., Tschumi, J., Blunier, T., Meyer, R., Stauffer, B., 1999. Holocene carbon-cycle dynamics based on CO2 trapped in ice at Taylor Dome, Antarctica. Nature 398, 121-126.

Jordan, R., Kleijne, A., 1994. A classification system of living coccolithophorids, in: Winter, A., Siesser, W.G. (Eds.), Coccolithpphores. Cambridge University Press, Cambridge, pp. 83-105.

Jordan, R.W., Cros, L., Young, J.R., 2004. A revised classification scheme for living haptophytes, Micropaleontology, pp. 55-79.

Kleypas, J.A., Buddemeier, R.W., Archer, D., Gattuso, J.P., Langdon, C., Opdyke, B.N., 1999. Geochemical consequences of increased atmospheric carbon dioxide on coral reefs. Science 284, 118-120.

Krug, S.A., Schulz, K.G., Riebesell, U., 2011. Effects of changes in carbonate chemistry speciation on Coccolithus braarudii: a discussion of coccolithophorid sensitivities. Biogeosciences 8, 771-777.

Langdon, C., Atkinson, M.J., 2005. Effect of elevated pCO_2 on photosynthesis and calcification of corals and interactions with seasonal change in temperature/irradiance and nutrient enrichment. Journal of Geophysical Research Oceans 110, C09S07.

Langer, G., Geisen, M., Baumann, K.H., Klas, J., Riebesell, U., Thoms, S., Young, J.R., 2006. Species-specific responses of calcifying algae to changing seawater carbonate chemistry. Geochemistry Geophysics Geosystems 7, Q09006.

Langer, G., Nehrke, G., Probert, I., Ly, J., Ziveri, P., 2009. Strain-specific responses of *Emiliania huxleyi* to changing seawater carbonate chemistry. Biogeosciences 6, 2637-2646.

Lohbeck, K.T., Riebesell, U., Reusch, T.B.H., 2012. Adaptive evolution of a key phytoplankton species to ocean acidification. Nature Geoscience, advance online publication.

Lourey, M.J., Trull, T.W., 2001. Seasonal nutrient depletion and carbon export in the Subantarctic and Polar Frontal Zones of the Southern Ocean south of Australia. Journal of Geophysical Research-Oceans 106, 31463-31487.

Lowenstam, H.A., Weiner, S., 1989. On Biomineralization. Oxford University Press, Inc., New York.

Lumpkin, R., Speer, K., 2007. Global ocean meridional overturning. Journal of Physical Oceanography 37, 2550-2562.

Malinverno, E., Triantaphyllou, M.V., Stavrakakis, S., Ziveri, P., Lykousis, V., 2009. Seasonal and spatial variability of coccolithophore export production at the South-Western margin of Crete (Eastern Mediterranean). Marine Micropaleontology 71, 131-147.

Margalef, R., 1978. LIFE-FORMS OF PHYTOPLANKTON AS SURVIVAL ALTERNATIVES IN AN UNSTABLE ENVIRONMENT. Oceanologica Acta 1, 493-509.

McIntyre, A., Be, A.W.H., 1967. Modern Coccolithophoridae of Atlantic Ocean .I. Placoliths and Cyrtoliths. Deep-Sea Research 14, 561-597.

McNeil, B.I., Matear, R.J., 2008. Southern Ocean acidification: A tipping point at 450-ppm atmospheric CO2. Proceedings of the National Academy of Sciences of the United States of America 105, 18860-18864.

McNeil, B.I., Metzl, N., Key, R.M., Matear, R., Corbiere, A., 2007. An empirical estimate of the Southern Ocean air-sea CO_2 flux. Global Biogeochemical Cycles 21, GB3011.

McNeil, B.I., Tilbrook, B., 2009. A seasonal carbon budget for the sub-Antarctic Ocean, South of Australia. Marine Chemistry 115, 196-210.

Mehrbach, C., Culberson, C.H., Hawley, J.E., Pytkowicz, R.M., 1973. Measurement of the apparent dissociation constants of Carbonic Acid in seawater at atmospheric pressure. Limnology and Oceanography 18, 897-907.

Milliman, J.D., 1993. Production and Accumulation of Calcium-Carbonate in the Ocean - Budget of a Nonsteady State. Global Biogeochemical Cycles 7, 927-957.

Mitchell- Innes, B.A., Winter, A., 1987. Coccolithophores - a Major Phytoplankton Component in Mature Upwelled Waters Off the Cape Peninsula, South-Africa in March, 1983. Marine Biology 95, 25-30.

Mohan, R., Mergulhao, L.P., Guptha, M.V.S., Rajakurnar, A., Thamban, M., AnilKurnar, N., Sudhakar, M., Ravindra, R., 2008. Ecology of coccolithophores in the Indian sector of the Southern Ocean. Marine Micropaleontology 67, 30-45.

Mohan, R., Quarshi, A.A., Meloth, T., Sudhakar, M., 2011. Diatoms from the surface waters of the Southern Ocean during the austral summer of 2004. Current Science 100, 1323-1327.

Mostajo, E.L., 1985. Nanoplancton calcareo del océano Atlántico sur. . Rev. Española Micropal 17, 261-280

Moy, A.D., 2005. Late Pleistocene Palaeoceanographic and Geochemical Evolution of the South Tasman Rise, Institue of Academic and Southern Ocean Studies. University of Tasmania, Hobart, p. 235.

Moy, A.D., Howard, W.R., Bray, S.G., Trull, T.W., 2009. Reduced calcification in modern Southern Ocean planktonic foraminifera. Nature Geoscience 2, 276-280.

Moy, A.D., Howard, W.R., Gagan, M.K., 2006. Late Quaternary palaeoceanography

of the Circumpolar Deep Water from the South Tasman Rise. Journal of Quaternary Science 21, 763-777.

Muller, M.N., Kisakurek, B., Buhl, D., Gutperlet, R., Kolevica, A., Riebesell, U., Stoll, H., Eisenhauer, A., 2011. Response of the coccolithophores Emiliania huxleyi and Coccolithus braarudii to changing seawater Mg(2+) and Ca(2+) concentrations: Mg/Ca, Sr/Ca ratios and delta(44/40)Ca, delta(26/24)Mg of coccolith calcite. Geochimica et Cosmochimica Acta 75, 2088-2102.

Muller, M.N., Schulz, K.G., Riebesell, U., 2009. Effects of long-term high CO_2 exposure on two species of coccolithophores. Biogeosciences 6, 10963-10982.

Nishida, S., 1986. Nannoplankton flora in the Southern Ocea, with special reference to siliceous varieties. Memoirs of National Intitue of Polar Research, 56-68.

Okada, H., Honjo, S., 1973. The distribution of oceanic coccolithophores in the Pacific. . Deep-Sea Oceanography 20, 355-374.

Okada, H., Honjo, S., 1975. Distribution of Coccolithophores in marginal seas along Western Pacific Ocean and in Red Sea Marine Biology 54, 319-328.

Okada, H., McIntyre, A., 1979. Seasonal Distribution of Modern Coccolithophores in the Western North-Atlantic Ocean. Marine Biology 54, 319-328.

Olguin, H.F., Alder, V.A., 2011. Species composition and biogeography of diatoms in antarctic and subantarctic (Argentine shelf) waters (37-76 degrees S). Deep-Sea Research Part Ii-Topical Studies in Oceanography 58, 139-152.

Orr, J.C., Fabry, V.J., Aumont, O., Bopp, L., Doney, S.C., Feely, R.A., Gnanadesikan, A., Gruber, N., Ishida, A., Joos, F., Key, R.M., Lindsay, K., Maier-Reimer, E., Matear, R., Monfray, P., Mouchet, A., Najjar, R.G., Plattner, G.K., Rodgers, K.B., Sabine, C.L., Sarmiento, J.L., Schlitzer, R., Slater, R.D., Totterdell, I.J., Weirig, M.F., Yamanaka, Y., Yool, A., 2005. Anthropogenic ocean acidification over the twenty-first century and its impact on calcifying organisms. Nature 437, 681-686.

Orr, J.C., Maier-Reimer, E., Mikolajewicz, U., Monfray, P., Sarmiento, J.L., Toggweiler, J.R., Taylor, N.K., Palmer, J., Gruber, N., Sabine, C.L., Le Quere, C., Key, R.M., Boutin, J., 2001. Estimates of anthropogenic carbon uptake from four three-dimensional global ocean models. Global Biogeochemical Cycles 15, 43-60

Orsi, A.H., Whitworth, T., Nowlin, W.D., 1995. On the Meridional Extent and Fronts of the Antarctic Circumpolar Current. Deep-Sea Research Part I-Oceanographic Research Papers 42, 641-673.

Parente, A., Cachao, M., Baumann, K.H., de Abreu, L., Ferreira, J., 2004. Morphometry of *Coccolithus pelagicus* s.l. (Coccolithophore, Haptophyta) from offshore Portugal, during the last 200 kyr. Micropaleontology 50, 107-120.

Petit, J.R., Jouzel, J., Raynaud, D., Barkov, N.I., Barnola, J.M., Basile, I., Bender, M., Chappellaz, J., Davis, M., Delaygue, G., Delmotte, M., Kotlyakov, V.M., Legrand, M., Lipenkov, V.Y., Lorius, C., Pepin, L., Ritz, C., Saltzman, E., Stievenard, M., 1999. Climate and atmospheric history of the past 420,000 years from the Vostok ice core, Antarctica. Nature 399, 429-436.

Pelejero, C., Calvo, E., Hoegh-Guldberg, O., 2010. Paleo-perspective on ocean acidification. Trends in Ecology and Evolution 25(6), 332-344.

Pierrot, D., Lewis, E., Wallace, D., 2006. MS Excel program developed for CO_2 system calculations, ORNL/CDIAC-105, in: Laboratory, B.N. (Ed.). Carbon Dioxide Information Analysis Center, Oak Ridge National Laboratory, U.S Departement of Energy, Oak Ridge, Tennessee

Raven, J.A., Falkowski, P.G., 1999. Oceanic sinks for atmospheric CO2. Plant Cell and Environment 22, 741-755.

Redfield, A.C., Ketchum, B.H., Richards, F.H., 1963. The influence of organisms on the composition of seawater, in: Hill, M.N. (Ed.), The Sea. Inter-Science, New York, pp. 26-77.

Renaud, S., Klaas, C., 2001. Seasonal variations in the morphology of the coccolithophore Calcidiscus leptoporus off Bermuda (N. Atlantic). Journal of Plankton Research 23, 779-795.

Renaud, S., Ziveri, P., Broerse, A.T.C., 2002. Geographical and seasonal differences in morphology and dynamics of the coccolithophore Calcidiscus leptoporus. Marine Micropaleontology 46, 363-385.

Ridgwell, A., Zeebe, R., 2005. The role of the global carbonate cycle in the regulation and evolution of the earth system. Earth and planetary science letters 234, 299-315.

Riebesell, U., Bellerby, R.G.J., Grossart, H.P., Thingstad, F., 2008. Mesocosm CO_2 perturbation studies: from organism to community level. Biogeosciences 5, 1157-1164.

Riebesell, U., Schulz, K.G., Bellerby, R.G.J., Botros, M., Fritsche, P., Meyerhofer, M., Neill, C., Nondal, G., Oschlies, A., Wohlers, J., Zollner, E., 2007. Enhanced biological carbon consumption in a high CO_2 ocean. Nature 450, 545-548.

Riebesell, U., Zondervan, I., Rost, B., Tortell, P.D., Zeebe, R.E., Morel, F.M.M., 2000. Reduced calcification of marine plankton in response to increase atmospheric CO_2. Nature 407, 364-367.

Ries, J.B., 2005. Aragonite production in calcite seas: effect of seawater Mg/Ca ratio on the calcification and growth of the calcareous alga Penicillus capitatus. Paleobiology 31, 445-458.

Ries, J.B., Cohen, A.L., McCorkle, D.C., 2009. Marine calcifiers exhibit mixed responses to CO_2-induced ocean acidification. Geology 37, 1131-1134.

Rintoul, S.R., 2008. The role of Southern Ocean in past, present and future climate: A strategy for the International Polar Year. Indian Journal of Marine Sciences 37, 373-385.

Rintoul, S.R., Bullister, J.L., 1999. A late winter hydrographic section from Tasmania to Antarctica. Deep-Sea Research Part I-Oceanographic Research Papers 46, 1417-1454.

Rintoul, S.R., England, M.H., 2002. Ekman transport dominates local air-sea fluxes in driving variability of subantarctic mode water. Journal of Physical Oceanography 32, 1308-1321.

Rintoul, S.R., Trull, T.W., 2001. Seasonal evolution of the mixed layer in the Subantarctic Zone south of Australia. Journal of Geophysical Research-Oceans 106, 31447-31462.

Roberts, D., Howard, W.R., Moy, A.D., Roberts, J.L., Trull, T.W., Bray, S.G., Hopcroft, R.R., 2011. Interannual pteropod variability in sediment traps deployed above and below the aragonite saturation horizon in the Sub-Antarctic Southern Ocean. Polar Biology 34, 1739-1750.

Rost, B., Riebesell, U., 2004. Coccolithophores and the biological carbon pump: responses to environmental changes, in: Thierstein, H.R., Young, J.R. (Eds.), Coccolithophores: From Molecular processes to Global Impact. Springer, London, p. 565.

Royal_Society, 2005. Ocean Acidification Due to Increasing Atmospheric Carbon Dioxide, The Royal Society, London, UK, p. 57.

Sabine, C.L., Feely, R.A., Gruber, N., Key, R.M., Lee, K., Bullister, J.L., Wanninkhof, R., Wong, C.S., Wallace, D.W.R., Tilbrook, B., Millero, F.J., Peng, T.H., Kozyr, A., Ono, T., Rios, A.F., 2004. The oceanic sink for anthropogenic CO2. Science 305, 367-371.

Saez, A.G., Probert, I., Geisen, M., Quinn, P., Young, J.R., Medlin, L.K., 2003. Pseudo-cryptic speciation in coccolithophores. Proceedings of the National Academy of Sciences of the United States of America 100, 7163-7168.

Sarmiento, J.L., Dunne, J., Gnanadesikan, A., Key, R.M., Matsumoto, K., Slater, R., 2002. A new estimate of the CaCO(3) to organic carbon export ratio. Global Biogeochemical Cycles 16, 1107, doi:1110.1029/2002GB001919.

Sarmiento, J.L., Orr, J.C., 1991. 3-Dimensional simulations of the impact of Southern-Ocean nutrients depletion on atmospheric CO_2 and ocean chemistry. Limnology and Oceanography 36, 1928-1950.

Schiebel, R., 2002. Planktic foraminiferal sedimentation and the marine calcite budget. Global Biogeochemical Cycles 16.

Scott, F.J., Thomas, D.P., 2005. Diatoms, in: Scott, F.J., Marchant, H.J. (Eds.), Antarctic Marine Protists. ABRS and AAD, Hobart.

Siegenthaler, U., Monnin, E., Kawamura, K., Spahni, R., Schwander, J., Stauffer, B., Stocker, T.F., Barnola, J.M., Fischer, H., 2005. Supporting evidence from the EPICA Dronning Maud Land ice core for atmospheric CO2 changes during the past millennium. Tellus Series B-Chemical and Physical Meteorology 57, 51-57.

Sigman, D.M., Boyle, A., 2000. Glacial/interglacial variations in atmospheric carbon dioxide. Nature 407, 859-869.

Sigman, D.M., Hain, M.P., Haug, G.H., 2010. The polar ocean and glacial cycles in atmospheric CO(2) concentration. Nature 466, 47-55.

Silva, A., Palma, S., Oliveira, P.B., Moita, M.T., 2009. Composition and interannual variability of phytoplankton in a coastal upwelling region (Lisbon Bay, Portugal). Journal of Sea Research 62, 238-249.

Smith, H.J., Fischer, H., Wahlen, M., Mastroianni, D., Deck, B., 1999. Dual modes of the carbon cycle since the Last Glacial Maximum. Nature 400, 248-250.

Sokolov, S., Rintoul, S.R., 2007a. Multiple jets of the Antarctic circumpolar current South of Australia. Journal of Physical Oceanography 37, 1394-1412.

Sokolov, S., Rintoul, S.R., 2007b. On the relationship between fronts of the Antarctic Circumpolar Current and surface chlorophyll concentrations in the Southern Ocean. Journal of Geophysical Research-Oceans 112, C07030, doi:07010.01029/02006JC004072.

Sokolov, S., Rintoul, S.R., 2009a. Circumpolar structure and distribution of the Antarctic Circumpolar Current fronts: 1. Mean circumpolar paths. Journal of Geophysical Research-Oceans 114, C11019, doi:11010.11029/12008JC005248.

Sokolov, S., Rintoul, S.R., 2009b. Circumpolar structure and distribution of the Antarctic Circumpolar Current fronts: 2. Variability and relationship to sea surface height. Journal of Geophysical Research-Oceans 114, C11018, doi:11010.11029/12008JC005108.

Speer, K., Rintoul, S.R., Sloyan, B., 2000. The diabatic Deacon cell. Journal of Physical Oceanography 30, 3212-3222.

Stanley, S.M., 2006. Influence of seawater chemistry on biomineralization throughout phanerozoic time: Paleontological and experimental evidence. Palaeogeography Palaeoclimatology Palaeoecology 232, 214-236.

Stanley, S.M., 2008. Effects of Global Seawater Chemistry on Biomineralization: Past, Present, and Future. Chemical Reviews 108, 4483-4498.

Stanley, S.M., Ries, J.B., Hardie, L.A., 2005. Seawater chemistry, coccolithophore population growth, and the origin of Cretaceous chalk. Geology 33, 593-596.

Takahashi, T., Sutherland, S.C., Sweeney, C., Poisson, A., Metzl, N., Tilbrook, B., Bates, N., Wanninkhof, R., Feely, R.A., Sabine, C., Olafsson, J., Nojiri,

Y., 2002. Global sea-air CO2 flux based on climatological surface ocean pCO(2), and seasonal biological and temperature effects. Deep-Sea Research Part Ii-Topical Studies in Oceanography 49, 1601-1622.

Takahashi, T., Sutherland, S.C., Wanninkhof, R., Sweeney, C., Feely, R.A., Chipman, D.W., Hales, B., Friederich, G., Chavez, F., Sabine, C., Watson, A., Bakker, D.C.E., Schuster, U., Metzl, N., Yoshikawa-Inoue, H., Ishii, M., Midorikawa, T., Nojiri, Y., Kortzinger, A., Steinhoff, T., Hoppema, M., Olafsson, J., Arnarson, T.S., Tilbrook, B., Johannessen, T., Olsen, A., Bellerby, R., Wong, C.S., Delille, B., Bates, N.R., de Baar, H.J.W., 2009. Climatological mean and decadal change in surface ocean pCO(2), and net sea-air CO2 flux over the global oceans Deep-Sea Research Part I-Oceanographic Research Papers 56, 2075-2076.

Thierstein, H.R., Cortes, M.Y., Haidar, A.T., 2004. Plankton community behavior on ecological and evolutionary time-scales: when models confront evidence, in: Thierstein, H.R., Young, J.R. (Eds.), Coccolithophores: From Molecular Processes to Global Impact. Springer-Verlag Berlin, Berlin, pp. 455-479.

Tribollet, A., Godinot, C., Atkinson, M., Langdon, C., 2009. Effects of elevated pCO(2) on dissolution of coral carbonates by microbial euendoliths. Global Biogeochemical Cycles 23, GB3008.

Trull, T., Rintoul, S.R., Hadfield, M., Abraham, E.R., 2001a. Circulation and seasonal evolution of polar waters south of Australia: Implications for iron fertilization of the Southern Ocean. Deep-Sea Research Part Ii-Topical Studies in Oceanography 48, 2439-2466.

Trull, T., Sedwick, P.N., Griffiths, F.B., Rintoul, S.R., 2001b. Introduction to special section: SAZ Project. Journal of geophysical Research 106, 425-429.

Trull, T.W., Bray, S.G., Manganini, S.J., Honjo, S., Fancois, R., 2001c. Moored sediment trap measurements of carbon export in the Subantarctic and Polar Frontal Zones of the Southern Ocean, south of Australia. Journal of Geophysical Research-Oceans 103, 31489-31509.

Tyrrell, T., Merico, A., 2004. *Emiliania huxley*i: bloom observations and the conditions that induce them, in: Thierstein, H.R., Young, J.R. (Eds.), Coccolithophores: From Molecular Processes to Global Impact. Springer, London.

Verbeek, J.W., 1989. Recent calcareous nannoplakton in the Southernmost Atlantic. Polarforschung 59, 45-60.

Villa, G., Palandri, S., Wise, S.W., 2005. Quaternary calcareous nannofossils from Periantarctic basins: Paleoecological and paleoclimatic implications. Marine Micropaleontology 56, 103-121.

Warton, D.I., Wright, I.J., Falster, D.S., Westoby, M., 2006. Bivariate line-fitting methods for allometry. Biological Reviews 81, 259-291.

Weiner, S., Dove, P.M., 2003. An overview of Biomineralization processes and the Problem of the Vital Effect, in: Dove, P.M., De Yoreo, J.J., S., W. (Eds.), Biomineralization. The mieralogical Society of America, Washington, p. 381.

Wells, P., Okada, H., 1997. Response of nannoplankton to major changes in sea-surface temperature and movements of hydrological fronts over Site DSDP 593 (south Chatham Rise, southeastern New Zealand), during the last 130yrs. . Marine Micropaleontology 32, 341-363.

Wolf-Gladrow, D.A., Zeebe, R.E., Klaas, C., Kortzinger, A., Dickson, A.G., 2007. Total alkalinity: The explicit conservative expression and its application to biogeochemical processes. Marine Chemistry 106, 287-300.

Young, J., Bown, P.R., 1997. Proposals for a revised classification system for calcareous nannoplankton. Journal of Nannoplankton research 19, 15-47.

Young, J.R., 1992. The description and analysis of coccolith structure, in: Hamrsmid, B., Young, J.R. (Eds.), Proceedings of the 4th INA Conference. Knihovnicka ZPN, Prague 1992, pp. 35-71.

Young, J.R., Bown, P.R., 1991. An Ontogenic Sequence of Coccoliths from the Late Jurassic Kimmeridge Clay of England. Palaeontology 34, 843-850.

Young, J.R., Davis, S.A., Bown, P.R., Mann, S., 1999. Coccolith ultrastructure and biomineralisation. Journal of Structural Biology 126, 195-215.

Young, J.R., Didymus, J.M., Bown, P.R., Prins, B., Mann, S., 1992a. Crystal assembly and phylogenetic evolution in heterococcoliths. Nature 356, 516-519.

Young, J.R., Didymus, J.M., Bown, P.R., Prins, B., Mann, S., 1992b. Crystal Assembly and Phylogenetic Evolution in Heterococcoliths. Nature 356, 516-518.

Young, J.R., Geisen, M., Cross, L., Kleijne, A., Sprengel, C., Probert, I., J, O., 2003. A guide to extant coccolithophore taxonomy. Journal of Nannoplankton research.

Young, J.R., Geisen, M., Probert, I., 2005. A review of selected aspects of coccolithophore biology with implications for paleobiodiversity estimation. Micropaleontology 51, 267-288.

Young, J.R., Henriksen, K., 2003. Biomineralization within Vesicles: The calcite of Coccoliths, in: Dove, P.M., De Yoreo, J.J., S., W. (Eds.), Biomineralization. The mieralogical Society of America, Washington, p. 381.

Young, J.R., Henriksen, K., Probert, I., 2004. Structure and morphogenesis of the coccoliths of the CODENET species, in: Thierstein, H.R., Young, J.R. (Eds.), Coccolithophores: From molecular Processes to Global Impact. Springer, London, p. 565.

Young, J.R., Ziveri, P., 2000. Calculation of coccolith volume and its use in calibration of carbonate flux estimates. Deep-Sea Research Part Ii-Topical Studies in Oceanography 47, 1679-1700.

Zhengyu, L., Philander, S.G.H., 2001. Tropical-extratropical oceanic exchange pathways, in: Siedler, G., Chung, C.W., Gould, J. (Eds.), Ocean circulation and climate. Academic Press, London, pp. 247-254.

List of plates

Plate 1. Electron micrograph of *Coccolithus pelagicus (s.l)* coccoliths

a. Sediment sample, deglaciation period, 158cm depth in core MD972106;
b. Holocene sediment, 13 cm depth in core MD972106;
c. Example of a coccolith with serrated edges from sediment trap samples, November 2003, 2000 m depth (46^{o} 49.47'S, 141^{o} 38.73'E) (white arrows);
d. Typical coccolith from sediment trap samples, September 2003, 2000 m depth (46^{o} 49.47'S, 141^{o} 38.73'E);
e. Example of some possible dissolution in specimens from the deglaciation, 158 cm depth in core MD972106 (white arrow);
f. Central bar of coccolith from sediment trap sample, November 2003, 2000 m depth (46^{o} 49.47'S, 141^{o} 38.73'E) (white arrow);

Scale bars: a-e = 5µm, f = 2µm

Plate 2. Light micrographs of *Coccolithus pelagicus (s.l)* coccoliths

a, c. Coccoliths with central bar in brightfield (BF). Note the presence of serrated and incomplete (broken) proximal shields.
b, d. Central area of corresponding coccoliths (a) and (c) in cross-polarised light (POL). Note central bars do not appear birefringent in POL;
e. Coccolith in BF with complete proximal shield, lacking central bar;
f. Central area of (e) in POL.

Scale bars: 2µm

Plate 3. Light micrographs of *Coccolithus braarudii* from the Southern Ocean.

a. Coccolith from sediment trap samples, South Tasman Rise (STR) 46^{o} 49.47'S, 141^{o} 38.73'E, September 2003;
b. Coccolith from core-top sediment, core GCO7, 3 cm depth (STR, 46^{o}09'S, 146^{o}17'E)
c. Coccolith, culture strain CPTX01, from water surface samples, Tinderbox, Tasmania;
d. Coccolith, culture strain CPBMB02, from water surface samples, Blackmans Bay, Tasmania;
e, f. Single coccospheres from sediment trap samples, October 2003, 2000 m depth, (STR, 46^{o} 49.47'S, 141^{o} 38.73'E);

Scale bars: 5µm

Plate 4. Electron micrograph of *Coccolithus braarudii* from the Southern Ocean.

a. *C. braarudii* coccosphere, culture strain CPBMB02, from water surface samples, Blackmans Bay, Tasmania (image: Miguel de Salas)
b. *C. braarudii* single coccosphere, culture strain CPTX01, from water surface samples, Tinderbox, Tasmania (image: Miguel de Salas);
c, d. C. *braarudii* single coccosphere, sediment trap samples, October 2003, 2000 m depth (STR, 46^{o} 49.47'S, 141^{o} 38.73'E);
e. C. *braarudii* coccospheres, culture strain CPTX01, from water surface samples, Tinderbox, Tasmania (image: Miguel de Salas) ;
f. Diatom *Fragilariopsis kerguelensis* from sediment trap samples, December 2003, 2000 m depth (STR, 46^{o} 49.47'S, 141^{o} 38.73'E);

Scale bars: 5µm

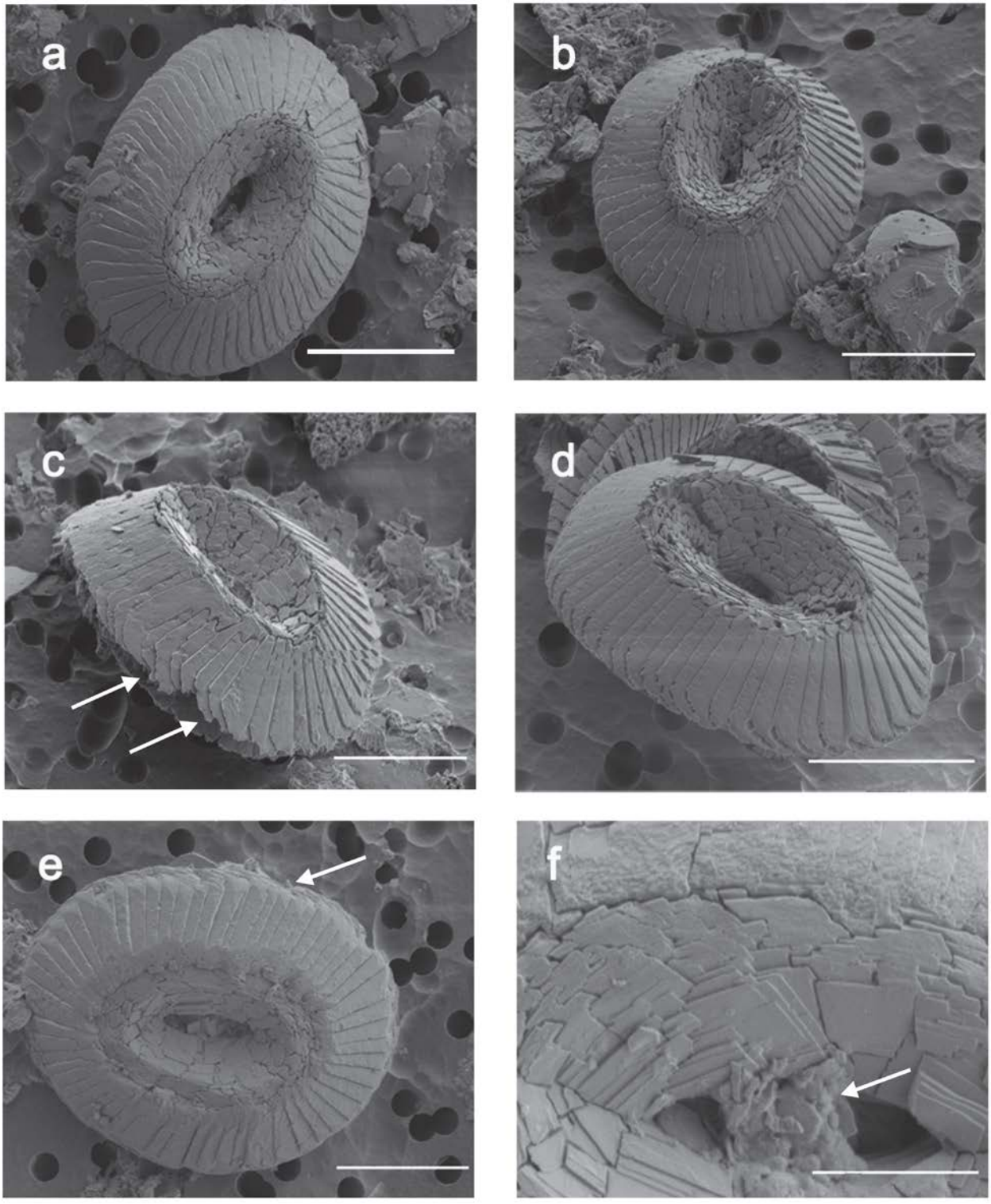

Plate 1. Electron micrograph of *Coccolithus pelagicus (s.l)* coccoliths.

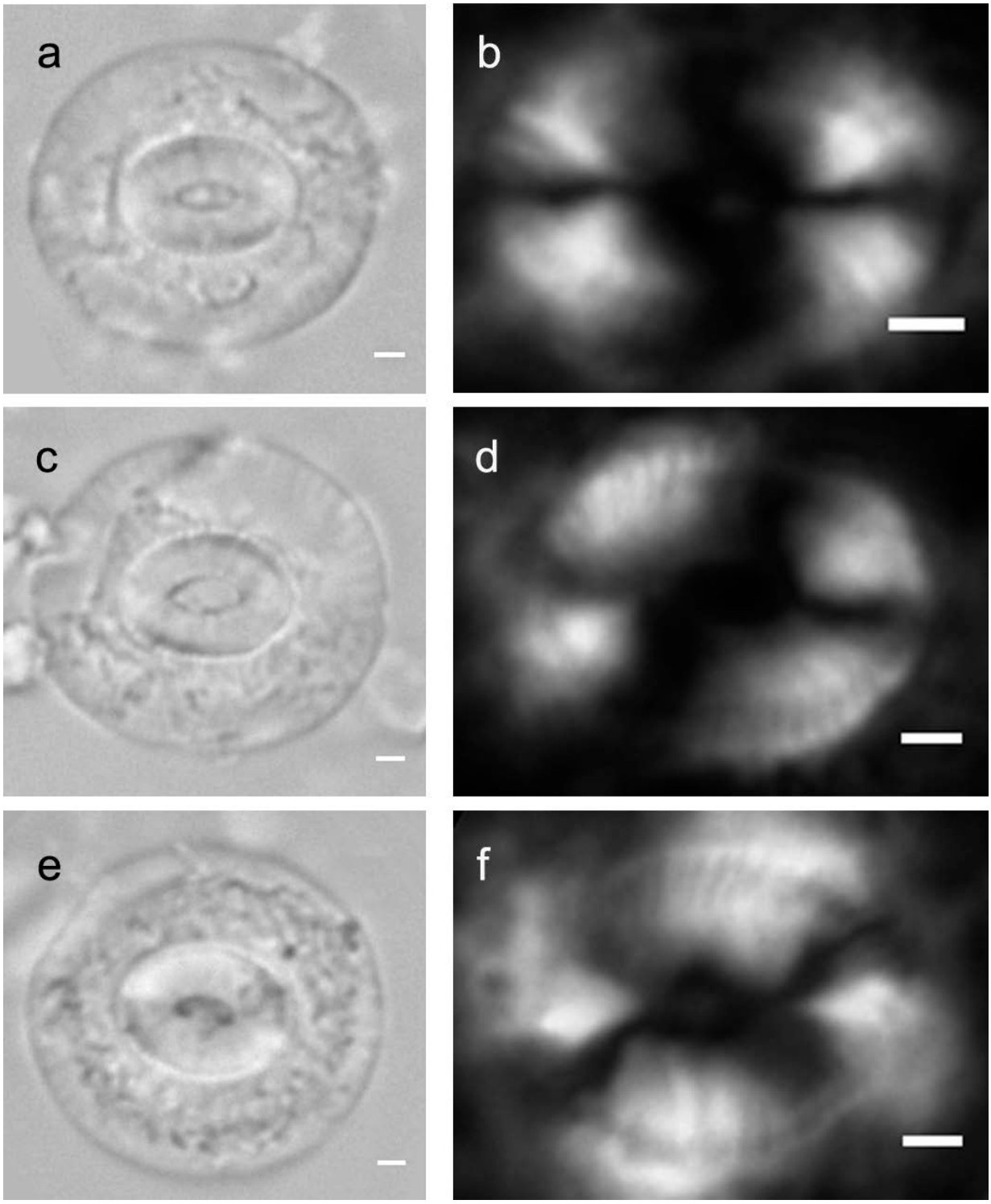

Plate 2. Light micrographs of *Coccolithus pelagicus (s.l)* coccoliths.

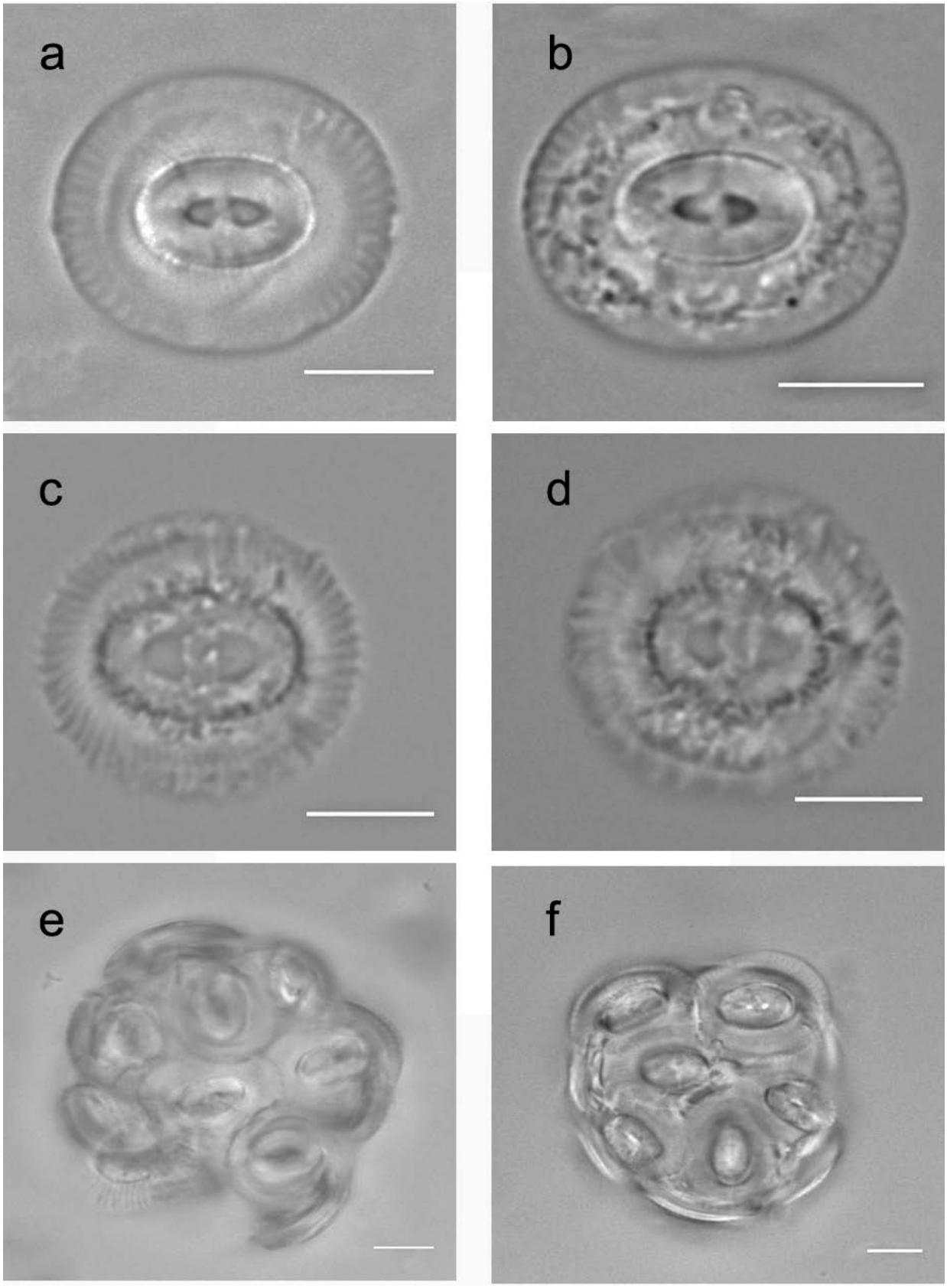

Plate 3. Light micrographs of *Coccolithus braarudii* from the Southern Ocean.

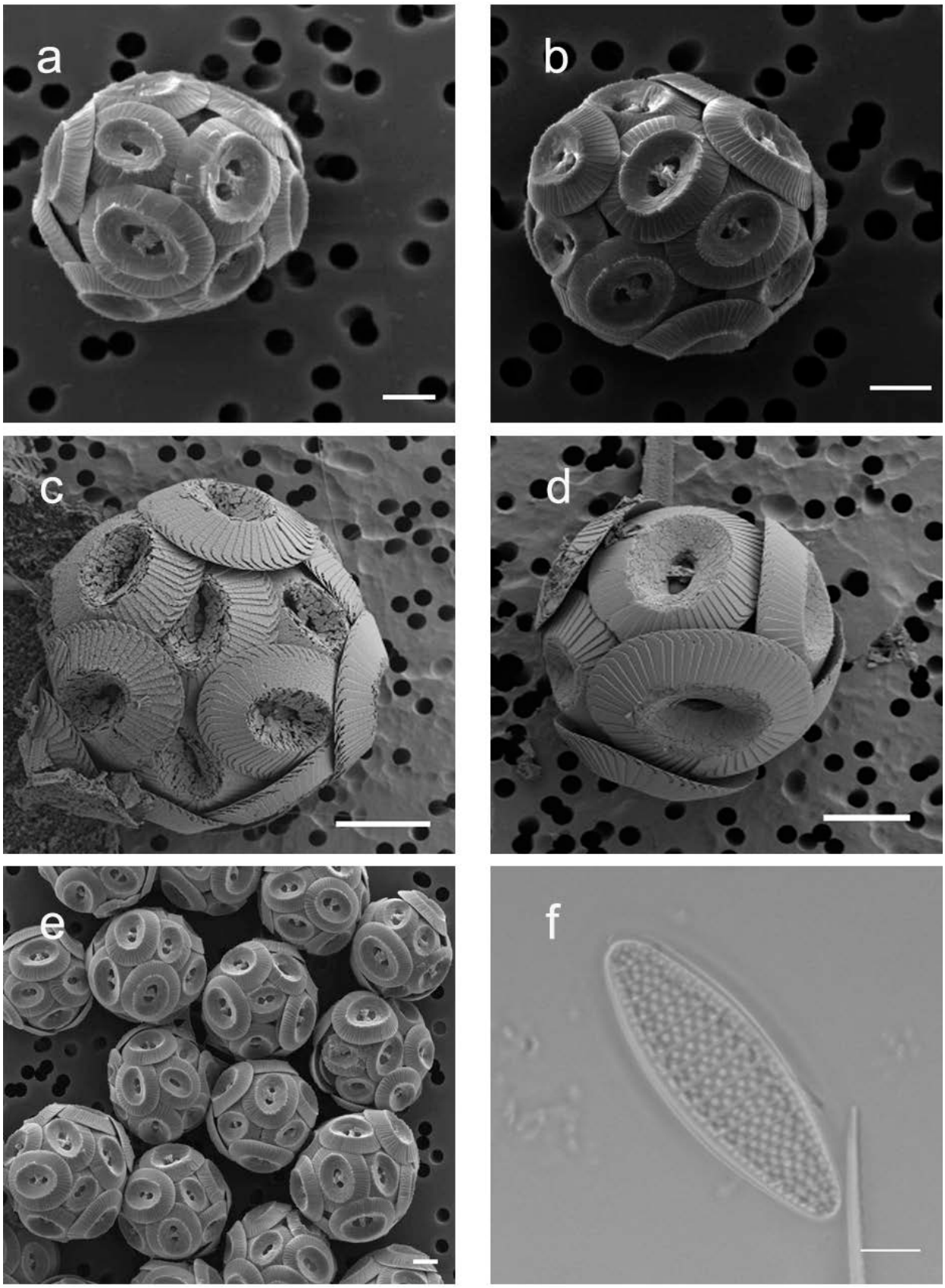

Plate 4. Electron micrograph of *Coccolithus braarudii* from the Southern Ocean.